DYNAMIC IMPACT TESTING
OF
CRT WOOD POSTS IN A RIGID SLEEVE

Submitted by

Steven W. Arens, B.S.C.E., E.I.T.
Graduate Research Assistant

Ronald K. Faller, Ph.D., P.E.
Research Assistant Professor

John R. Rohde, Ph.D., P.E.
Associate Professor

Karla A. Polivka, M.S.M.E., E.I.T.
Research Associate Engineer

MIDWEST ROADSIDE SAFETY FACILITY
University of Nebraska-Lincoln
527 Nebraska Hall
Lincoln, Nebraska 68588-0529
(402) 472-0965

Submitted to

MINNESOTA DEPARTMENT OF TRANSPORTATION (MnDOT)
Transportation Building
395 John Ireland Boulevard
Saint Paul, MN 55155

MwRSF Research Report No. TRP-03-198-08

April 11, 2008

TECHNICAL REPORT DOCUMENTATION PAGE

1. Report No.	2.	3. Recipient's Accession No.
TRP-03-198-08		

4. Title and Subtitle	5. Report Date
Dynamic Impact Testing of CRT Wood Posts in a Rigid Sleeve	April 11, 2008
	6.

7. Author(s)	8. Performing Organization Report No.
Arens, S.W., Faller, R.K., Rohde, J.R., and Polivka K.A.	TRP-03-198-08

9. Performing Organization Name and Address	10. Project/Task/Work Unit No.
Midwest Roadside Safety Facility (MwRSF) University of Nebraska-Lincoln 527 Nebraska Hall Lincoln, Nebraska 68588-0529	11. Contract © or Grant (G) No.

12. Sponsoring Organization Name and Address	13. Type of Report and Period Covered
Minnesota Department of Transportation (MnDOT) Transportation Building 395 John Ireland Boulevard Saint Paul, MN 55155	Final Report, 2007-2008
	14. Sponsoring Agency Code

15. Supplementary Notes

Prepared in cooperation with U.S. Department of Transportation, Federal Highway Administration

16. Abstract (Limit: 200 words)

Dynamic impact testing was performed on 152-mm x 203-mm (6-in. x 8-in.) CRT wood posts placed in a rigid sleeve at various angles. A total of nine bogie tests were performed with three tests each at 0, 90, and 45 degree rotation angles relative to the strong axis of bending. For each bogie test, the raw acceleration data was obtained from accelerometers and was filtered. Then, force-displacement and energy-displacement graphs were plotted. Based on the results, the properties and strengths of the CRT wood posts at the different impact angles were determined. The results of this study will be the basis in a future R&D effort to design a new, Universal Breakaway Steel Post for various guardrail applications.

17. Document Analysis/Descriptors	18. Availability Statement
Highway Safety, Wood Posts, Guardrail Posts, Bogie Testing, Impact Testing	No restrictions. Document available from: National Technical Information Services, Springfield, Virginia 22161

19. Security Class (this report)	20. Security Class (this page)	21. No. of Pages	22. Price
Unclassified	Unclassified	89	

DISCLAIMER STATEMENT

The contents of this report reflect the views of the authors who are responsible for the facts and the accuracy of the data presented herein. The contents do not reflect the official views nor policies of the Federal Highway Administration nor the Minnesota Department of Transportation. This report does not constitute a standard, specification, or regulation.

ACKNOWLEDGMENTS

The authors wish to acknowledge the Minnesota Department of Transportation for sponsoring this project.

Acknowledgment is also given to the following individuals who made a contribution to the completion of this research project.

Midwest Roadside Safety Facility

D.L. Sicking, Ph.D., P.E., Professor and MwRSF Director
J.D. Reid, Ph.D., Professor
R.W. Bielenberg, M.S.M.E., E.I.T., Research Associate Engineer
S.K. Rosenbaugh, M.S.C.E., E.I.T., Research Associate Engineer
J.C. Holloway, M.S.C.E., E.I.T., Research Manager
C.L. Meyer, B.S.M.E., E.I.T., Research Engineer II
A.T. Russell, B.S.B.A., Laboratory Mechanic II
K.L. Krenk, B.S.M.A, Field Operations Manager
A.T. McMaster, Laboratory Mechanic I
Undergraduate and Graduate Assistants

TABLE OF CONTENTS

TECHNICAL REPORT DOCUMENTATION PAGE ..... **i**

DISCLAIMER STATEMENT ..... **ii**

ACKNOWLEDGMENTS ..... **iii**

TABLE OF CONTENTS ..... **iv**

List of Figures vi
List of Tables ix

1 INTRODUCTION **1**

1.1 Background 1
1.2 Objective 2

2 LITERATURE REVIEW **3**

2.1 Prior Post Testing Results 3

3 PHYSICAL TESTING **4**

3.1 Purpose 4
3.2 Test Facility 4
3.3 Scope 4

4 SYSTEM DETAILS **6**

4.1 Wood Post 6
4.2 Knots and Imperfections 9
4.3 Moisture Content 11
4.4 Post Dimensions and Mass (Weight) 11
4.5 Rigid Sleeve and Wood Shims 12
4.6 Equipment and Instrumentation 13
4.6.1 Bogie *14*
4.6.2 Accelerometer *15*
4.6.3 Pressure Tape Switches *16*
4.6.4 Photography Cameras *16*
4.4 Methodology of Testing 16
4.5 End of Test Determination 21
4.6 Data Processing 21

5 TEST RESULTS AND DISCUSSION **23**

5.1 Introduction 23
5.2 Individual Test Results and Discussion 24

5.2.1 Test MNCRT-1 – Strong-Axis (0 Degree) Impact on CRT Post 25
5.2.2 Test MNCRT-2 – Strong-Axis (0 Degree) Impact on CRT Post 28
5.2.3 Test MNCRT-3 – Strong-Axis (0 Degree) Impact on CRT Post 31
5.2.4 Test MNCRT-4 – Weak-Axis (90 Degree) Impact on CRT Post 34
5.2.5 Test MNCRT-5 – Weak-Axis (90 Degree) Impact on CRT Post 37
5.2.6 Test MNCRT-6 – Weak-Axis (90 Degree) Impact on CRT Post 40
5.2.7 Test MNCRT-7 – Diagonal-Axis (45 Degree) Impact on CRT Post 43
5.2.8 Test MNCRT-8 – Diagonal-Axis (45 Degree) Impact on CRT Post 46
5.2.9 Test MNCRT-9 – Diagonal-Axis (45 Degree) Impact on CRT Post 49
5.3 Force Discussion 52
5.3.1 Force Results for Test Nos. MNCRT-1, MNCRT-2 and MNCRT-3 53
5.3.2 Force Results for Test Nos. MNCRT-4, MNCRT-5 and MNCRT-6 55
5.3.3 Force Results for Test Nos. MNCRT-7, MNCRT-8 and MNCRT-9 57
5.4 Energy Discussion 59
5.4.1 Energy Results for Test Nos. MNCRT-1, MNCRT-2 and MNCRT-3 60
5.4.2 Energy Results for Test Nos. MNCRT-4, MNCRT-5 and MNCRT-6 62
5.4.3 Energy Results for Test Nos. MNCRT-7, MNCRT-8 and MNCRT-9 65

6 CONCLUSIONS AND RECOMMENDATIONS 67

7 REFERENCES 69

8 APPENDICES 71

Appendix A 71
A.1 Test Summary Information 71

List of Figures

Figure 1a. Cross-Section Dimensions of the Wood Posts - Metric 7
Figure 1b. Cross-Section Dimensions of the Wood Posts - English..... 7
Figure 2. Wood Post Knot Orientation..... 9
Figure 3. Shimmed CRT in Rigid Sleeve 13
Figure 4. Bogie and Test Setup..... 15
Figure 5. Test Setup for Test Nos. MNCRT-1 to MNCRT-3 (0 Degree Tests) 18
Figure 6. Test Setup for Test Nos. MNCRT-4 to MNCRT-6 (90 Degree Tests) 19
Figure 7. Test Setup for Test Nos. MNCRT-7 to MNCRT-9 (45 Degree Tests) 20
Figure 8. Time Sequential Photographs, Test MNCRT-1..... 25
Figure 9a. Force versus Deflection Curve for MNCRT-1 – Metric 26
Figure 9b. Force versus Deflection Curve for MNCRT-1 – English..... 26
Figure 10a. Energy versus Deflection Curve for MNCRT-1 – Metric..... 26
Figure 10b. Energy versus Deflection Curve for MNCRT-1 – English 26
Figure 11. Post-Impact Images of MNCRT-1 27
Figure 12. Time Sequential Photographs, Test MNCRT-2..... 28
Figure 13a. Force versus Deflection Curve for MNCRT-2 – Metric 29
Figure 13b. Force versus Deflection Curve for MNCRT-2 – English..... 29
Figure 14a. Energy versus Deflection Curve for MNCRT-2 – Metric..... 29
Figure 14b. Energy versus Deflection Curve for MNCRT-2 – English 29
Figure 15. Post-Impact Images of MNCRT-2 30
Figure 16. Time Sequential Photographs, Test MNCRT-3..... 31
Figure 17a. Force versus Deflection Curve for MNCRT-3 – Metric 32
Figure 17b. Force versus Deflection Curve for MNCRT-3 – English..... 32
Figure 18a. Energy versus Deflection Curve for MNCRT-3 – Metric..... 32
Figure 18b. Energy versus Deflection Curve for MNCRT-3 – English 32
Figure 19. Post-Impact Images of MNCRT-3 33
Figure 20. Time Sequential Photographs, Test MNCRT-4..... 34
Figure 21a. Force versus Deflection Curve for MNCRT-4 – Metric 35
Figure 21b. Force versus Deflection Curve for MNCRT-4 – English..... 35
Figure 22a. Energy versus Deflection Curve for MNCRT-4 – Metric..... 35
Figure 22b. Energy versus Deflection Curve for MNCRT-4 – English 35
Figure 23. Post-Impact Images of MNCRT-4 36
Figure 24. Time Sequential Photographs, Test MNCRT-5..... 37
Figure 25a. Force versus Deflection Curve for MNCRT-5 – Metric 38
Figure 25b. Force versus Deflection Curve for MNCRT-5 – English..... 38
Figure 26a. Energy versus Deflection Curve for MNCRT-5 – Metric..... 38
Figure 26b. Energy versus Deflection Curve for MNCRT-5 – English 38
Figure 27. Post-Impact Images of MNCRT-5 39
Figure 28. Time Sequential Photographs, Test MNCRT-6..... 40
Figure 29a. Force versus Deflection Curve for MNCRT-6 – Metric 41
Figure 29b. Force versus Deflection Curve for MNCRT-6 – English..... 41
Figure 30a. Energy versus Deflection Curve for MNCRT-6 – Metric..... 41
Figure 30b. Energy versus Deflection Curve for MNCRT-6 – English 41

Figure 31. Post-Impact Images of MNCRT-6 42
Figure 32. Time Sequential Photographs, Test MNCRT-7 43
Figure 33a. Force versus Deflection Curve for MNCRT-7 – Metric 44
Figure 33b. Force versus Deflection Curve for MNCRT-7 – English 44
Figure 34a. Energy versus Deflection Curve for MNCRT-7 – Metric 44
Figure 34b. Energy versus Deflection Curve for MNCRT-7 – English 44
Figure 35. Post-Impact Images of MNCRT-7 45
Figure 36. Time Sequential Photographs, Test MNCRT-8 46
Figure 37a. Force versus Deflection Curve for MNCRT-8 – Metric 47
Figure 37b. Force versus Deflection Curve for MNCRT-8 – English 47
Figure 38a. Energy versus Deflection Curve for MNCRT-8 – Metric 47
Figure 38b. Energy versus Deflection Curve for MNCRT-8 – English 47
Figure 39. Post-Impact Images of MNCRT-8 48
Figure 40. Time Sequential Photographs, Test MNCRT-9 49
Figure 41a. Force versus Deflection Curve for MNCRT-9 – Metric 50
Figure 41b. Force versus Deflection Curve for MNCRT-9 – English 50
Figure 42a. Energy versus Deflection Curve for MNCRT-9 – Metric 50
Figure 42b. Energy versus Deflection Curve for MNCRT-9 – English 50
Figure 43 Post-Impact Images of MNCRT-9 51
Figure 44a. Force-Deflection Curves for MNCRT-1, 2, and 3 - Metric 54
Figure 44b. Force-Deflection Curves for MNCRT-1, 2, and 3 – English 54
Figure 45a. Force-Deflection Curves for MNCRT-4, 5, and 6 - Metric 56
Figure 45b. Force-Deflection Curves for MNCRT-4, 5, and 6 – English 56
Figure 46a. Force-Deflection Curves for MNCRT-7, 8, and 9 - Metric 58
Figure 46b. Force-Deflection Curves for MNCRT-7, 8, and 9 – English 58
Figure 47a. Energy-Deflection Curves for MNCRT-1, 2, and 3 - Metric 61
Figure 47b. Energy-Deflection Curves for MNCRT-1, 2, and 3 - English 61
Figure 48a. Energy-Deflection Curves for MNCRT-4, 5, and 6 - Metric 64
Figure 48b. Energy-Deflection Curves for MNCRT-4, 5, and 6 - English 64
Figure 49a. Energy-Deflection Curves for MNCRT-7, 8, and 9 - Metric 66
Figure 49b. Energy-Deflection Curves for MNCRT-7, 8, and 9 - English 66
Figure 50a. Peak Forces and Energy Levels of the CRT Post - Metric 68
Figure 50b. Peak Forces and Energy Levels of the CRT Post - English 68
Figure A-1. Results of MNCRT-1 (EDR3) 72
Figure A-2. Results of MNCRT-1 (EDR4) 73
Figure A-3. Results of MNCRT-2 (EDR3) 74
Figure A-4. Results of MNCRT-2 (EDR4) 75
Figure A-5. Results of MNCRT-3 (EDR3) 76
Figure A-6. Results of MNCRT-3 (EDR4) 77
Figure A-7. Results of MNCRT-4 (EDR3) 78
Figure A-8. Results of MNCRT-4 (EDR4) 79
Figure A-9. Results of MNCRT-5 (EDR3) 80
Figure A-10. Results of MNCRT-5 (EDR4) 81
Figure A-11. Results of MNCRT-6 (EDR3) 82
Figure A-12. Results of MNCRT-6 (EDR4) 83

Figure A-13. Results of MNCRT-7 (EDR3)..... 84
Figure A-14. Results of MNCRT-7 (EDR4)..... 85
Figure A-15. Results of MNCRT-8 (EDR3)..... 86
Figure A-16. Results of MNCRT-8 (EDR4)..... 87
Figure A-17. Results of MNCRT-9 (EDR3)..... 88
Figure A-18. Results of MNCRT-9 (EDR4)..... 89

List of Tables

Page

Table 1a. Scope of Physical Testing - Metric **5**
Table 1b. Scope of Physical Testing - English **5**
Table 2a. Wood CRT Post Peak Load Capacities - Metric **8**
Table 2b. Wood CRT Post Peak Load Capacities - English **8**
Table 3a. CRT Post Knot Location Details - Metric **10**
Table 3b. CRT Post Knot Location Details - English **10**
Table 4. Moisture Contents of Wood Posts **11**
Table 5a. Dimensions of CRT Wood Posts - Metric **12**
Table 5b. Dimensions of CRT Wood Posts - English **12**
Table 6. Test Parameters **16**
Table 7a. Peak Force Results for MNCRT-1, MNCRT-2, and MNCRT-3 - Metric **53**
Table 7b. Peak Force Results for MNCRT-1, MNCRT-2, and MNCRT-3 - English **53**
Table 8a. Peak Force Results for MNCRT-4, MNCRT-5, and MNCRT-6 - Metric **55**
Table 8b. Peak Force Results for MNCRT-4, MNCRT-5, and MNCRT-6 - English **55**
Table 9a. Peak Force Results for MNCRT-7, MNCRT-8, and MNCRT-9 - Metric **57**
Table 9b. Peak Force Results for MNCRT-7, MNCRT-8, and MNCRT-9 - English **57**
Table 10a. Energy Results for MNCRT-1, MNCRT-2, and MNCRT-3 - Metric **60**
Table 10b. Energy Results for MNCRT-1, MNCRT-2, and MNCRT-3 - English **60**
Table 11a. Energy Results for MNCRT-4, MNCRT-5, and MNCRT-6 - Metric **62**
Table 11b. Energy Results for MNCRT-4, MNCRT-5, and MNCRT-6 - English **63**
Table 12a. Energy Results for MNCRT-7, MNCRT-8, and MNCRT-9 - Metric **65**
Table 12b. Energy Results for MNCRT-7, MNCRT-8, and MNCRT-9 - English **65**
Table A-1. Post Testing Summary **71**
Table A-2. Post Testing Results Reference **71**

1 INTRODUCTION

1.1 Background

From 1997 through 2000, the Midwest Roadside Safety Facility (MwRSF) developed a thrie-beam bullnose guardrail system for shielding median hazards found between divided highways [1-3]. The new, non-proprietary bullnose guardrail system was successfully developed, full-scale vehicle crash tested, and evaluated according to the Test Level 3 (TL-3) safety performance criteria provided in National Cooperative Highway Research Program (NCHRP) Report No. 350 [4].

In the bullnose guardrail system, controlled release terminal (CRT) wood posts were used. Although the CRT posts adequately met the TL-3 safety requirements, these wood posts contain several drawbacks. First, the properties and performance of wood posts can be variable due to the existence of knots, checks, and splits, leading to the necessity of grading and inspection requirements. In the CRT wood posts two holes are drilled in the post to allow the post to breakaway upon impact, these holes further expose the interior of the wood to the environment, which may accelerate deterioration. Wood posts can swell under certain environmental conditions causing difficulty in the removal of broken posts from steel foundation tubes after impact. Chemical preservatives used to treat the wood posts have been claimed to be harmful to the environment. As such, the treated wood posts may require special consideration during their disposal. As a result of these concerns about wood CRT posts, there exists a need for the development of a new breakaway steel post to replace wood CRT posts for use in bullnose guardrail systems, guardrail end terminals, and any longitudinal barrier systems.

For this study, several dynamic bogie tests on CRT wood posts oriented at varying angles were performed. The results from the bogie tests will establish the performance criteria in the development of a Universal Breakaway Steel Post for bullnose guardrail systems, guardrail end terminals, and other longitudinal barrier systems. It is envisioned that the new steel post should match the longitudinal, lateral, and torsional resistances of the existing CRT post, thus allowing it to replace the CRT wood post in any guardrail application.

1.2 Objective

The objective of the research project was to determine the dynamic properties of the CRT wood posts in different axes, thus later assisting the research team in the design of a Universal Breakaway Steel Post. The breakaway steel post will need to reasonably reproduce the existing properties of the CRT post that are observed in the dynamic bogie tests.

2 LITERATURE REVIEW

2.1 Prior Post Testing Results

Due to the wide variations of posts in roadside hardware, many post studies have been previously performed. Hascall et al. [5] reviewed and summarized the previous post studies completed from 1960 through 2004. The only relevant study of CRT post properties was performed in the Ensco study “Safety Modification of Turned Down Guardrail Terminals” in which the CRT post was developed [6]. This Ensco report consisted of three volumes and described the development a safer turned-down guardrail terminal. The CRT wood post was developed for use as a breakaway post in the turned-down terminal to allow the rail to fall freely when impacted near the terminal and to redirect impacts occurring downstream of the first post of the terminal.

3 PHYSICAL TESTING

3.1 Purpose

Physical testing of components is an important aspect of any design process. This study is aimed at quantifying the mechanical properties of southern yellow pine CRT posts to set design objectives for replacing them.

3.2 Test Facility

Physical testing of the control releasing terminal (CRT) wood posts was performed at the MwRSF's outdoor testing facility located at the Lincoln airpark, on the northwest side of the Lincoln Municipal Airport.

3.3 Scope

The research objective was achieved by performing bogie crash tests on the CRT wood posts oriented at different angles with known installation conditions. The dynamic properties of the CRT wood post were determined with target impact conditions of a speed of 24.1 km/h (15 mph), rotation angles of 0, 45, and 90 degrees relative to the strong axis, and a height of 632 mm (24.875 in.) above the ground line. The scope of the physical testing is listed in Table 1.

A total of nine tests, MNCRT-1 through MNCRT-9, were conducted with the posts embedded in a rigid sleeve. All nine posts were embedded 1,016 mm (40 in.), as designed, into the rigid sleeve, which placed the breakaway hole in the CRT at ground level. Design details for the CRT posts are provided in Section 4.

The test results were analyzed and documented. Conclusions were then drawn that pertain to the behavior of the wood posts under dynamic loading.

Table 1a. Scope of Physical Testing - Metric

Test No.	Speed		Embedment Depth (mm)	Embedment Material	Impact Angle* (Degrees)
	km/h	m/s			
MNCRT-1	23.17	6.44	1,016	Rigid Sleeve	0
MNCRT-2	25.59	7.11	1,016	Rigid Sleeve	0
MNCRT-3	24.35	6.76	1,016	Rigid Sleeve	0
MNCRT-4	26.46	7.35	1,016	Rigid Sleeve	90
MNCRT-5	25.38	7.05	1,016	Rigid Sleeve	90
MNCRT-6	24.59	6.83	1,016	Rigid Sleeve	90
MNCRT-7	25.85	7.18	1,016	Rigid Sleeve	45
MNCRT-8	25.78	7.16	1,016	Rigid Sleeve	45
MNCRT-9	25.01	6.95	1,016	Rigid Sleeve	45

*****Angle Relative to Strong Axis Impact

Table 1b. Scope of Physical Testing - English

Test No.	Speed		Embedment Depth (inches)	Embedment Material	Impact Angle* (Degrees)
	mph	ft/s			
MNCRT-1	14.40	21.12	40	Rigid Sleeve	0
MNCRT-2	15.90	23.32	40	Rigid Sleeve	0
MNCRT-3	15.13	22.19	40	Rigid Sleeve	0
MNCRT-4	16.44	24.11	40	Rigid Sleeve	90
MNCRT-5	15.77	23.13	40	Rigid Sleeve	90
MNCRT-6	15.28	22.41	40	Rigid Sleeve	90
MNCRT-7	16.06	23.55	40	Rigid Sleeve	45
MNCRT-8	16.02	23.50	40	Rigid Sleeve	45
MNCRT-9	15.54	22.79	40	Rigid Sleeve	45

*****Angle Relative to Strong Axis Impact

4 SYSTEM DETAILS

4.1 Wood Post

The posts evaluated in this study were southern yellow pine (SYP) and grade No. 1 or better controlled release terminal (CRT) wood posts. The 1,829-mm (72-in.) long CRT wood post are designed to break away when impacted about its weak axis of bending. A 152-mm x 203-mm (6-in. x 8-in.) cross section is weakened by drilling out two 889-mm (3.5-in.) holes in the middle region of the post. The first hole, located 400-mm (15.75-in.) below ground level, was designed to allow the post to break away for the typical strong (S-1) soil conditions, as described in NCHRP Report No. 230 [7]. The second hole was located at ground level to weaken the wood post and allow it to break away for very stiff (frozen) soils.

For this bogie testing study, CRT wood posts only utilized the top hole. Since the post was located in a rigid foundation only the top hole located at the ground level contributed to the breakaway properties and capacity of the CRT wood post. The CRT wood post is illustrated in Figure 1.

From the cross-sectional dimensions and the properties of the wood CRT posts, an estimate was made for the peak load capacities about both axes of bending. As shown in Table 2, the peak load is a function of the assumed modulus of rupture, which was chosen as 37,232 MPa (5,400 psi) [8]. The results from Table 2 show that the strong axis should fail at about twice the peak load as the weak axis of the post.

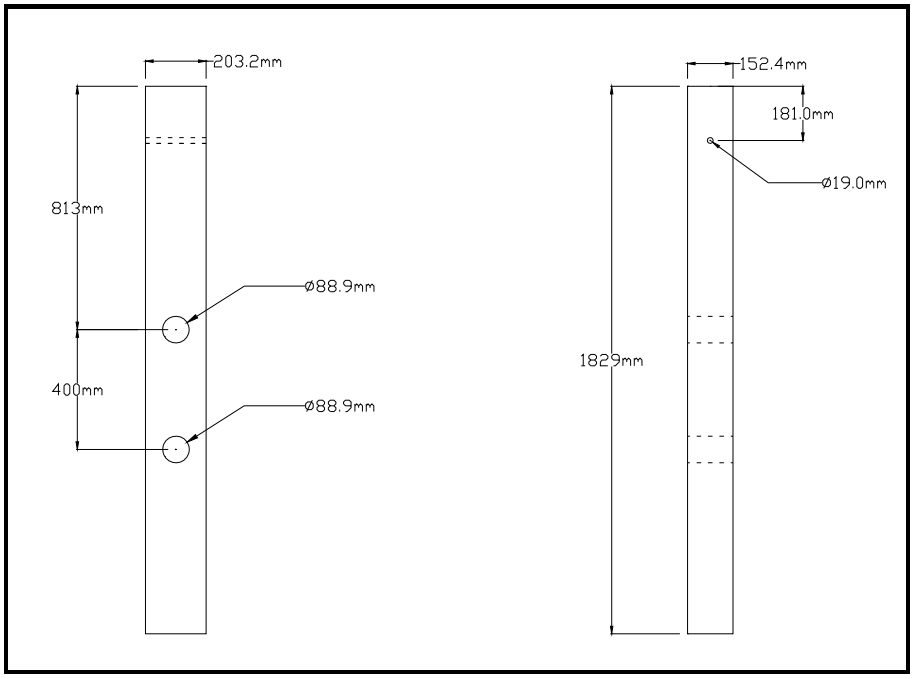

Figure 1a. Cross-Sectional Dimensions for CRT Wood Posts - Metric

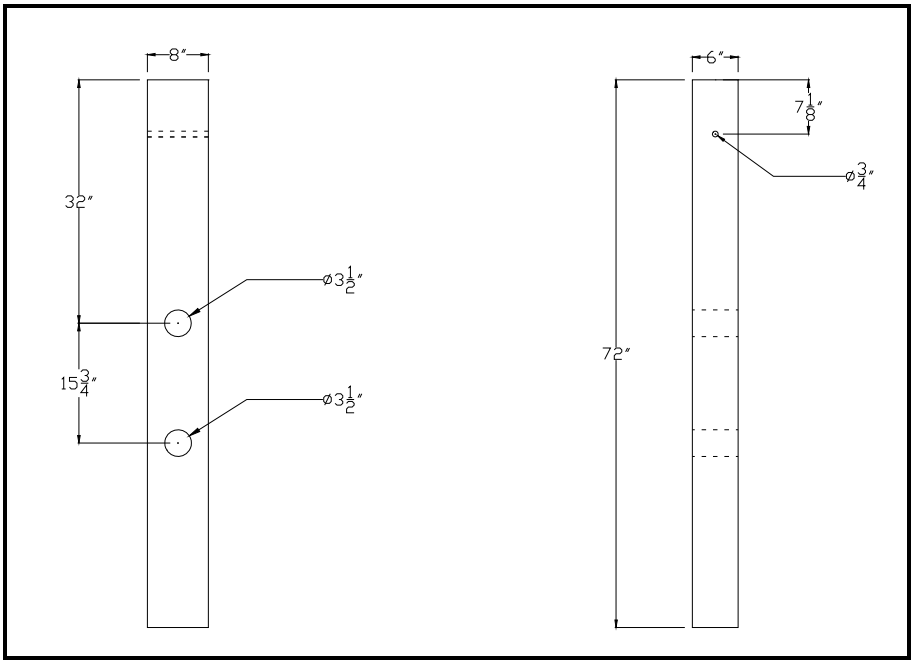

Figure 1b. Cross-Sectional Dimensions for CRT Wood Posts - English

Table 2a. Wood CRT Post Peak Load Capacities – Metric

CRT Post Properties							Strong Axis of Bending					Weak Axis of Bending				
Assumed Modulus of Rupture (Mpa)	Post Width (mm)	Post Depth (mm)	C x-x (mm)	C y-y (mm)	Hole Diameter (mm)	Load Height (mm)	Igross x-x (mm^4)	Ihole x-x (mm^4)	Inet x-x (mm^4)	Snet x-x (mm^3)	Bending Moment x-x (kJ)	Igross y-y (mm^4)	Ihole y-y (mm^4)	Inet y-y (mm^4)	Snet y-y (mm^3)	Bending Moment y-y (kJ)
37.232	152.4	203.2	101.6	76.2	88.9	631.8	1.066E+08	8.920E+06	9.763E+07	9.609E+05	35.82	5.994E+07	2.622E+07	3.371E+07	4.425E+05	16.50

Peak Load Capacities	
Strong Axis x-x	Weak Axis y-y
(kN)	(kN)
56.67	26.11

Table 2b. Wood CRT Post Peak Load Capacities - English

CRT Post Properties							Strong Axis of Bending					Weak Axis of Bending				
Assumed Modulus of Rupture (psi)	Post Width (In.)	Post Depth (In.)	C x-x (In.)	C y-y (In.)	Hole Diameter (In.)	Load Height (In.)	Igross x-x ($In.^4$)	Ihole x-x ($In.^4$)	Inet x-x ($In.^4$)	Snet x-x ($In.^3$)	Bending Moment x-x (Kip-In.)	Igross y-y ($In.^4$)	Ihole y-y ($In.^4$)	Inet y-y ($In.^4$)	Snet y-y ($In.^3$)	Bending Moment y-y (Kip-In.)
5,400	6.00	8.00	4.00	3.00	3.50	24.88	256.00	21.44	234.56	58.64	317	144.00	63.00	81.00	27.00	146

Peak Load Capacities	
Strong Axis x-x	Weak Axis y-y
(Kips)	(Kips)
12.74	5.87

4.2 Knots and Imperfections

Wood is a highly variable material. Knots and imperfections can significantly affect the strength of the wood post. Therefore, the number, size, and location of knots on each post were carefully recorded and are given in Figure 2 and Table 3.

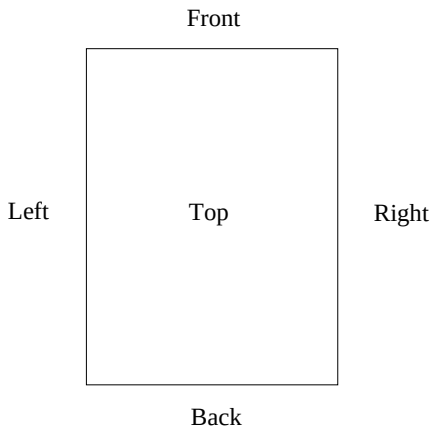

Figure 2. Wood Post Knot Orientation

Table 3a. CRT Post Knot Location Details – Metric (All measurements in mm)

Test No.	Knots*			
MNCRT-1	Ø25.4 @ 1041 Left	Ø25.4 @ 1092 Left	Ø25.4 @ 470 Back and Left	Ø38.1 @ 1067 Right
MNCRT-2	None			
MNCRT-3	Ø34.925 @ 660 Left and Back	Ø38.1 @ 445 Right		
MNCRT-4	Ø19.05 @ 1067 Left	Ø22.225 @ 1003 Back		
MNCRT-5	Ø6.35 @ 990.6 Right	Split running length down middle parallel to front and back faces		
MNCRT-6	Ø34.925 @ 559 Front	Ø31.75 @ 1194 Right	Ø101.6 @ 584.2 Left and Back	
MNCRT-7	Ø41.275 @ 991 Left	Ø31.75 @ 1016 Back	Ø19.05 @ 467 Right	
MNCRT-8	None			
MNCRT-9	Ø31.75 @ 889 Left	Ø44.45 @ 1016 Back	Ø6.35 @ 610 Left	Ø6.35 @ 775 Front

*****Distance measured from top with orientation illustrated in Figure 2.

Table 3b. CRT Post Knot Location Details – English

Test No.	Knots*			
MNCRT-1	Ø1” @ 41” Left	Ø1” @ 43” Left	Ø1” @ 18.5” Back and Left	Ø1.5” @ 42” Right
MNCRT-2	None			
MNCRT-3	Ø1.375” @ 26” Left and Back	Ø1.5” @ 17.5” Right		
MNCRT-4	Ø0.75” @ 42” Left	Ø0.875” @ 39.5” Back		
MNCRT-5	Ø0.25” @ 39” Right	Split running length down middle parallel to front and back faces		
MNCRT-6	Ø1.375” @ 22” Front	Ø1.25” @ 47” Right	Ø4” @ 23” Left and Back	
MNCRT-7	Ø1.625” @ 39” Left	Ø1.25” @ 40” Back	Ø0.75” @ 18.5” Right	
MNCRT-8	None			
MNCRT-9	Ø1.25” @ 35” Left	Ø1.75” @ 40” Back	Ø0.25” @ 24” Left	Ø0.25” @ 30.5” Front

*****Distance measured from top with orientation illustrated in Figure 2.

4.3 Moisture Content

The strength of a wood post can also be affected by the moisture content. When the moisture content reaches 23 percent or above, the wood is typically saturated, resulting in a reduced strength. The moisture content for each post was carefully measured at three locations - 533 mm (21 in.) from the top of the post, centerline of the post, and 533 mm (21 in.) from the bottom of the post - using a pin-type moisture meter [9]. The area within this length was considered the critical zone, or the zone where fracture was likely to occur. The moisture contents for all nine wood posts are provided in Table 4.

Table 4. Moisture Contents for Wood Posts

Test No.	Moisture Content (%)*		
	533 mm (21") From Top	Center Line	533 mm (21") From Bottom
MNCRT-1	12	12	12
MNCRT-2	15	10	10
MNCRT-3	14	15	15
MNCRT-4	16	14	11
MNCRT-5	14	11	13
MNCRT-6	12	13	12
MNCRT-7	11	13	14
MNCRT-8	15	11	14
MNCRT-9	12	13	12

*****Measured at impact face

4.4 Post Dimensions and Mass (Weight)

Due to variances in mill operations, wood guardrail posts are fabricated within an acceptable range of dimensional tolerances. The CRT posts used in this study nominally measured 152 mm x 203 mm (6 in. x 8 in.). The dimensions were measured at three locations of the posts - at the top of the post, at the breakaway hole in the post, and at the bottom of the post. Due to the differences in moisture contents, densities, and dimensions, each CRT post had

different weights. The results of the measurements and weights for each post test are given in Table 5.

Table 5a. Dimensions of CRT Wood Posts – Metric

Test No.	Mass (kg)	Post Dimensions (mm)		
		@ Top	@ Hole	@ Bottom
MNCRT-1	24.9	154 x 205	152 x 202	152 x 203
MNCRT-2	35.4	151 x 203	149 x 198	152 x 202
MNCRT-3	25.9	154 x 200	149 x 200	151 x 203
MNCRT-4	29.0	152 x 203	156 x 203	156 x 202
MNCRT-5	28.6	152 x 200	149 x 200	149 x 203
MNCRT-6	30.8	151 x 200	151 x 197	149 x 198
MNCRT-7	29.5	151 x 200	149 x 200	149 x 202
MNCRT-8	28.6	149 x 200	151 x 202	151 x 203
MNCRT-9	29.5	149 x 202	151 x 200	152 x 200

Table 5b. Dimensions of CRT Wood Posts – English

Test No.	Weight (lbs)	Post Dimensions (inches)		
		@ Top	@ Hole	@ Bottom
MNCRT-1	55	6.06” x 8.06”	6” x 7.94”	6” x 8”
MNCRT-2	78	5.94” x 8”	5.88” x 7.81”	6” x 7.94”
MNCRT-3	57	6.06” x 7.88”	5.88” x 7.88”	5.94” x 8”
MNCRT-4	64	6” x 8”	6.13” x 8”	6.13” x 7.94”
MNCRT-5	63	6” x 7.88”	5.88” x 7.88”	5.88” x 8”
MNCRT-6	68	5.94” x 7.88”	5.94” x 7.75”	5.88” x 7.81”
MNCRT-7	65	5.94” x 7.88”	5.88” x 7.88”	5.88” x 7.94”
MNCRT-8	63	5.88” x 7.88”	5.94” x 7.94”	5.94” x 8”
MNCRT-9	65	5.88” x 7.94”	5.94” x 7.88”	6” x 7.88”

4.5 Rigid Sleeve and Wood Shims

For all nine tests, a rigid sleeve was utilized to anchor the post. The post was fitted into the sleeve with wood blocks and shims to rigidly hold the post upright. The rigid placement of the posts in the sleeve allowed for the determination of the dynamic wood properties before and

during fracture. It should be noted that there was no post interaction with soil. An example of a post placed in the rigid sleeve with a 45 degree orientation is shown in Figure 3.

Figure 3. Shimmed CRT in Rigid Sleeve

4.6 Equipment and Instrumentation

The main equipment and instruments used for the tests were:

- Bogie
- Accelerometer
- Pressure Tape Switches
- Digital Photographic Cameras

4.6.1 Bogie

A rigid frame bogie was used to impact the posts. The bogie impact head was constructed of 203-mm (8-in.) diameter by 12.5-mm (0.5-in.) thick, standard steel pipe, with 19-mm (0.75-in.) thick, neoprene belting wrapped around the pipe to prevent local damage to the post from the impact. The bogie with the impact head is shown in Figure 4. The mass (weight) of the bogie, with the addition of the mountable impact head, was 728 kg (1,605 lbs). The impact height was 632 mm (24.875 in.) above the ground. The target speed for the tests was 24.14 km/h (15 mph).

In all tests, a pickup truck with a reverse cable tow and guide rail system was used to propel the bogie. The bogie was accelerated toward the post along the guidance system, which consisted of a steel pipe anchored above the tarmac. In all of the tests, the bogie wheels were aligned for caster and toe-in values of zero so that the bogie would track properly. When the bogie reached the end of the guidance system, it was released from the tow cable, allowing it to be free rolling when it impacted the post. A remote braking system was installed on the bogie, thus allowing it to be safely brought to rest after the test.

Figure 4. Bogie and Test Setup

4.6.2 Accelerometer

One tri-axial, piezo-resistive, accelerometer system Model EDR-4 with a range of ± 200 g's was developed by Instrumented Sensor Technology (IST) of Okemos, Michigan and was mounted on the frame of the bogie near its center of gravity. Data sampling was at 10,000 Hz with a Butterworth low-pass filter with a –3dB cut-off frequency of 1,500 Hz was used for anti-aliasing.

Another tri-axial, piezo-resistive, accelerometer system Model EDR-3 with a range of ± 200 g's was also developed by Instrumented Sensor Technology (IST) of Okemos, Michigan and was mounted on the frame on the bogie near its center of gravity. Data sampling was at 3,200 Hz with a 1,120 Hz Butterworth low-pass filter with a -3dB cut-off.

A laptop computer downloaded the raw acceleration data immediately following each test. The computer made the use of "DynaMax 1.75" accelerometer software [10] and then

loaded into "DADiSP 4.0" data processing program [11]. The data was processed according to the SAE J211/1 specifications [12].

4.6.3 Pressure Tape Switches

Three pressure tape switches spaced at a distance of 0.457-m (1.5-ft) intervals were used to determine the speed of the bogie before the impact. As the left-front tire of the bogie passed over each tape switch, a strobe light was fired, sending an electronic timing signal to the data acquisition system. Test speeds were determined by knowing the time between these signals from the data acquisition system and the distance between the switches.

4.6.4 Photography Cameras

One high-speed AOS VIT cam digital video camera, with a Sigma 24-70 mm lens and an operating speed of 500 frames/sec, was located perpendicular to the post impact direction. One JVC digital video camera, with an operating speed of 29.97 frames/sec, was also used to film the bogie test.

4.7 Methodology of Testing

A total of nine impact tests were carried out on posts placed in a rigid sleeve with three tests each at 0, 45, and 90 degrees relative to the strong axis of bending. The test parameters are shown in Table 6.

Table 6. Test Parameters

MNCRT Test Parameters
MNCRT: Control Releasing Terminal Wood Post
Test: Impact in rigid sleeve at 0, 45, and 90 degrees with respect to strong axis
Accelerometer: EDR-3 and EDR-4 Data
Bogie Mass (Weight): 728.0 kg (1,605 lbs)
Bumper Height: 632 mm (24.875 in.)
Posts: 152 mm x 203 mm (6 in. x 8 in.)
Post Length: 1,829 mm (72 in.)

Three different test setups were used to conduct the tests. The test setup for the 0-degree, strong-axis bogie tests, test nos. MNCRT-1 through MNCRT-3, is shown in Figure 5. The test setup for the 90-degree, weak-axis bogie tests, test nos. MNCRT-4 through MNCRT-6, is shown in Figure 6. For the final setup, the wood post's orientation was changed for a 45 degree impact, as provided in Figure 7.

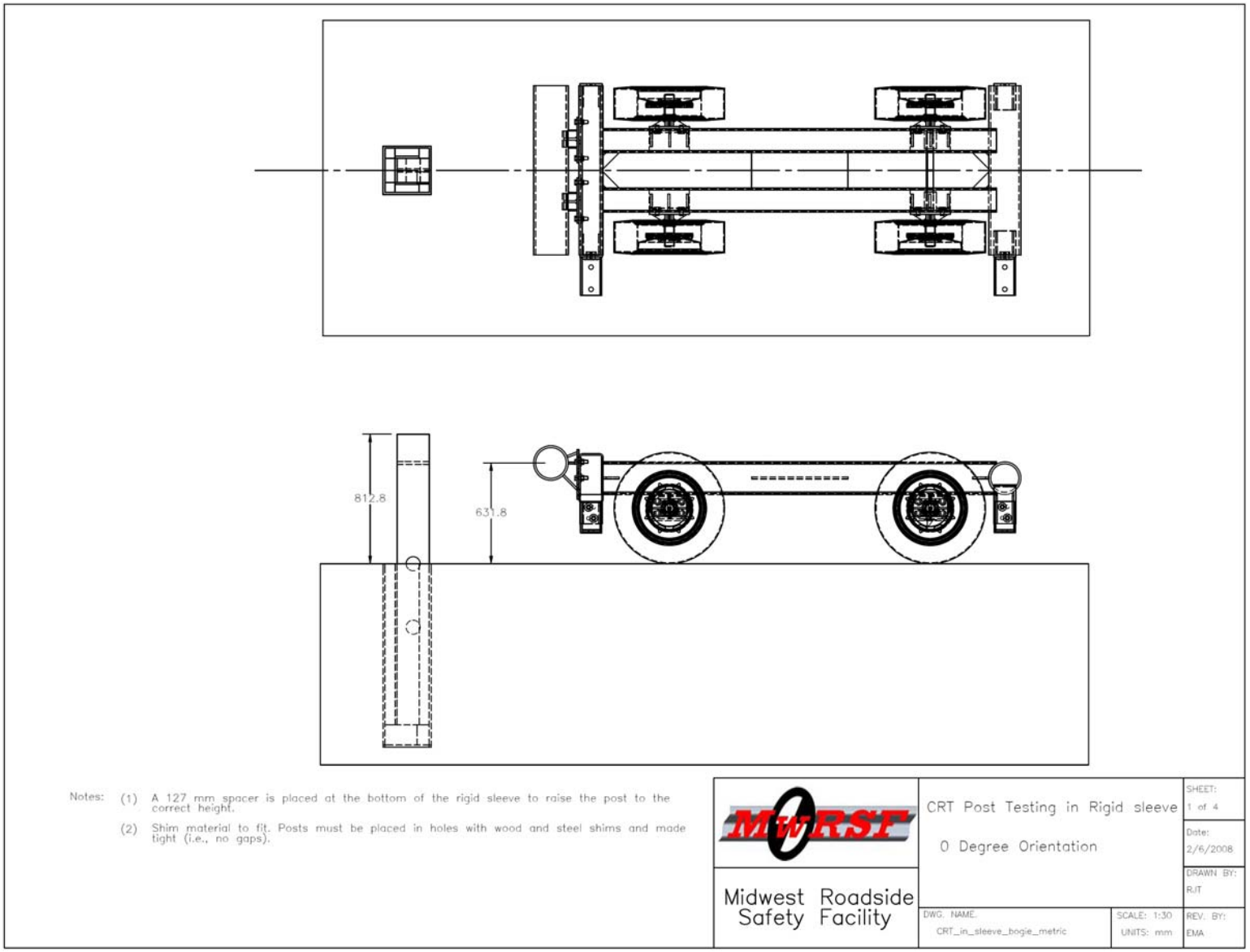

Figure 5. Test Setup for Test Nos. MNCRT-1 to MNCRT-3 (0 degree tests)

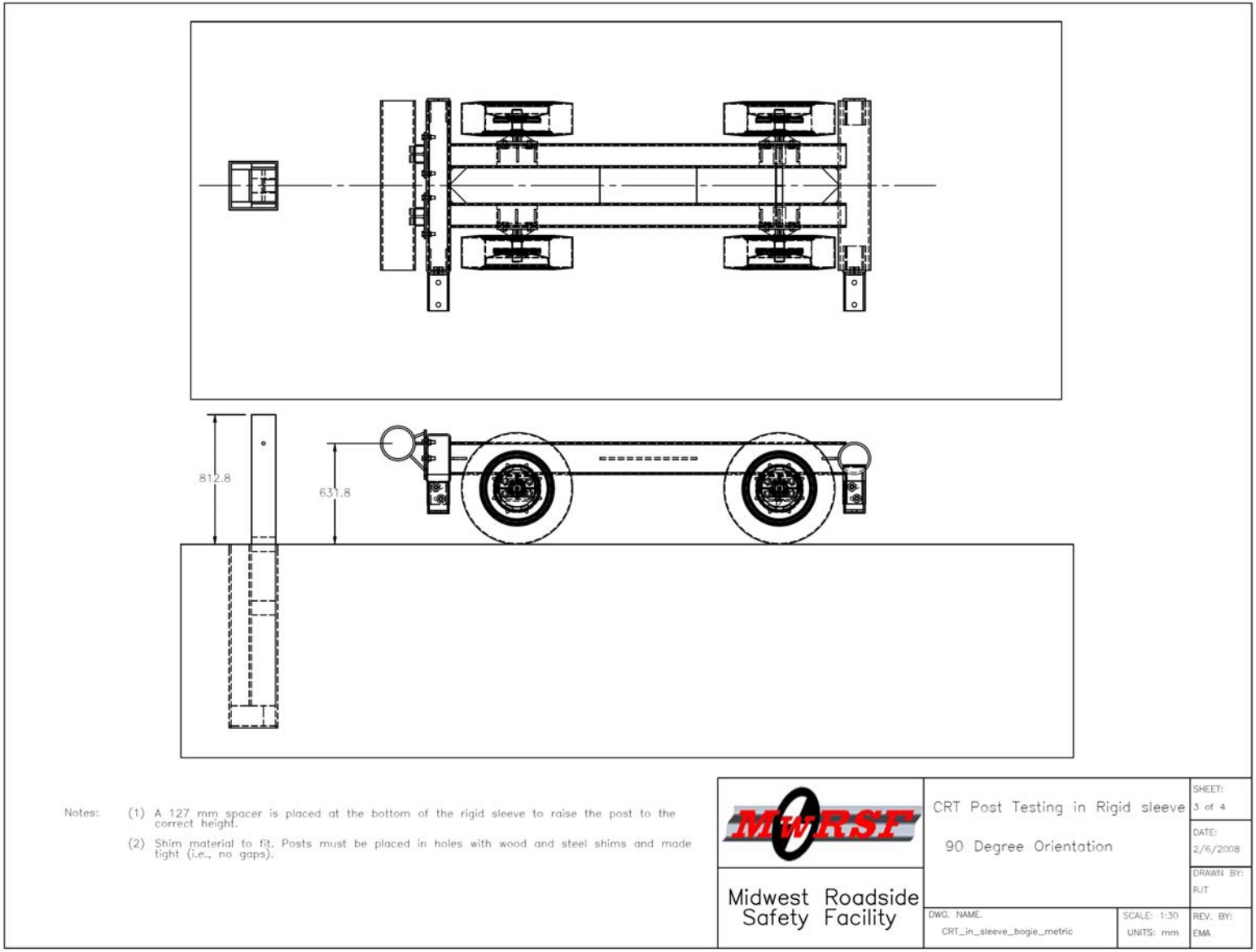

Figure 6. Test Setup for Test Nos. MNCRT-4 to MNCRT-6 (90 degree tests)

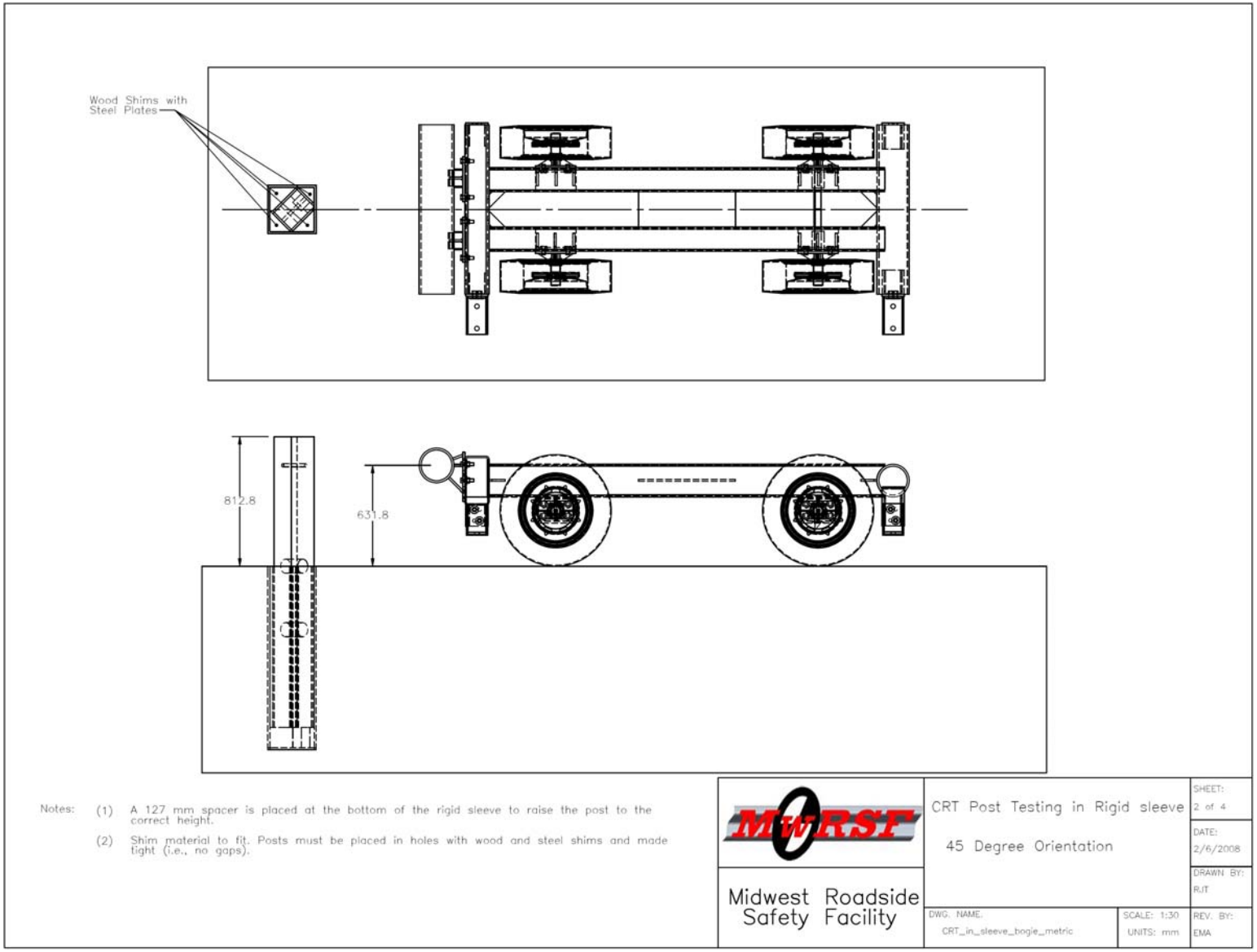

Figure 7. Test Setup for Test Nos. MNCRT-7 to MNCRT-9 (45 degree tests)

4.8 End of Test Determination

During an impact, the data acquisition system records the accelerations that the bogie observes from all sources, not just the post. Because of this, vibrations in the bogie vehicle, impact head, and accelerometer mounting assembly are also recorded and result in a high frequency acceleration trace. Since the bogie vehicle may still be vibrating after the impact event, the data may extend beyond the failure of the post. For this reason, the end of the test needed to be defined.

In general, this event time was identified as the time that the vibration peaks in the acceleration trace subsided back toward zero when it was clear that the continuation of vibrations were not caused by the interaction with the post. Also, some limitations were established so there were no unreasonably long test durations. First, all tests were limited to a 508-mm (20-in.) maximum deflection because it was decided that no post would have the capacity to deflect more than 508 mm (20 in.) in a rigid sleeve without complete fracture. Second, each test was limited by the bogie-post contact time. For each test, the high-speed video was used to establish the length of time that the bogie was actually in contact with the post. This time was then used to define the end of the test.

4.9 Data Processing

Initially, the bulk of the data was filtered using the SAE Class 60 Butterworth filter conforming to the SAE J211/1 specifications. The pertinent acceleration signal was extracted from the bulk of the data. The processed acceleration data was then multiplied by the mass of the bogie to get the impact force using Newton’s Second Law. Next, the acceleration trace was integrated to find the change in velocity. The initial velocity of the bogie, calculated using the data from the pressure tape switches, was then used to determine the actual bogie velocity versus

time. The calculated actual velocity trace versus time was integrated to find the displacement versus time trace. Subsequently, using the previous results, the force versus deflection curve was plotted for each test. Finally, integration of the force versus deflection curve provided the energy versus displacement curve for each test.

5 TEST RESULTS AND DISCUSSION

5.1 Introduction

The information desired from the physical tests was the relation between force on the post and deflection of the post at the impact location. This data was then used to find total energy (the area under the force versus deflection curve) dissipated during each test.

It should be noted that although the acceleration data was applied to the impact location, the data came from the center of gravity of the bogie. This added some error to the data, since the bogie was not perfectly rigid, causing vibrations in the bogie. Also, the bogie may have rotated during impact, causing differences in accelerations between the bogie center of mass and the bogie impact head. While these issues may affect the data, it was believed that the data was not greatly influenced by them, and as a result, the data was useful for analysis. One useful aspect of using accelerometer data was that it included influences of the post inertia on the reaction force. This is important since the post's mass would affect the results.

The accelerometer data was processed for each test in order to obtain acceleration, velocity, and displacement curves, as well as force versus deflection curves. This section discusses those results for the EDR-3 accelerometer. Although both the EDR-3 and EDR-4 data recorders were used for the tests, the current EDR-3 has a more accurate representation of the data than the existing EDR-4 unit, even with the lower sampling rate. However, for this post testing program, the two accelerometers provided similar results. Individual test results are provided in Appendix A for both the EDR-3 and EDR-4 recorders.

5.2 Individual Test Results and Discussion

The following sections discuss the dynamic behaviors and results for test nos. MNCRT-1 through MNCRT-9. However, it was not the objective of this section to draw comparisons between the posts tested but rather to identify the behaviors observed during each of the dynamic impact tests. Conclusions regarding the performance comparison of the posts are discussed in a subsequent chapter of this report.

5.2.1 Test No. MNCRT-1 – Strong-Axis (0 Degree) Impact on CRT Post

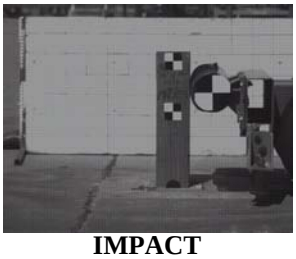

IMPACT

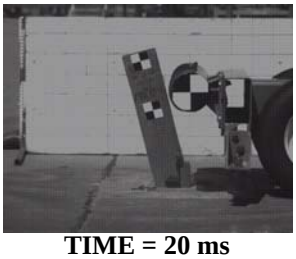

TIME = 20 ms

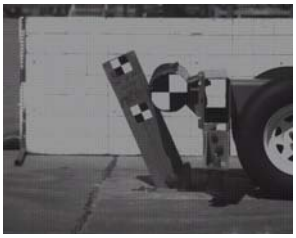

TIME = 40 ms

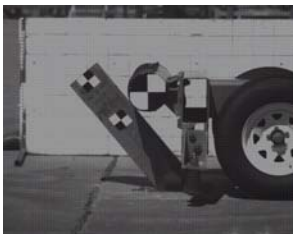

TIME = 60 ms

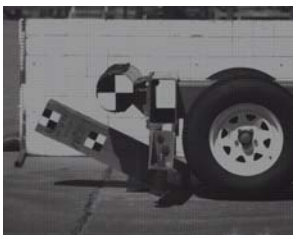

TIME = 90 ms

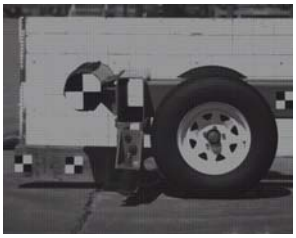

TIME = 120 ms

Test MNCRT-1 was a strong-axis impact at 0 degrees on the wood CRT post embedded in a rigid sleeve. Time-sequential photographs are shown in Figure 8. The post was observed to break at the ground level. Approximately 8 ms after impact, the wood CRT post fractured as a result of the impact and lost contact with the bogie's impact head. At approximately 34 ms, the bogie regained contact with the CRT post until losing all contact after 62 ms at a deflection of 406 mm (16.0 in).

The force versus deflection curve, as provided in Figure 9, indicated a significant initial peak in the force level, which can be attributed to inertial effects and initiating the failure of the post. After the initial peak, the wood post had fractured and absorbed little more energy, as seen in the energy versus deflection curve in Figure 10. Post-impact images of the fractured post can be seen in Figure 11.

Figure 8. Time Sequential Photographs, Test MNCRT-1

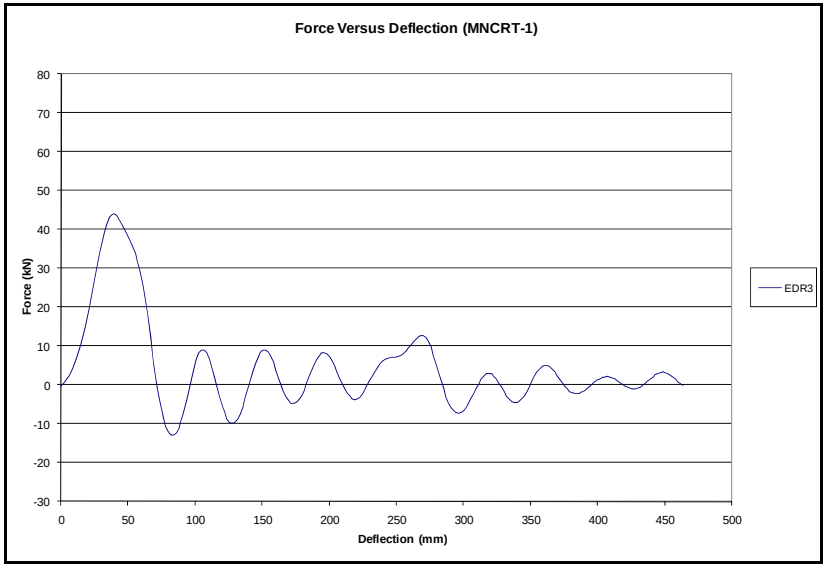

Figure 9a. Force versus Deflection Curve for MNCRT-1 – Metric

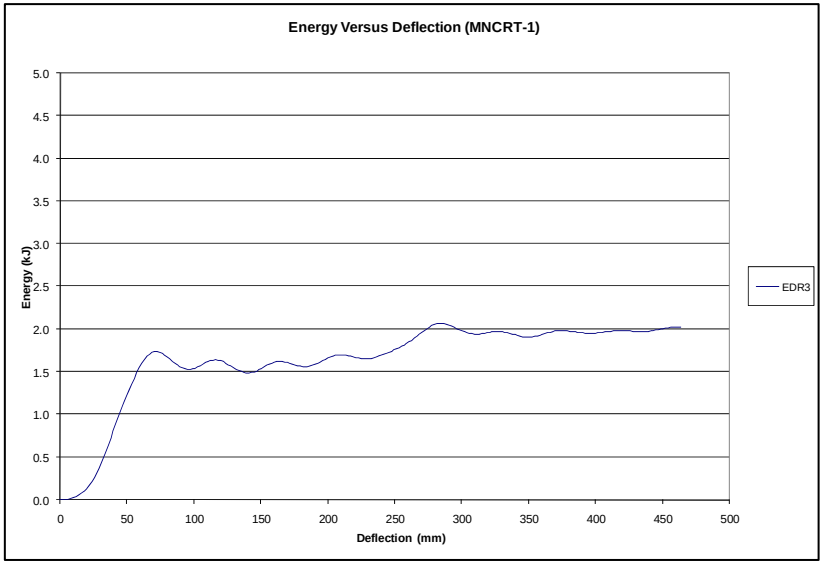

Figure 10a. Energy versus Deflection Curve for MNCRT-1 – Metric

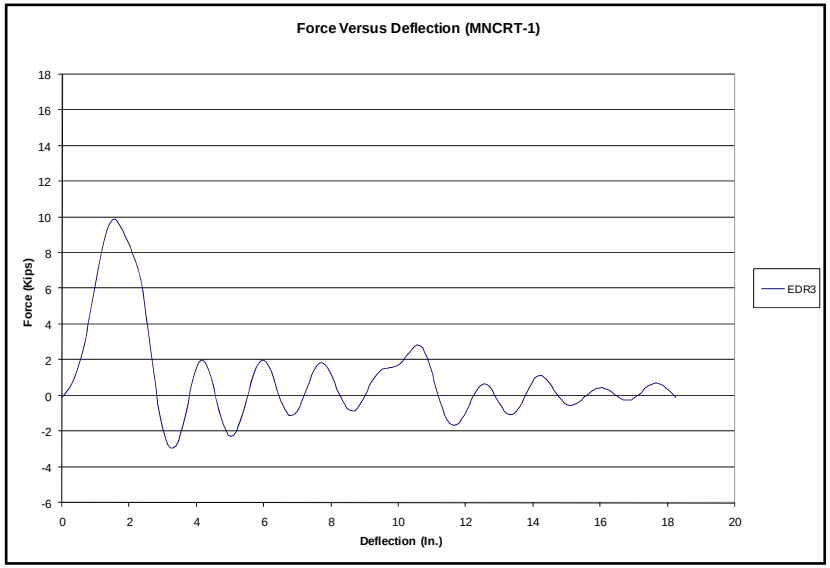

Figure 9b. Force versus Deflection Curve for MNCRT-1 – English

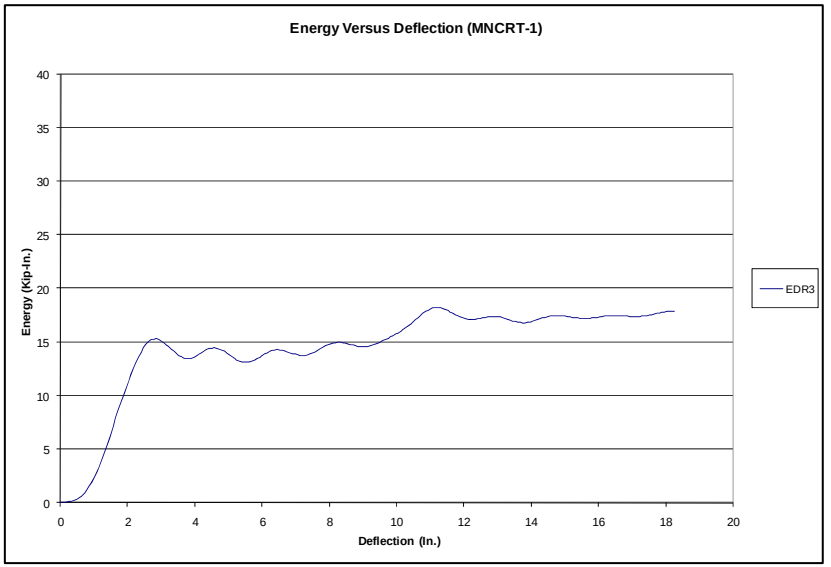

Figure 10b. Energy versus Deflection Curve for MNCRT-1 – English

Figure 11. Post-Impact Images of MNCRT-1

5.2.2 Test No. MNCRT-2 – Strong-Axis (0 Degree) Impact on CRT Post

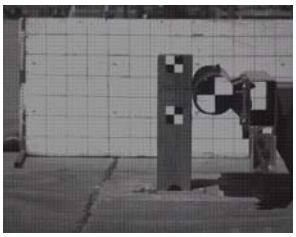

IMPACT

TIME = 20 ms

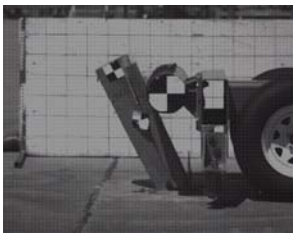

TIME = 40 ms

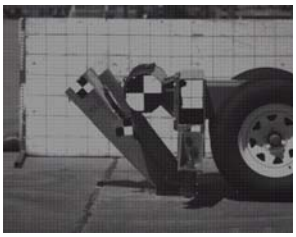

TIME = 60 ms

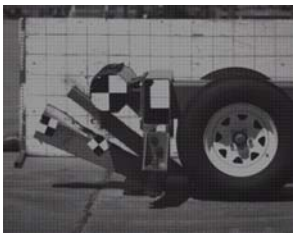

TIME = 90 ms

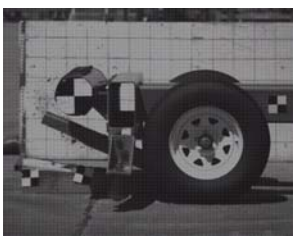

TIME = 120 ms

Figure 12. Time Sequential Photographs, Test MNCRT-2

Test MNCRT-2 was also a strong-axis impact at 0 degrees on the wood CRT post embedded in a rigid sleeve. Time-sequential photographs are shown in Figure 12. Even though this test repeated test MNCRT-1, the wood post exhibited different behaviors by splitting down the middle before fracturing at the breakaway hole. Also, when the post was impacted, it did not completely fracture immediately like in test MNCRT-1. These differences can be attributed to differences in the wood, especially with no knots present in the MNCRT-2 post. With the combination of the wood splitting down the middle of the post and the wood fracturing near the breakaway hole, the CRT post lost strength and broke into two pieces, eventually losing all contact after 110 ms.

Examination of the force versus deflection curve, as seen in Figure 13, indicated an initial large peak followed by a region of fairly uniform force levels. These forces can be attributed to the initial inertial effects and fracturing of the wood near the breakaway hole, respectively. The force level then tapered off for the duration of the test, and the post absorbed little more energy, as illustrated in the energy versus deflection curve in Figure 14. Post-impact images of the fractured post can be seen in Figure 15.

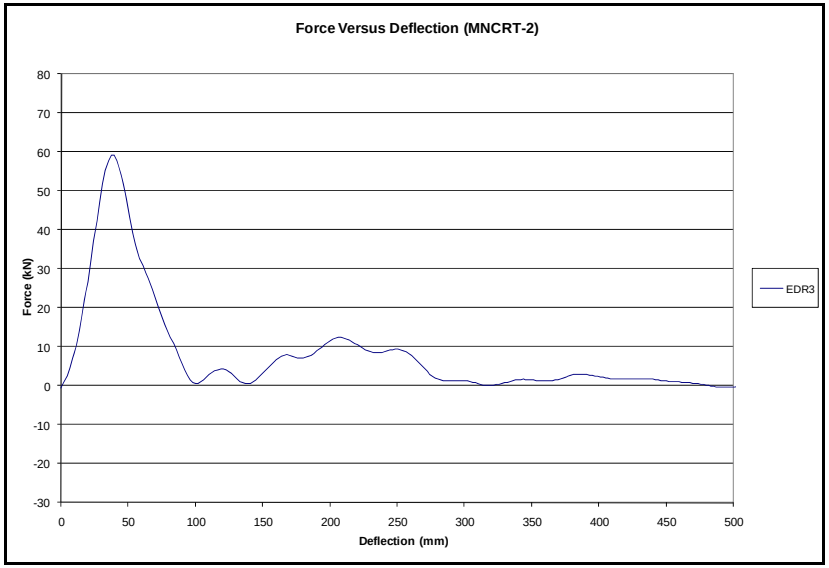

Figure 13a. Force versus Deflection Curve for MNCRT-2 – Metric

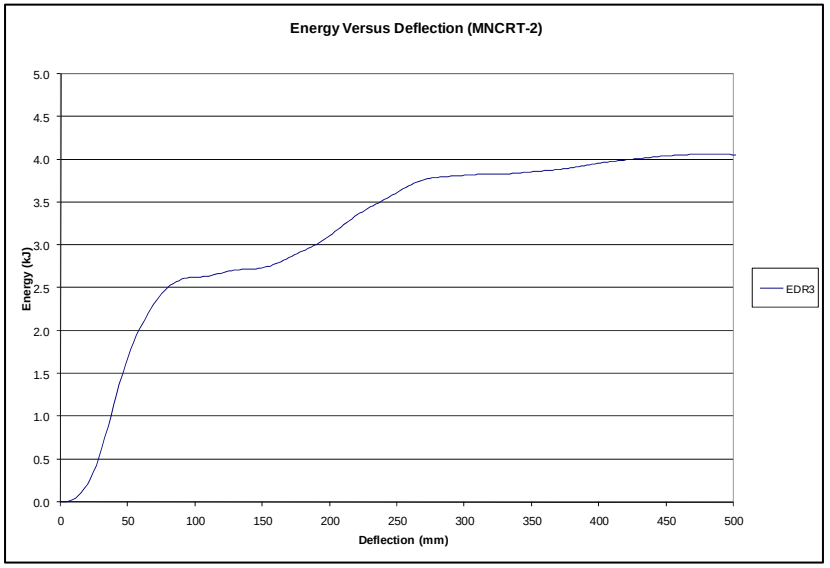

Figure 14a. Energy versus Deflection Curve for MNCRT-2 – Metric

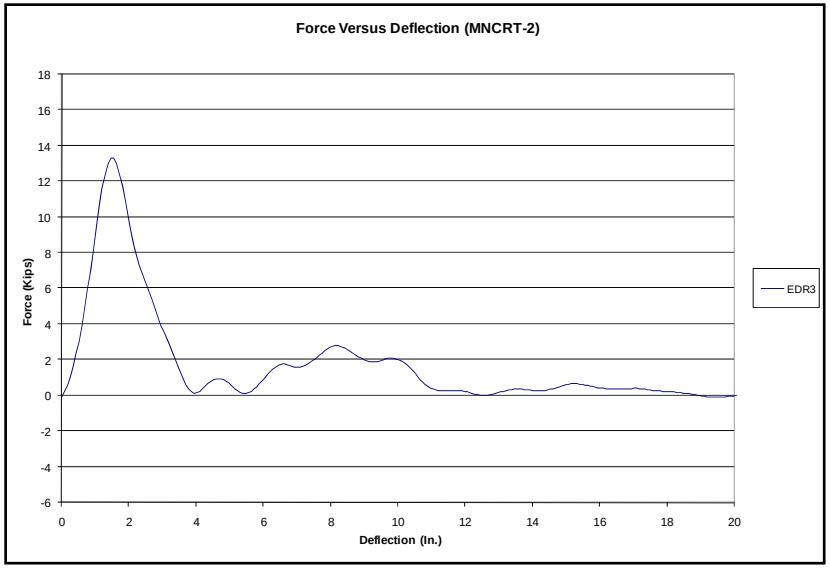

Figure 13b. Force versus Deflection Curve for MNCRT-2 – English

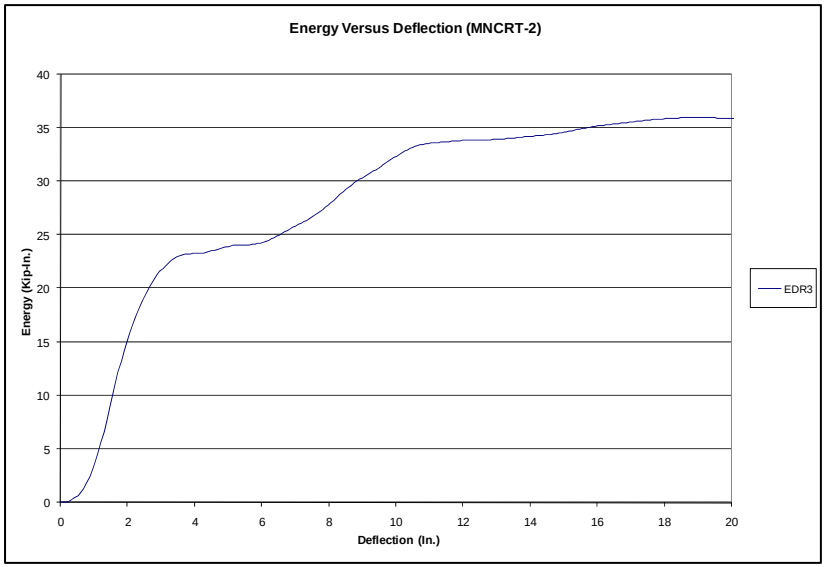

Figure 14b. Energy versus Deflection Curve for MNCRT-2 – English

Figure 15. Post-Impact Images of MNCRT-2

5.2.3 Test No. MNCRT-3 – Strong-Axis (0 Degree) Impact on CRT Post

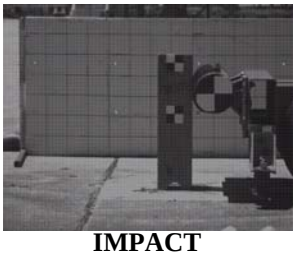

IMPACT

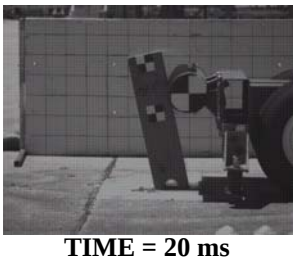

TIME = 20 ms

TIME = 40 ms

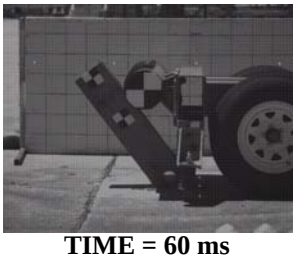

TIME = 60 ms

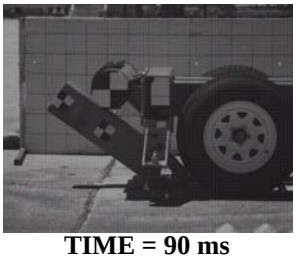

TIME = 90 ms

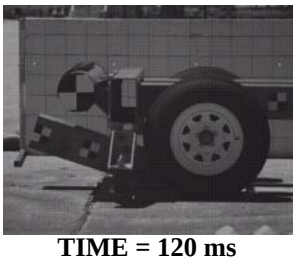

TIME = 120 ms

Test MNCRT-3 was the final test of a strong-axis impact at 0 degrees on the wood CRT post embedded in a rigid sleeve. Time-sequential photographs are shown in Figure 16. The post began to fracture at ground level near the breakaway hole almost immediately. The CRT post continued to rotate and lose strength, while more of the wood fractured. Eventually, the impact cylinder lost all contact with the post at 94 ms, resulting in the termination of the test.

The force versus deflection profile, as shown in Figure 17, indicated a similar behavior to that of test MNCRT-1. However, the magnitude of the initial peak was not as high, which can be attributed to the differences in the properties of the wood. Following the initial portion of the impact, the force level then tapered off in a comparable magnitude and duration to test MNCRT-1 due to their similar failure mode. In both tests, the wood only provided resistance in the initial inertial effects, which caused the wood to fracture and provide little more resistance, as shown in the energy versus deflection curve in Figure 18. Post-impact images of the fractured post can be seen in Figure 19.

Figure 16. Time Sequential Photographs, Test MNCRT-3

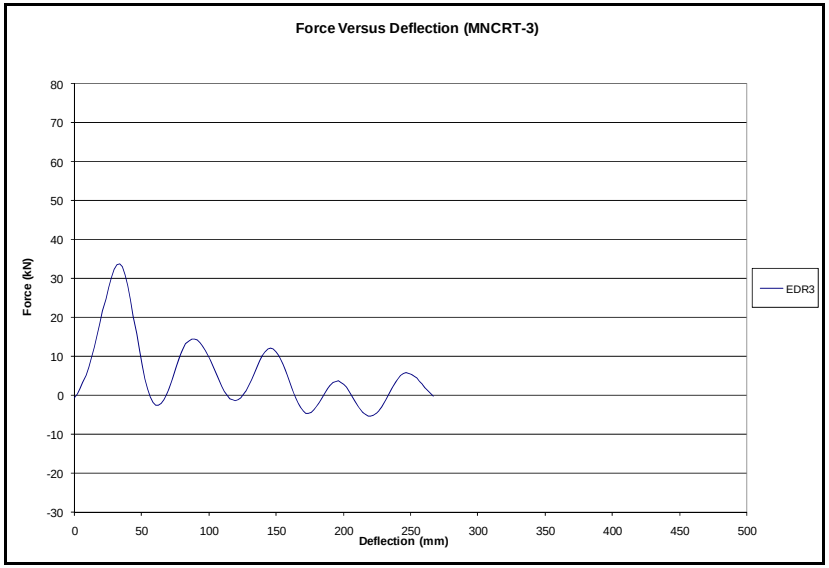

Figure 17a. Force versus Deflection Curve for MNCRT-3 – Metric

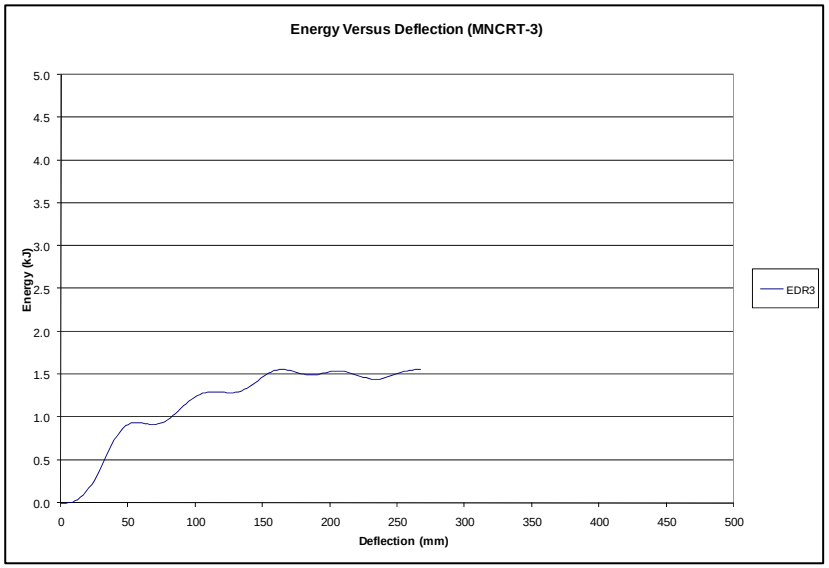

Figure 18a. Energy versus Deflection Curve for MNCRT-3 – Metric

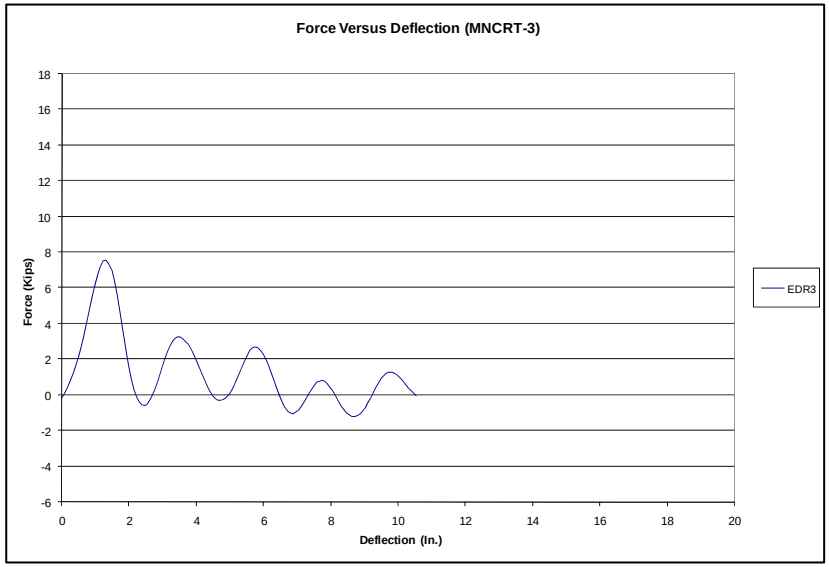

Figure 17b. Force versus Deflection Curve for MNCRT-3 – English

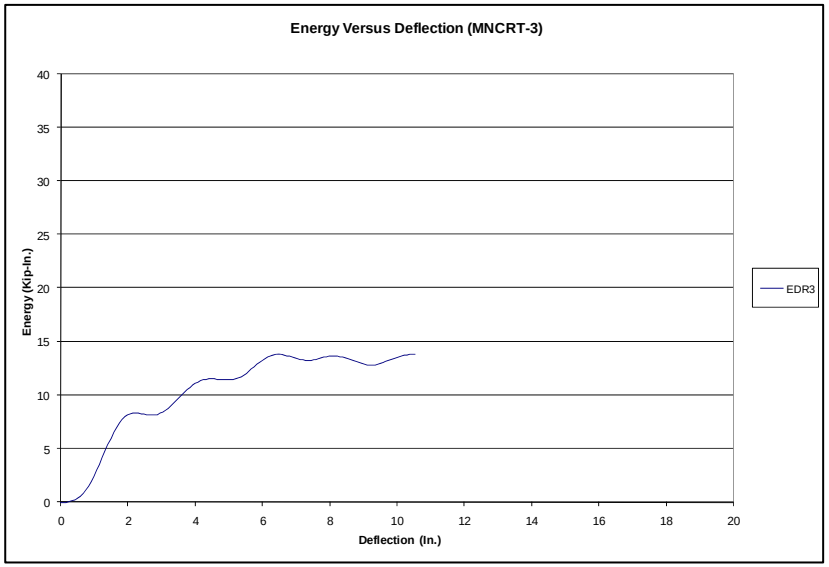

Figure 18b. Energy versus Deflection Curve for MNCRT-3 – English

Figure 19. Post-Impact Images of MNCRT-3

5.2.4 Test No. MNCRT-4 – Weak-Axis (90 Degree) Impact on CRT Post

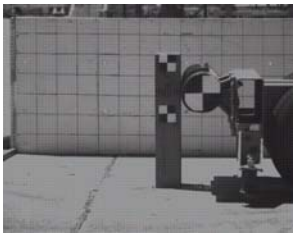

IMPACT

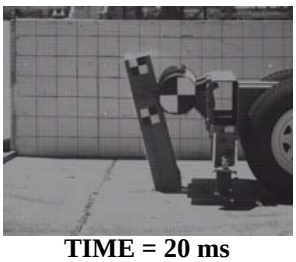

TIME = 20 ms

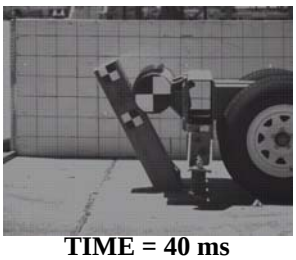

TIME = 40 ms

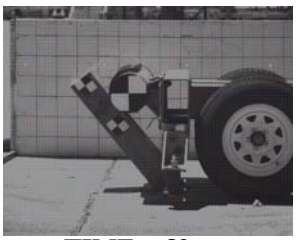

TIME = 60 ms

TIME = 90 ms

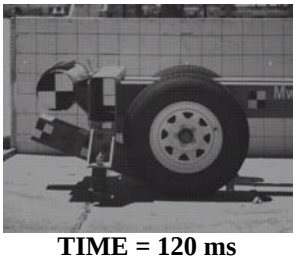

TIME = 120 ms

Test MNCRT-4 was a weak-axis impact at 90 degrees on the 152 mm x 203 mm (6 in. x 8 in.) wood CRT post embedded in a rigid sleeve. Time-sequential photographs are shown in Figure 20. Within 8 ms, the post began to fracture near the breakaway hole. The wood post continued to fracture near the breakaway hole as it was deflected by the bogie's impact head. As the post fractured, it lost more strength and eventually lost contact with the post at 96 ms.

The force versus deflection curve, as seen in Figure 21, shows a significant initial peak in the force level, which can be traced from the inertial effects and initiating the failure of the post. After the initial peak, the wood post had already begun to fracture, and as a result, it does not provide much more resistance for the duration of the test, as seen in the energy versus deflection curve in Figure 22. Post-impact images of the fractured post can be seen in Figure 23.

Figure 20. Time Sequential Photographs, Test MNCRT-4

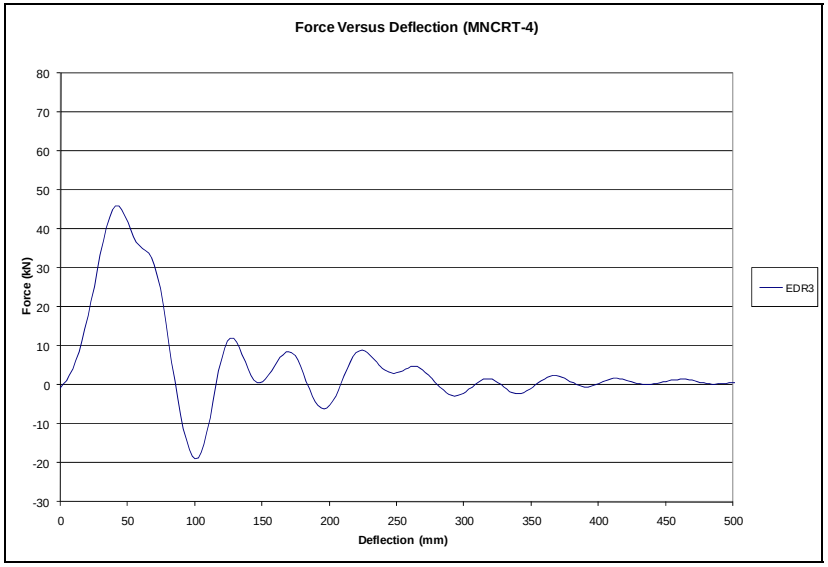

Figure 21a. Force versus Deflection Curve for MNCRT-4 – Metric

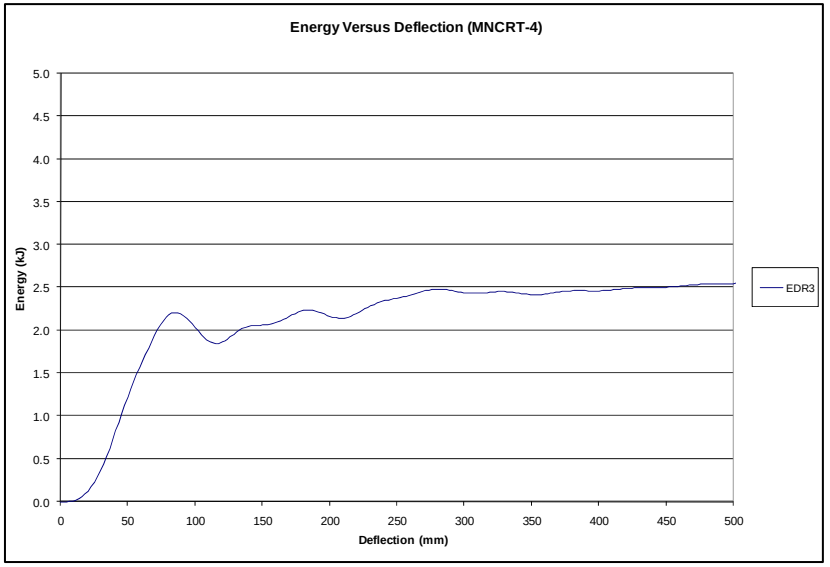

Figure 22a. Energy versus Deflection Curve for MNCRT-4 – Metric

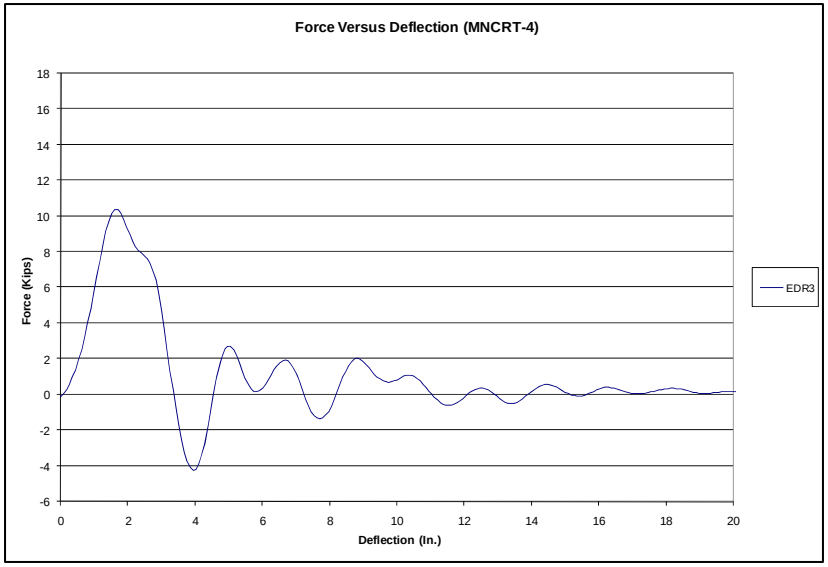

Figure 21b. Force versus Deflection Curve for MNCRT-4 – English

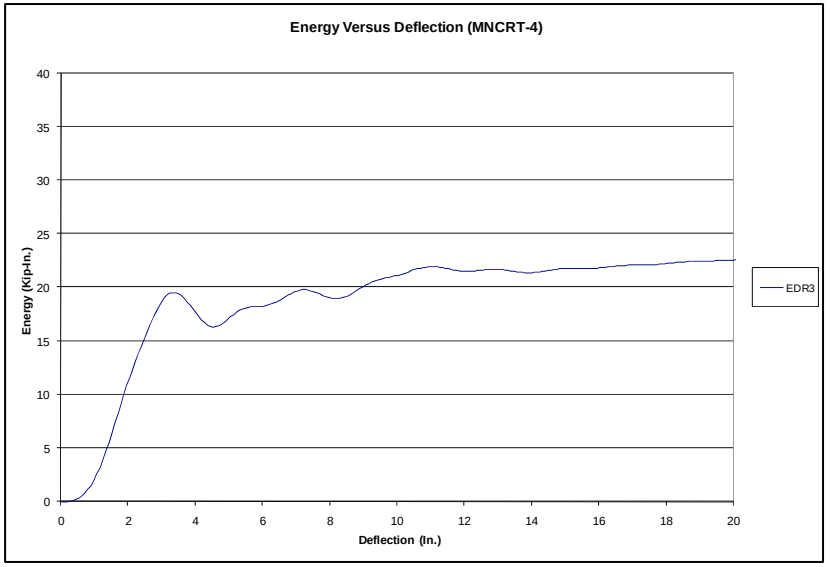

Figure 22b. Energy versus Deflection Curve for MNCRT-4 – English

Figure 23. Post-Impact Images of MNCRT-4

5.2.5 Test No. MNCRT-5 – Weak-Axis (90 Degree) Impact on CRT Post

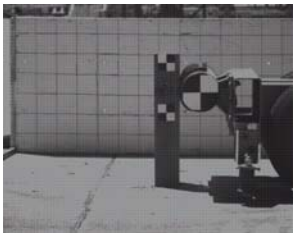

IMPACT

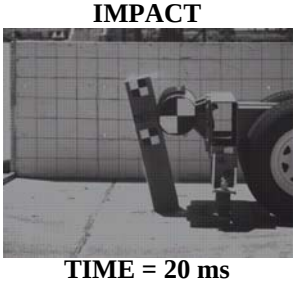

TIME = 20 ms

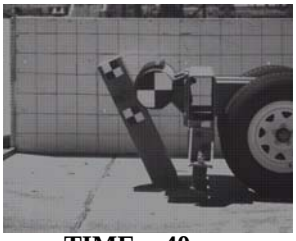

TIME = 40 ms

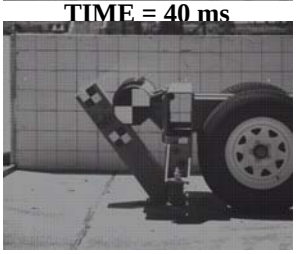

TIME = 60 ms

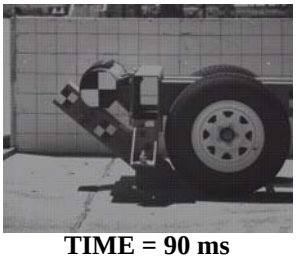

TIME = 90 ms

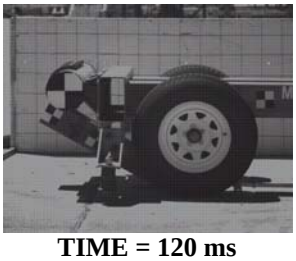

TIME = 120 ms

Test MNCRT-5 was a weak-axis impact at 90 degrees on the wood CRT post embedded in a rigid sleeve. Time-sequential photographs are shown in Figure 24. The observed dynamic behavior of the post was very similar to test MNCRT-4, and a similar explanation is offered. Almost instantly, the wood post began to fracture. It continued to fracture and rotate down until it lost contact with the bogie's impact head at 146 ms.

Examination of the force versus deflection curve in Figure 25 and the energy versus deflection curve in Figure 26 both indicated similar behavior to that observed in test MNCRT-4. Both tests had a large initial peak in the force level. After the initial peak, both CRT posts had already begun to fracture. Thus, there was little resistance from the wood posts even though the bogie head was still in contact with the post. Post-impact images of the fractured post can be seen in Figure 27.

Figure 24. Time Sequential Photographs, Test MNCRT-5

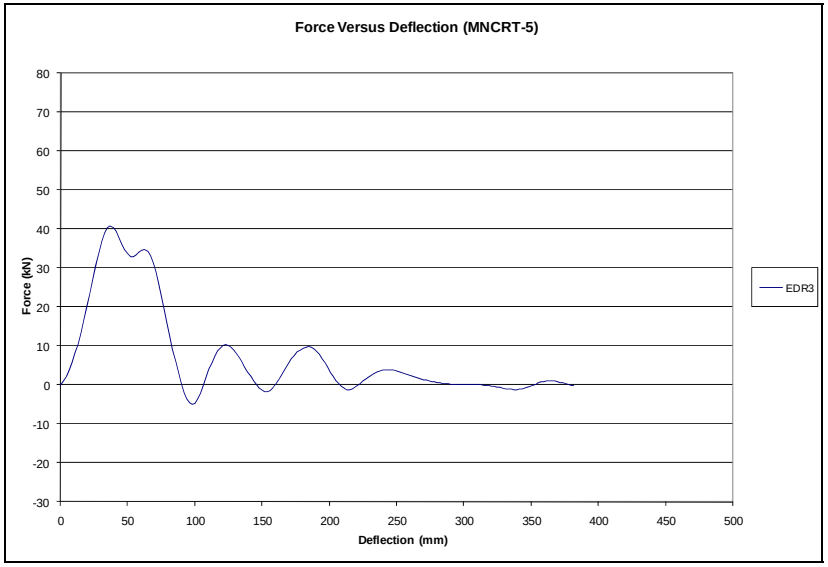

Figure 25a. Force versus Deflection Curve for MNCRT-5 – Metric

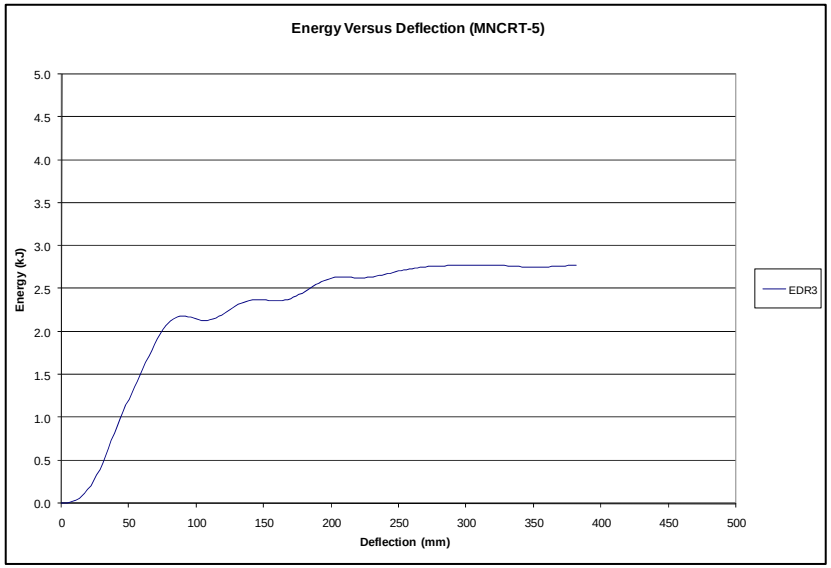

Figure 26a. Energy versus Deflection Curve for MNCRT-5 – Metric

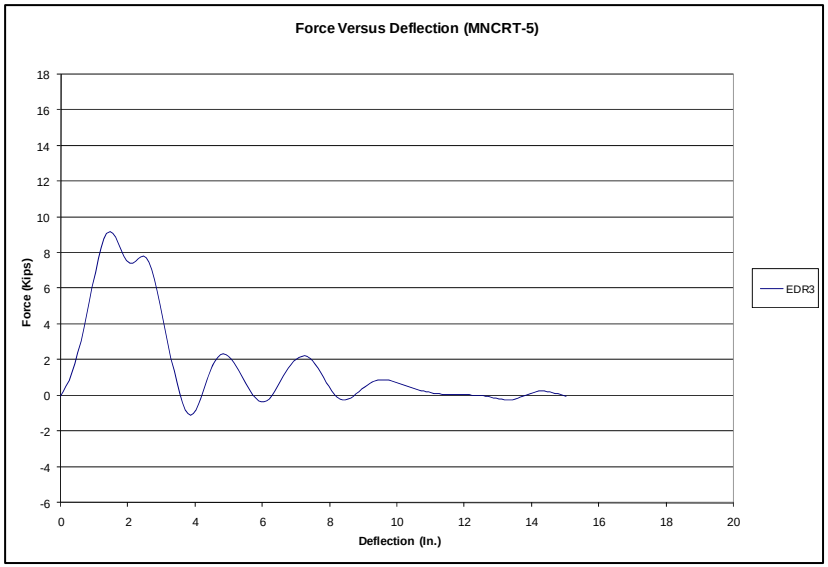

Figure 25b. Force versus Deflection Curve for MNCRT-5 – English

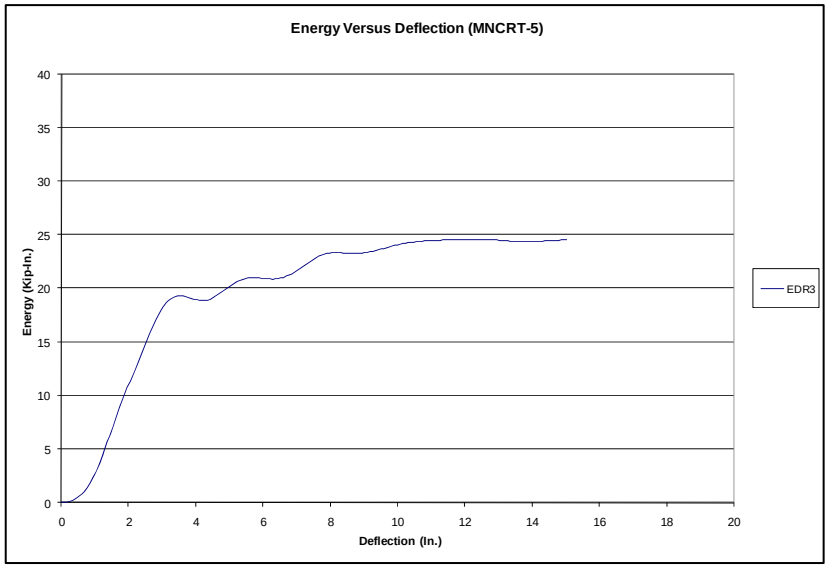

Figure 26b. Energy versus Deflection Curve for MNCRT-5 – English

Figure 27. Post-Impact Images of MNCRT-5

5.2.6 Test No. MNCRT-6 – Weak-Axis (90 Degree) Impact on CRT Post

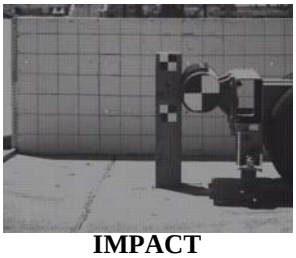

IMPACT

TIME = 20 ms

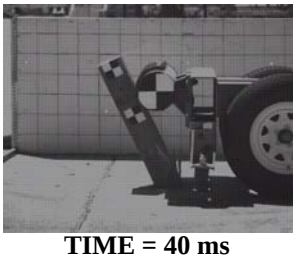

TIME = 40 ms

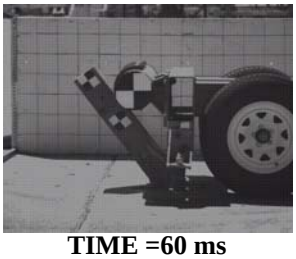

TIME =60 ms

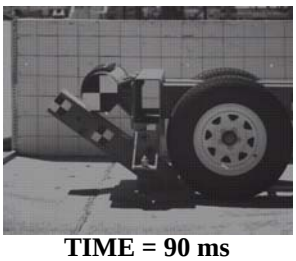

TIME = 90 ms

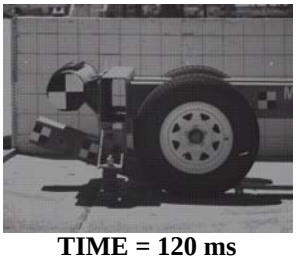

TIME = 120 ms

Test MNCRT-6 was also a weak-axis impact at 90 degrees on the wood CRT post embedded in a rigid sleeve. Time-sequential photographs are shown in Figure 28. The observed dynamic behavior of the post was very similar to tests MNCRT-4 and MNCRT-5. The wood CRT post immediately began to fracture near the breakaway post. However, the impact cylinder did not lose contact with the post until after 88 ms.

The force versus deflection curve in Figure 29 and the energy versus deflection curve in Figure 30 both indicated similar behavior to the previous two tests performed at 90 degrees. When compared with tests MNCRT-4 and MNCRT-5, the wood post in test MNCRT-6 has comparable duration and behavior. However, the only difference was in the magnitude of the force and energy levels. In test MNCRT-6, the wood post has lower force and energy levels than observed in either test MNCRT-4 or test MNCRT-5. This difference can be attributed to the differences in the properties of the wood. Post-impact images of the fractured post can be seen in Figure 31.

Figure 28. Time Sequential Photographs, Test MNCRT-6

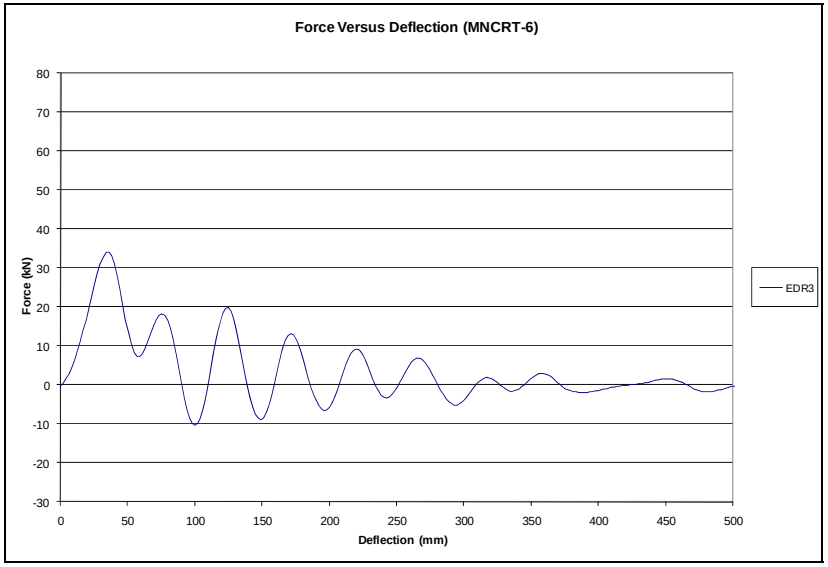

Figure 29a. Force versus Deflection Curve for MNCRT-6 – Metric

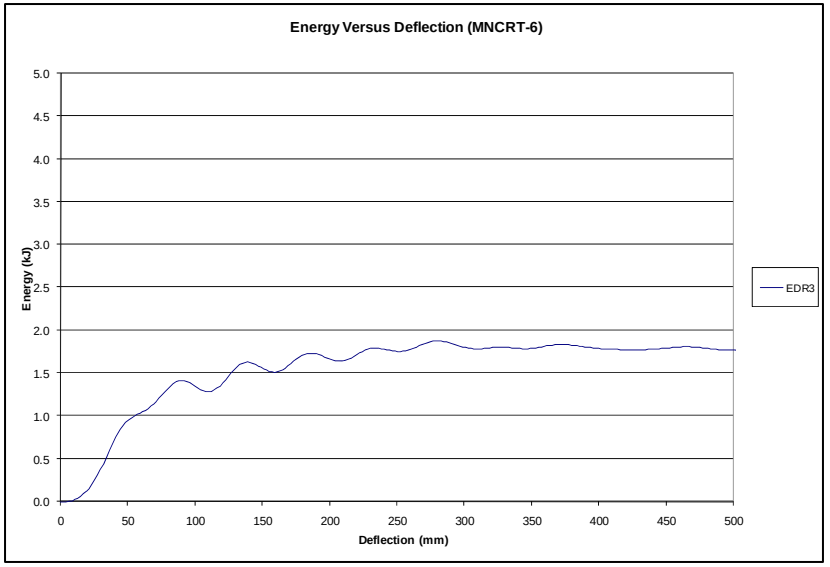

Figure 30a. Energy versus Deflection Curve for MNCRT-6 – Metric

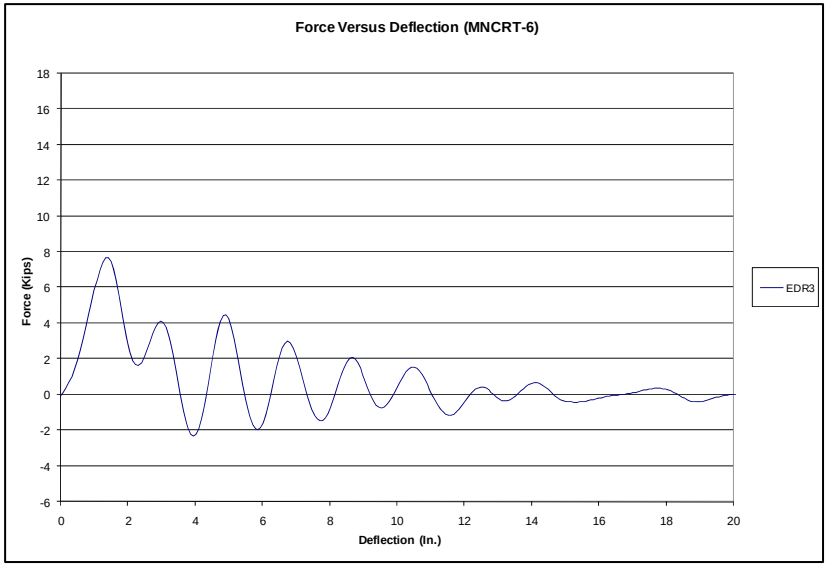

Figure 29b. Force versus Deflection Curve for MNCRT-6 – English

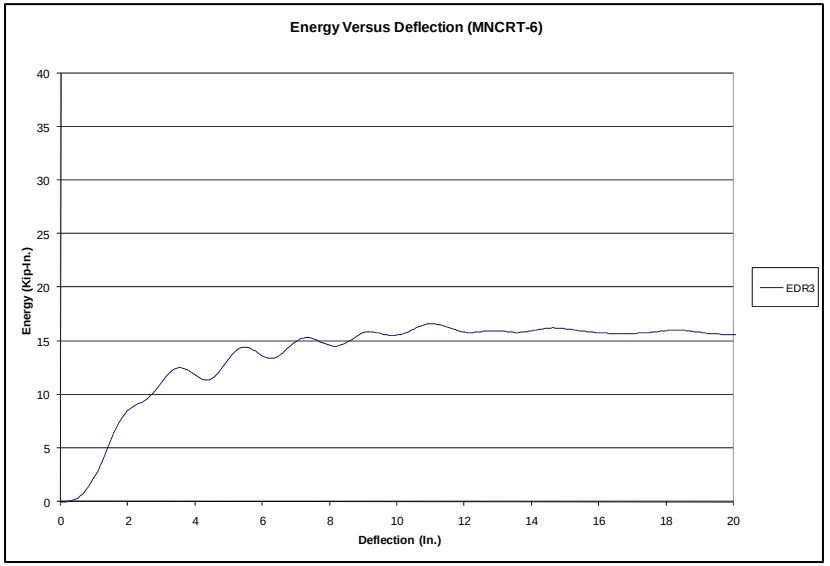

Figure 30b. Energy versus Deflection Curve for MNCRT-6 – English

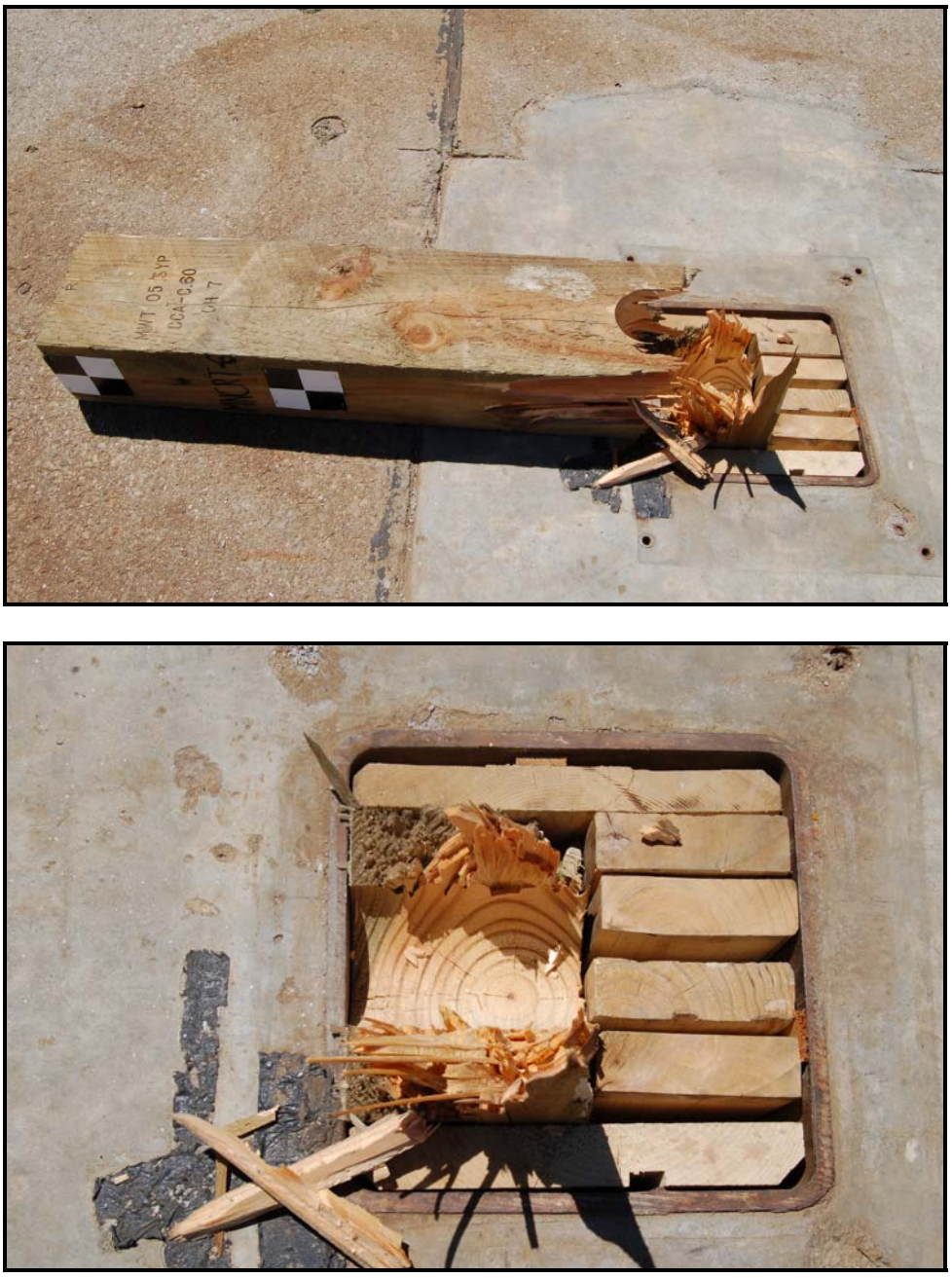

Figure 31. Post-Impact Images of MNCRT-6

5.2.7 Test No. MNCRT-7 – Diagonal-Axis (45 Degree) Impact on CRT Post

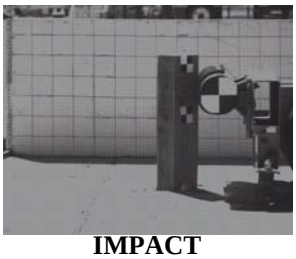

IMPACT

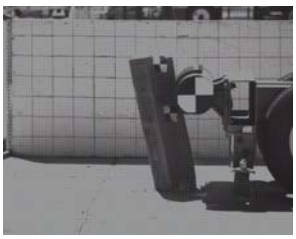

TIME = 20 ms

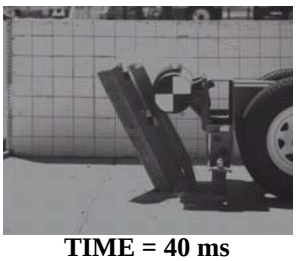

TIME = 40 ms

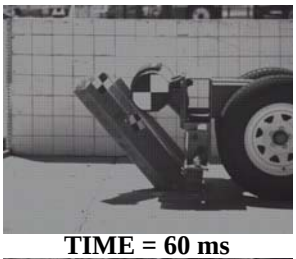

TIME = 60 ms

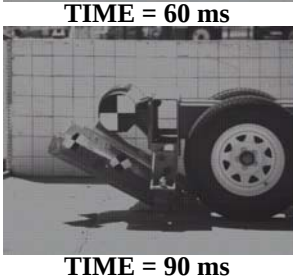

TIME = 90 ms

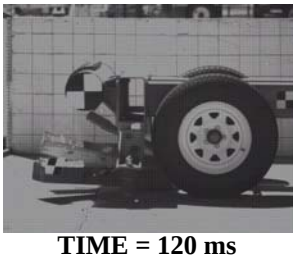

TIME = 120 ms

Test MNCRT-7 was a diagonal-axis impact at 45 degrees on the wood CRT post embedded in a rigid sleeve. Time-sequential photographs are shown in Figure 32. For the first 8 ms, it was observed that the post shifted in the rigid sleeve. This movement was unexpected and created some error as the wood post was not properly held rigidly in place. However, this fixture problem was deemed minor, since only a small amount of force was required to move the post. The fixture problem only added some inconsistency to the tests. After shifting in the rigid sleeve, the post began to fracture near ground level and split near the corner of the wood post. The post finally broke into three pieces and was in contact with the bogie's head until 112 ms.

Examination of the force versus deflection curve in Figure 33 shows the fixture problem with the initial spike in the force level. The second peak corresponds to the inertial effects of the wood post and initiating the failure of the post. After the first two peaks, the force levels subsided toward zero, as the post had already fractured and provided little resistance. The energy versus deflection curve can be seen in Figure 34, and post-impact images of the fractured post can be seen in Figure 35.

Figure 32. Time Sequential Photographs, Test MNCRT-7

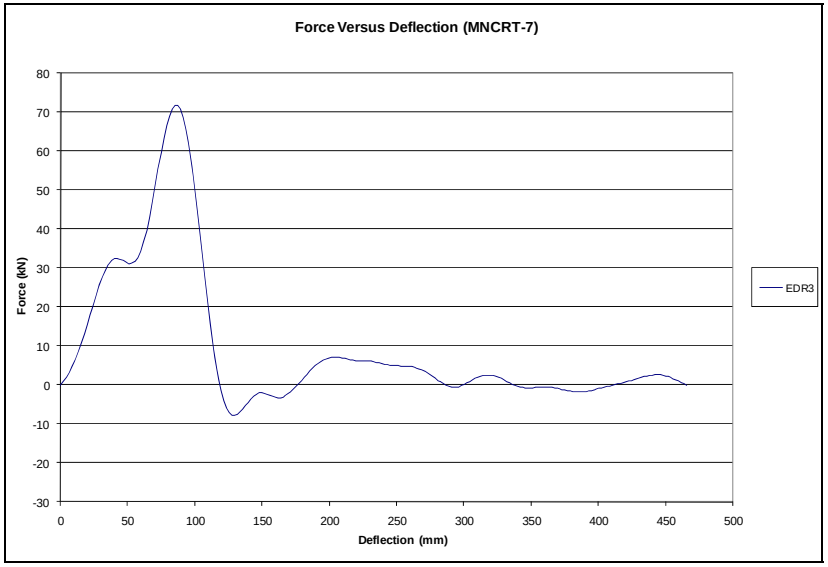

Figure 33a. Force versus Deflection Curve for MNCRT-7 – Metric

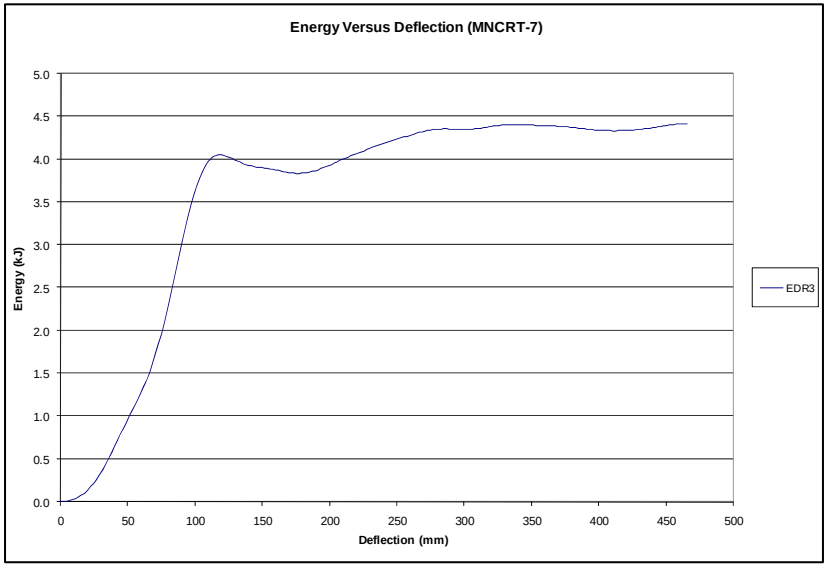

Figure 34a. Energy versus Deflection Curve for MNCRT-7 – Metric

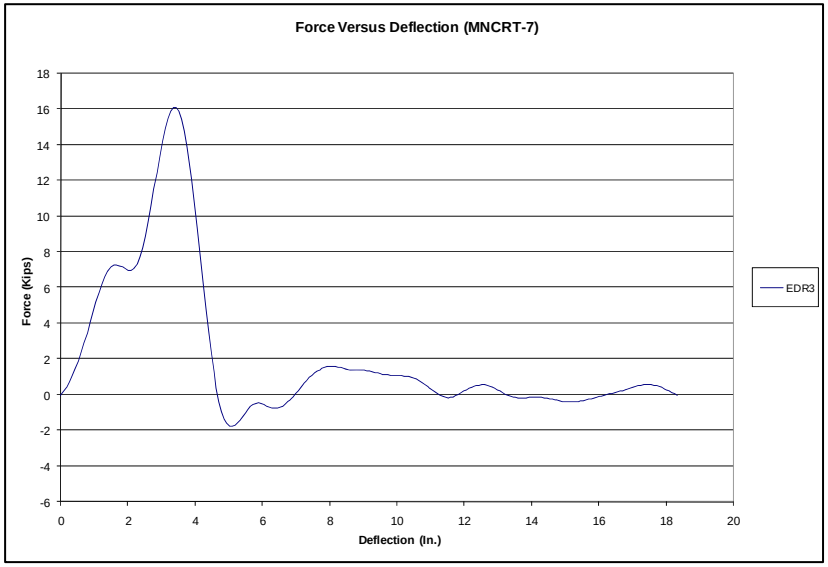

Figure 33b. Force versus Deflection Curve for MNCRT-7 – English

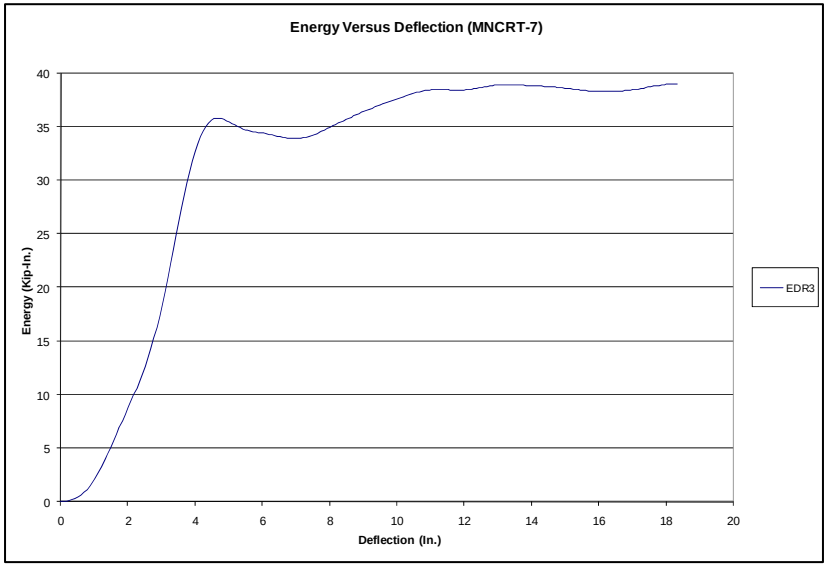

Figure 34b. Energy versus Deflection Curve for MNCRT-7 – English

Figure 35. Post-Impact Images of MNCRT-7

5.2.8 Test No. MNCRT-8 – Diagonal-Axis (45 Degree) Impact on CRT Post

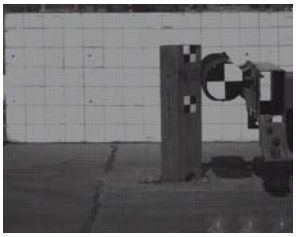

IMPACT

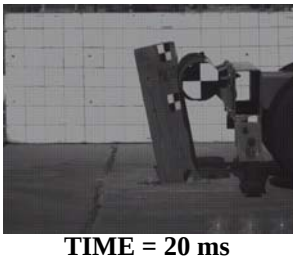

TIME = 20 ms

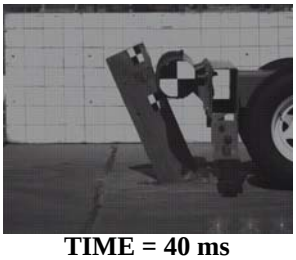

TIME = 40 ms

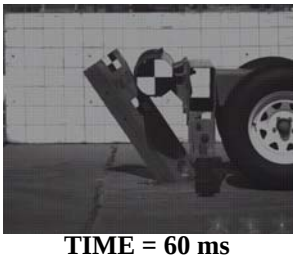

TIME = 60 ms

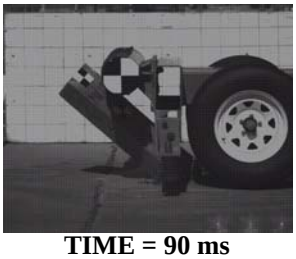

TIME = 90 ms

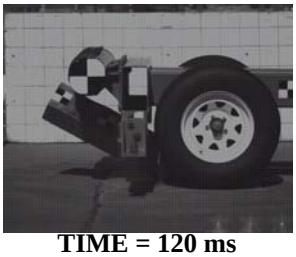

TIME = 120 ms

Test MNCRT-8 was also a diagonal-axis impact at 45 degrees on the wood CRT post embedded in a rigid sleeve. Time-sequential photographs are shown in Figure 36. The post was observed to move in the rigid sleeve for the first 6 ms. Even though this movement was another fixture error, it again was small enough to be irrelevant. Also, while the post shifted in the rigid sleeve, it began to rotate up, so that the breakaway hole moved above ground level. As a result, the post did not begin to fracture until at least 34 ms after impact. This behavior differed from previous tests, where the posts fractured immediately, and could be responsible for creating higher resistance than for a properly fixed post. After the initial behavior, the post did begin to fracture and eventually lost contact with the bogie at 128 ms.

The force versus deflection curve in Figure 37 and the energy versus deflection curve in Figure 38 both indicate similar behavior to test MNCRT-7. The only difference was in the magnitude of the force and energy levels. In test MNCRT-8, the post broke away in one piece near the breakaway hole. For test MNCRT-7, the post not only broke away near the breakaway hole but also broke into three pieces, which absorbed higher force and energy levels. Post-impact images of the fractured post can be seen in Figure 39.

Figure 36. Time Sequential Photographs, Test MNCRT-8

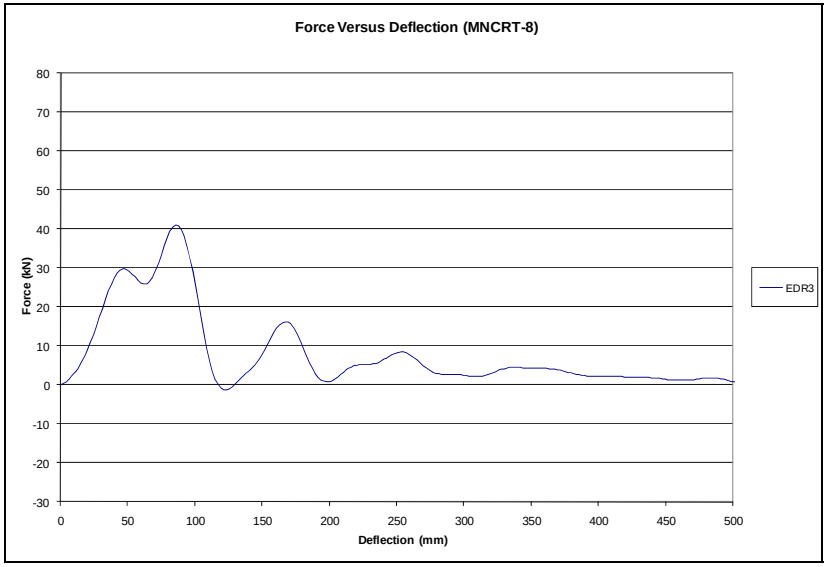

Figure 37a. Force versus Deflection Curve for MNCRT-8 – Metric

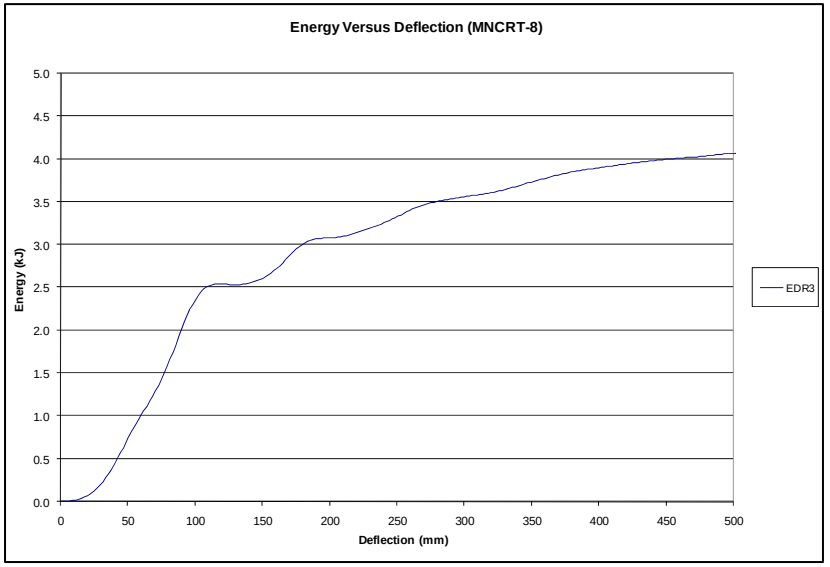

Figure 38a. Energy versus Deflection Curve for MNCRT-8 – Metric

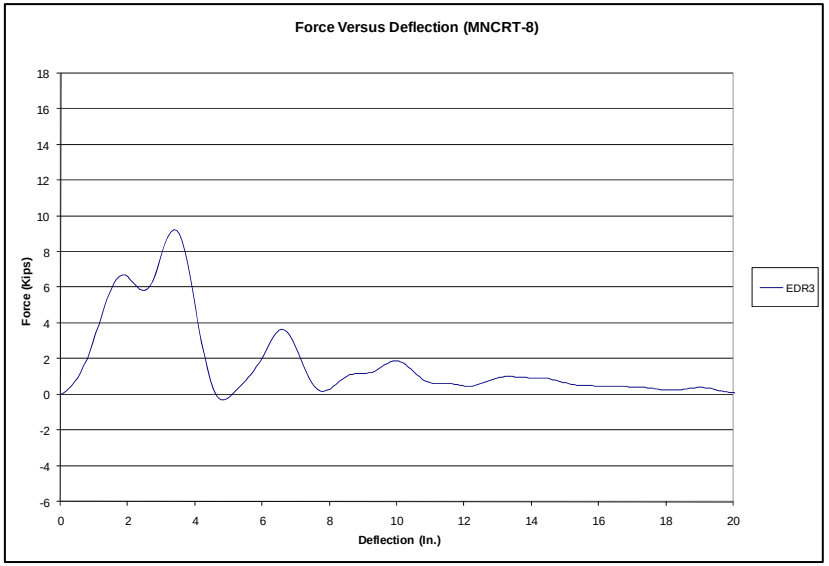

Figure 37b. Force versus Deflection Curve for MNCRT-8 – English

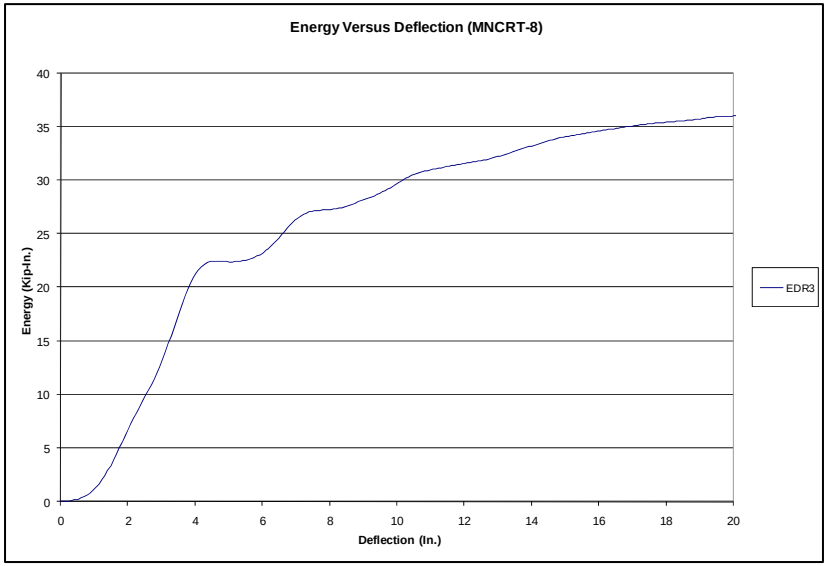

Figure 38b. Energy versus Deflection Curve for MNCRT-8 – English

Figure 39. Post-Impact Image of MNCRT-8

5.2.9 Test No. MNCRT-9 – Diagonal-Axis (45 Degree) Impact on CRT Post

IMPACT

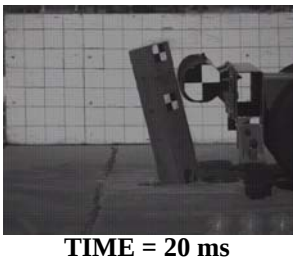

TIME = 20 ms

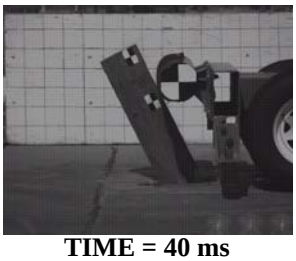

TIME = 40 ms

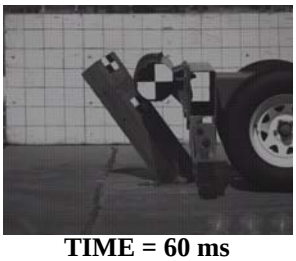

TIME = 60 ms

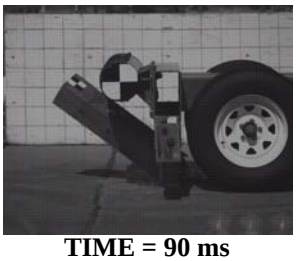

TIME = 90 ms

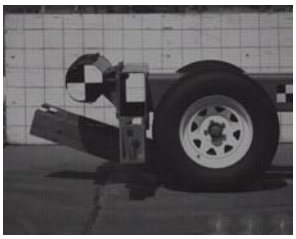

TIME = 120 ms

Test MNCRT-9 was the last diagonal-axis impact at 45 degrees on the wood CRT post embedded in a rigid sleeve. Time-sequential photographs are shown in Figure 40. Similar to tests MNCRT-7 and MNCRT-8, this test also had a fixture issue, but it was also deemed a minor concern, only creating some inconsistency. In this test, the post began to fracture immediately. The post lost contact with the bogie head at 16 ms until 36 ms. Then, the bogie continued to fracture and rotate the wood post until all contact was lost at 94 ms.

The force versus deflection curve in Figure 41 and the energy versus deflection curve in Figure 42 indicate both the fixture issue and the low strength of the wood CRT post. Similar to tests MNCRT-7 and MNCRT-8, the first peak in the force level illustrates the fixture issue. However, the second peak for this test was rather small and showed how easily the post fractured. After the initial peaks, the post had lost its strength and did not provide much more resistance for the duration of the test. Post-impact images of the fractured post can be seen in Figure 43.

Figure 40. Time Sequential Photographs, Test MNCRT-9

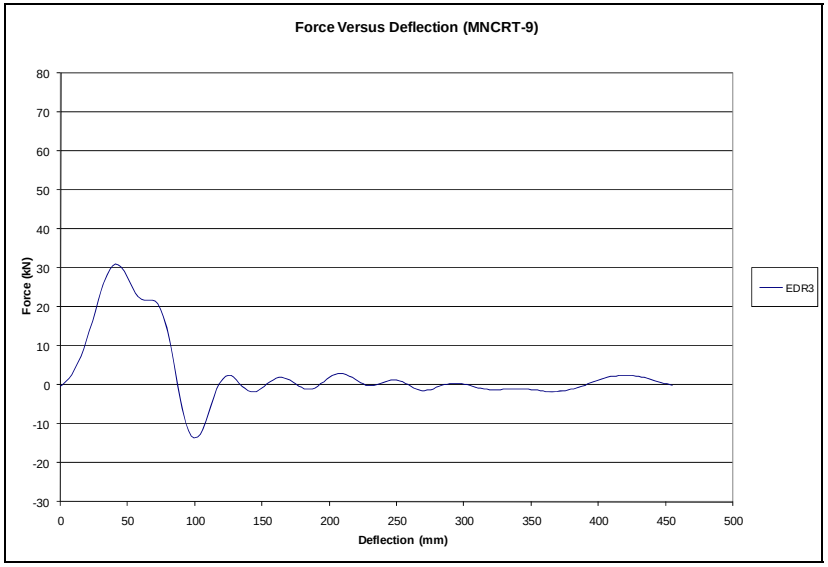

Figure 41a. Force versus Deflection Curve for MNCRT-9 – Metric

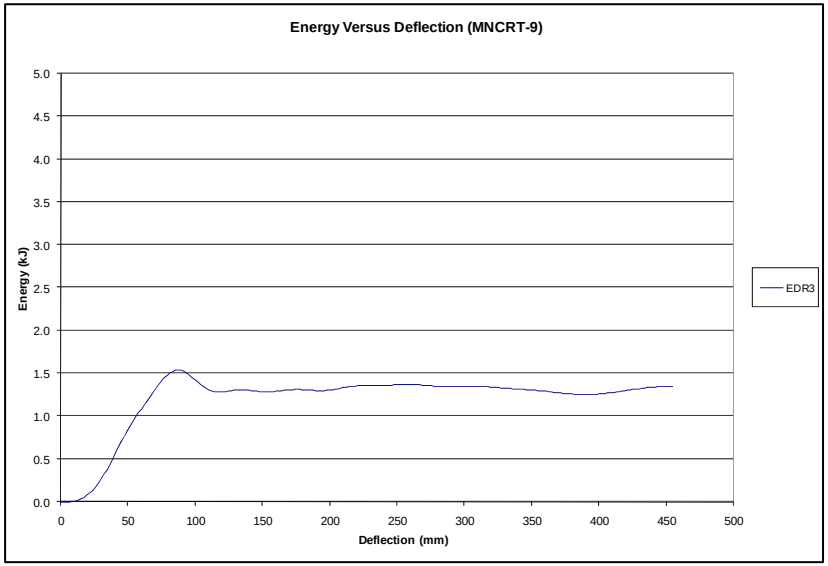

Figure 42a. Energy versus Deflection Curve for MNCRT-9 – Metric

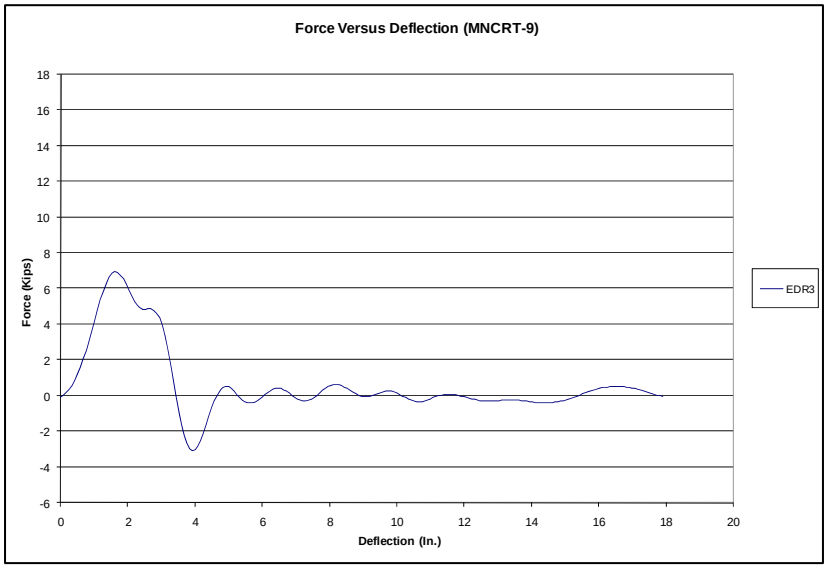

Figure 41b. Force versus Deflection Curve for MNCRT-9 – English

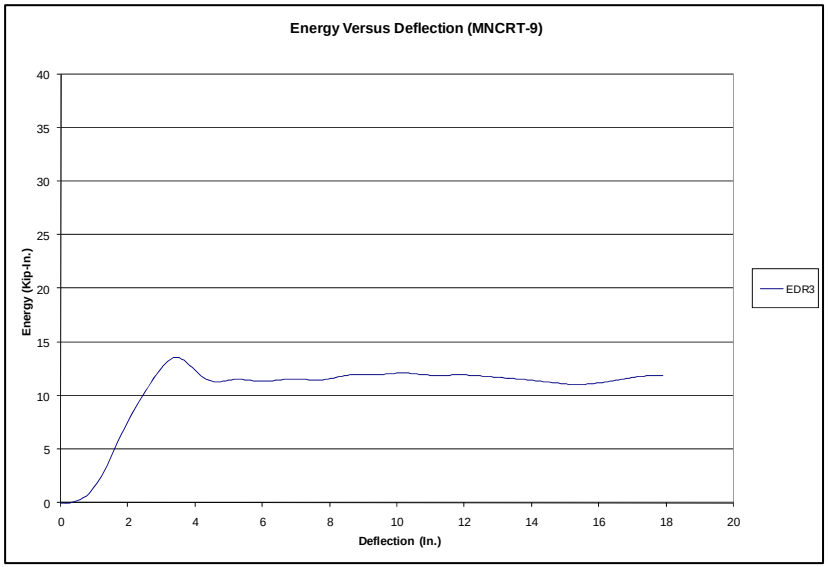

Figure 42b. Energy versus Deflection Curve for MNCRT-9 – English

Figure 43. Post-Impact Images of MNCRT-9

5.3 Force Discussion

The force levels observed during an impact are of significant interest in the design of the post. For all nine bogie tests, the CRT posts exhibited an initial peak in the force level due to the inertial effects and initiating the failure of the post near the ground line at the upper breakaway hole. After the initial peak in the force level, the CRT wood posts had fractured and had lost most of their strength, so the force level decreased toward zero. Although there was a visible trend of an initial peak force for all nine bogie tests, the angle for the dynamic impacts on CRT wood posts greatly affected the observed force levels. Therefore, it was desirable to compare the force levels during the dynamic impact events at the three different angles. The data presented in this section is grouped according to impact angle and provides insights into the properties of the CRT post at the three different impact orientations.

5.3.1 Force Results for Test Nos. MNCRT-1, MNCRT-2, and MNCRT-3

The first three bogie tests were performed on the strong-axis of the CRT wood posts. The force summaries for the three tests are given in Table 7, and the force versus displacement curve comparing the three tests is shown in Figure 44. For all three tests, the initial peak force occurred quickly at a similar displacement, averaging 36.9 mm (1.45 in.). The peak force levels were also similar, ranging from 33.72 kN (7.58 kips) to 59.21 kN (13.31 kips). Differences in the peak force levels can be attributed to variation in the wood properties of the posts. The post in test MNCRT-2 had no knots, while the other two posts in tests MNCRT-1 and MNCRT-3 had several knots that significantly reduced the strength of the posts.

Table 7a. Peak Force Results for MNCRT-1, MNCRT-2, and MNCRT-3 – Metric

Test No.	Impact Velocity (m/s)	Impact Angle (degrees)	Initial Peak Force	
			Displacement (mm)	Force (kN)
MNCRT-1	6.44	0	39.9	44.08
MNCRT-2	7.11	0	37. 3	59.21
MNCRT-3	6.76	0	33.5	33.72
Average	6.77	0	36.9	45.67

Table 7b. Peak Force Results for MNCRT-1, MNCRT-2, and MNCRT-3 – English

Test No.	Impact Velocity (mph)	Impact Angle (degrees)	Initial Peak Force	
			Displacement (in.)	Force (kips)
MNCRT-1	14.40	0	1.57	9.91
MNCRT-2	15.9	0	1.47	13.31
MNCRT-3	15.13	0	1.32	7.58
Average	15.14	0	1.45	10.27

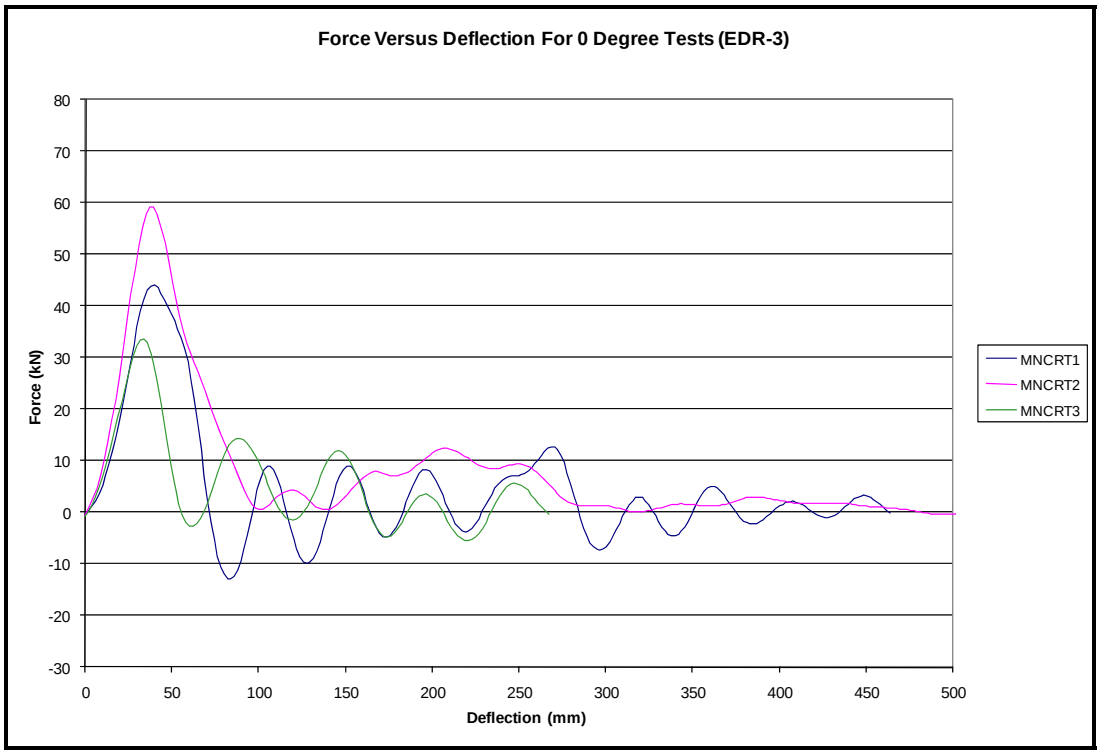

Figure 44a. Force-Deflection Curves for MNCRT-1, 2, and 3 – Metric

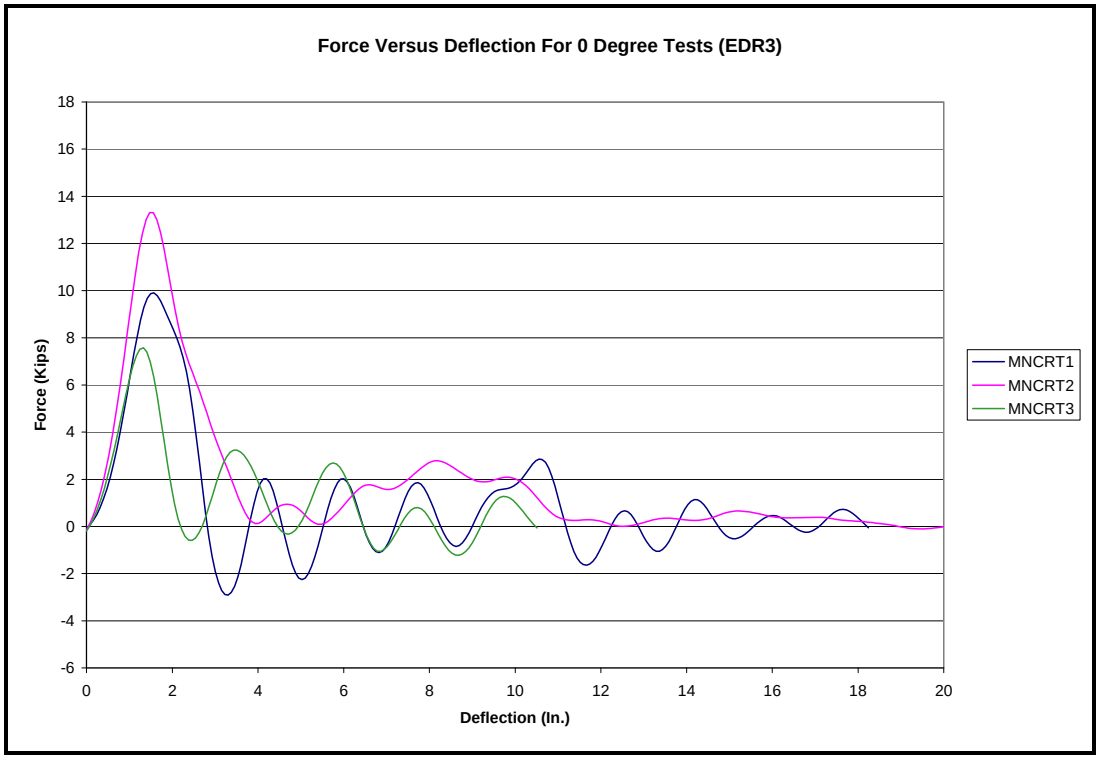

Figure 44b. Force-Deflection Curves for MNCRT-1, 2, and 3 - English

5.3.2 Force Results for Test Nos. MNCRT-4, MNCRT-5, and MNCRT-6

The second set of three bogie tests was performed on the weak axis of the CRT wood posts. The force summaries for the three tests are given in Table 8, and the force versus displacement curve comparing the three tests is shown in Figure 45. For all three tests, the initial peak force occurred quickly at a similar displacement, averaging 38.2 mm (1.50 in.). The peak force levels were also similar, ranging from 34.12 kN (7.67 kips) to 45.99 kN (10.34 kips). Differences in the peak force levels can be attributed to variation in the wood properties of the posts.

Table 8a. Peak Force Results for MNCRT-4, MNCRT-5, and MNCRT-6 – Metric

Test No.	Impact Velocity (m/s)	Impact Angle (degrees)	Initial Peak Force	
			Displacement (mm)	Force (kN)
MNCRT-4	7.35	90	41.1	45.99
MNCRT-5	7.05	90	37.3	40.88
MNCRT-6	6.83	90	36.1	34.12
Average	7.08	90	38.2	40.33

Table 8b. Peak Force Results for MNCRT-4, MNCRT-5, and MNCRT-6 – English

Test No.	Impact Velocity (mph)	Impact Angle (degrees)	Initial Peak Force	
			Displacement (in.)	Force (kips)
MNCRT-4	16.44	90	1.62	10.34
MNCRT-5	15.77	90	1.47	9.19
MNCRT-6	15.28	90	1.42	7.67
Average	15.82	90	1.50	9.07

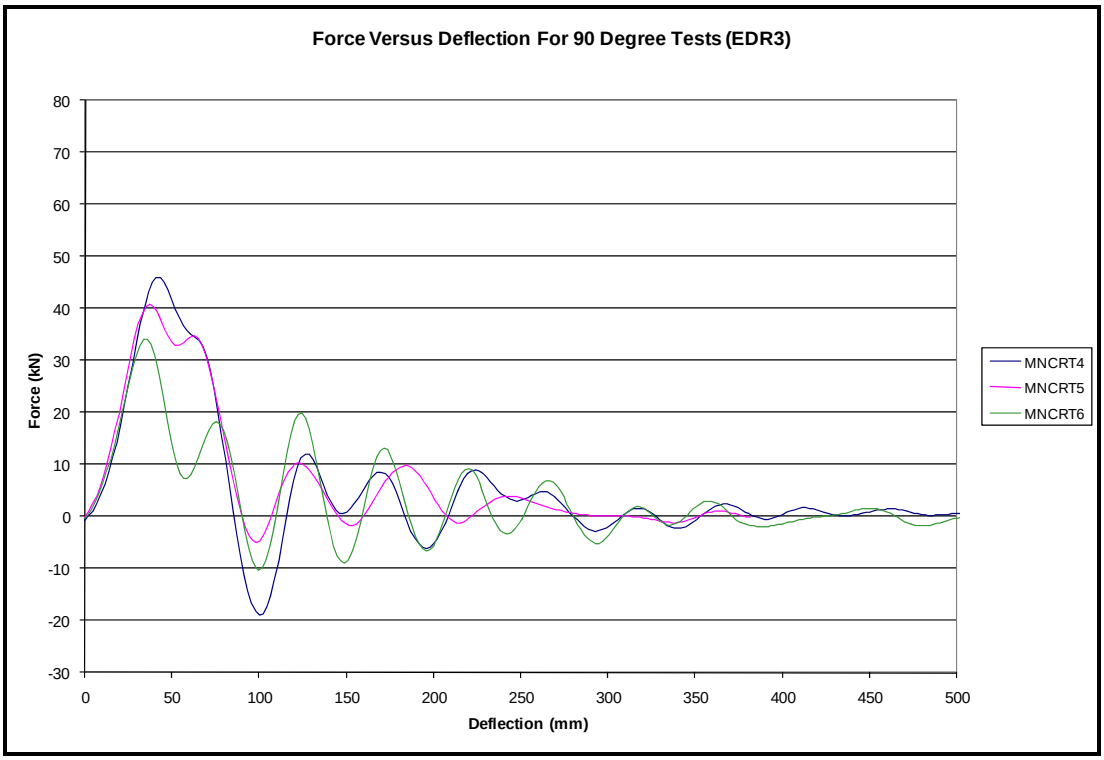

Figure 45a. Force-Deflection Curves for MNCRT-4, 5, and 6 – Metric

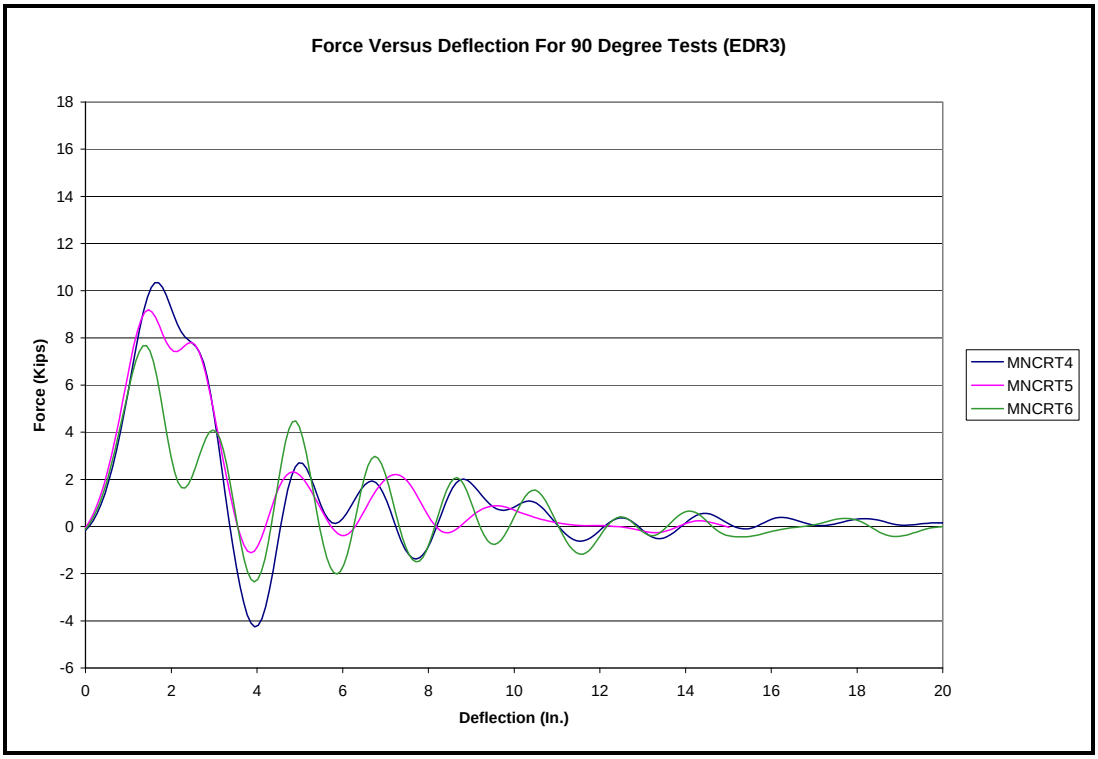

Figure 45b. Force-Deflection Curves for MNCRT-4, 5, and 6 – English

5.3.3 Force Results for Test Nos. MNCRT-7, MNCRT-8, and MNCRT-9

The final set of three bogie tests was performed on the diagonal axis (45 degrees) of the CRT wood posts. The force summaries for the three tests are given in Table 9, and the force versus displacement curve comparing the three tests is shown in Figure 46. The initial peak force occurred at an average displacement of 70.8 mm (2.79 in.). The peak force levels ranged from 31.05 kN (6.98 kips) to 71.66 kN (16.11 kips). The results in these tests were not as consistent as the previous impact angles due to a fixture issue in the rigid sleeve. Differences in the peak force levels can also be attributed to variation in the wood properties of the posts.

Table 9a. Peak Force Results for MNCRT-7, MNCRT-8, and MNCRT-9 – Metric

Test No.	Impact Velocity (m/s)	Impact Angle (degrees)	Initial Peak Force	
			Displacement (mm)	Force (kN)
MNCRT-7	7.18	45	85.3	71.66
MNCRT-8	7.16	45	85.9	41.10
MNCRT-9	6.95	45	41.1	31.05
Average	7.10	45	70.8	47.94

Table 9b. Peak Force Results for MNCRT-7, MNCRT-8, and MNCRT-9 – English

Test No.	Impact Velocity (mph)	Impact Angle (degrees)	Initial Peak Force	
			Displacement (in.)	Force (kips)
MNCRT-7	16.06	45	3.36	16.11
MNCRT-8	16.02	45	3.38	9.24
MNCRT-9	15.54	45	1.62	6.98
Average	15.87	45	2.79	10.78

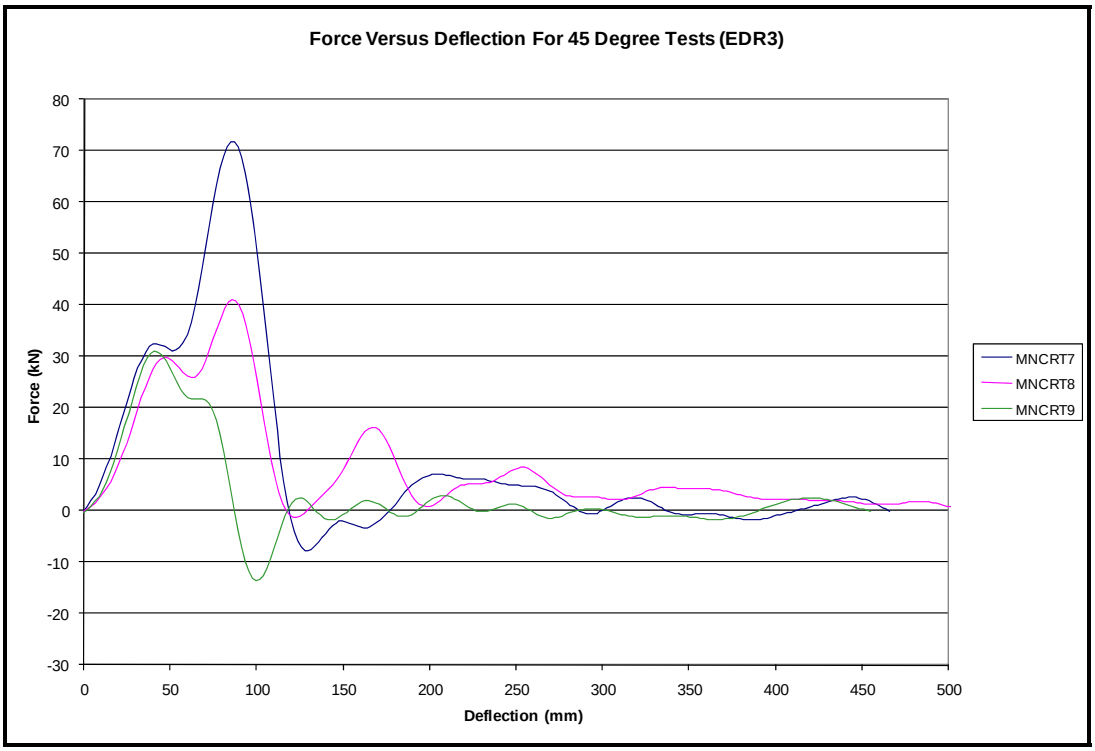

Figure 46a. Force-Deflection Curves for MNCRT-7, 8, and 9 – Metric

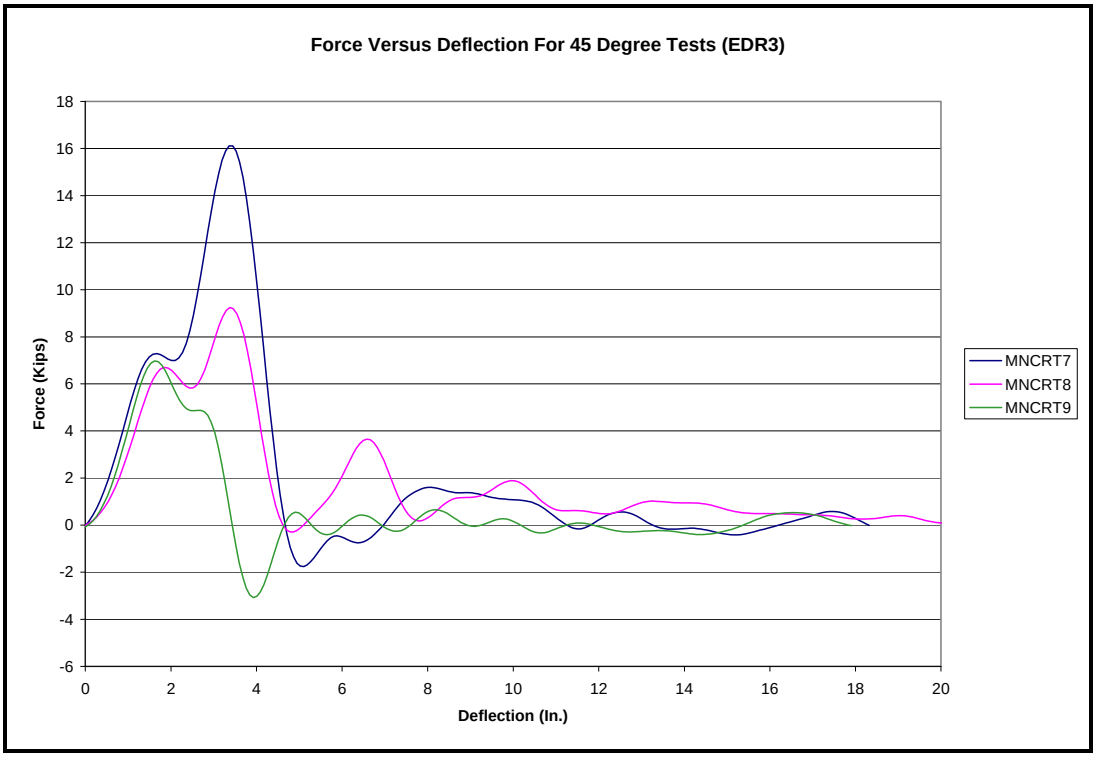

Figure 46b. Force-Deflection Curves for MNCRT-7, 8, and 9 - English

5.4 Energy Discussion

The energy dissipated during an impact is a significant factor in the performance of the post. The data presented in this section is grouped according to impact angle and will provide insights into the properties of the CRT post at the different impact angles.

Even with the high variation in wood, there still are visible trends in the energy levels at the different impact angles. For all tests, the CRT posts exhibited an initial rise in the energy level due to the inertial effects and initiating the failure of the post. This initial rise occurred before a deflection of 127 mm (5 in.) for every test. After the initial 127 mm (5 in.), the post had already fractured and had lost most of its resistance. As a result, energy levels at 127 mm (5 in.) of deflection were chosen to provide a consistent position to compare the different tests. The energy dissipated during each test was calculated by integrating the area under its force-deflection curve, shown previously in Figures 44 through 46.

5.4.1 Energy Results for Test Nos. MNCRT-1, MNCRT-2, and MNCRT-3

The first three bogie tests were performed on the strong-axis of the CRT wood posts, and the energy summaries are given in Table 10. Analysis of the energy versus deflection curves for the strong-axis at 0 degrees, as provided in Figure 47, illustrates the variation in the properties of the wood. In tests MNCRT-1 and MNCRT-3, the energy levels show similar results with 1.29 kJ (11.4 kip-in.) and 1.54 kJ (13.6 kip-in.) respectively. However, test MNCRT-2 had a significantly larger energy level of 2.70 kJ (23.9 kip-in.) at 127 mm (5 in.) of deflection. This difference can be attributed to variation in the wood properties. The post in test MNCRT-2 had no knots, while the other two posts in tests MNCRT-1 and MNCRT-3 had several knots that significantly reduced the strength, or energy levels, of both posts.

Table 10a. Energy Results for MNCRT-1, MNCRT-2, and MNCRT-3 – Metric

Test No.	Impact Velocity (m/s)	Impact Angle (degrees)	Energy @ 127 mm Displacement (kJ)	Final Total Energy	
				Displacement (mm)	Energy (kJ)
MNCRT-1	6.44	0	1.57	284.0	2.06
MNCRT-2	7.11	0	2.70	482.1	4.07
MNCRT-3	6.76	0	1.29	165.1	1.56
Average	6.77	0	1.85	310.4	2.56

Table 10b. Energy Results for MNCRT-1, MNCRT-2, and MNCRT-3 – English

Test No.	Impact Velocity (mph)	Impact Angle (degrees)	Energy @ 5 in. Displacement (kip-in.)	Final Total Energy	
				Displacement (in.)	Energy (kip-in.)
MNCRT-1	14.40	0	13.9	11.18	18.26
MNCRT-2	15.9	0	23.9	18.98	36.00
MNCRT-3	15.13	0	11.4	6.50	13.82
Average	15.14	0	16.4	12.22	22.69

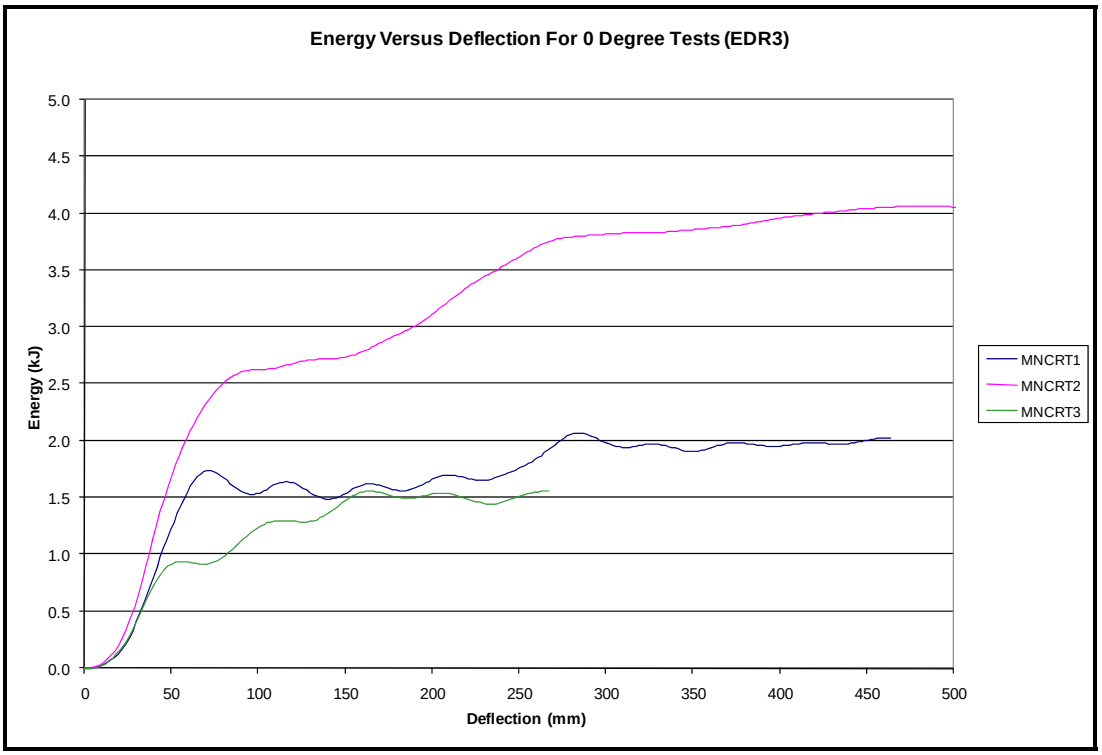

Figure 47a. Energy-Deflection Curves for MNCRT-1, 2, and 3 – Metric

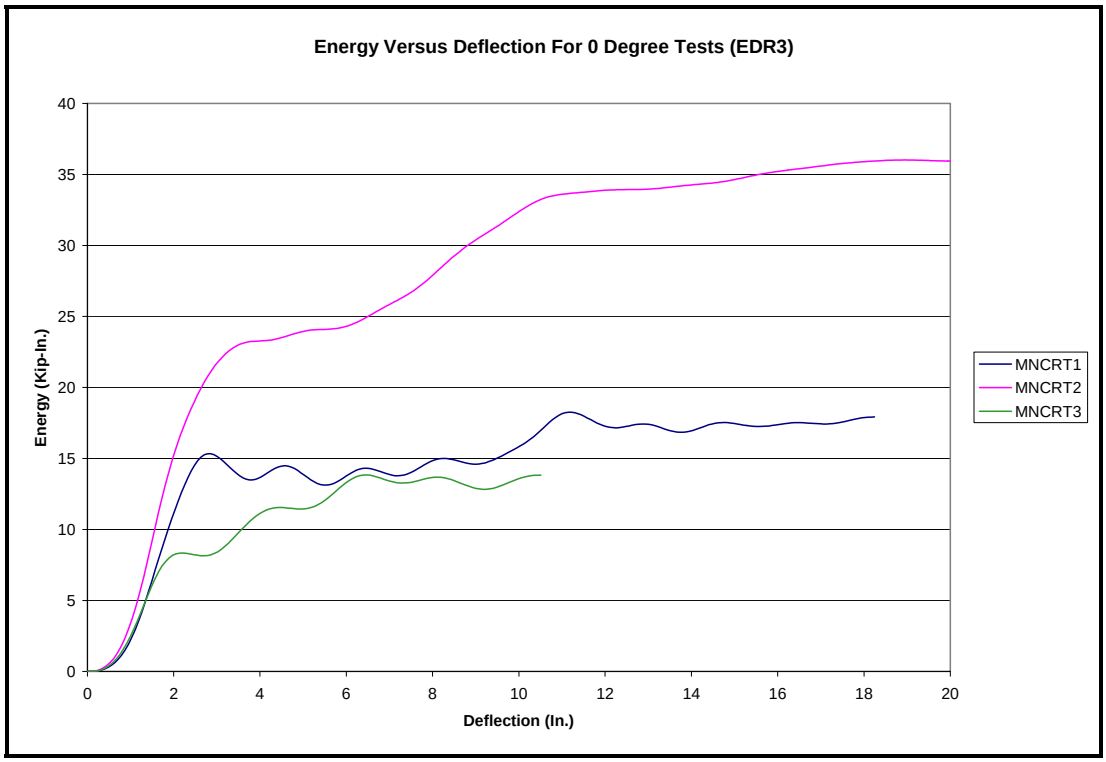

Figure 47b. Energy-Deflection Curves for MNCRT-1, 2, and 3 – English

5.4.2 Energy Results for Test Nos. MNCRT-4, MNCRT-5, and MNCRT-6

For the weak axis tests at 90 degrees, all three post tests had consistent behavior, as seen in Table 11 and Figure 48. Test MNCRT-4 had an energy level of 1.93 kJ (17.1 kip-in.), test MNCRT-5 had energy level of 2.28 kJ (20.2 kip-in.), and test MNCRT-6 had an energy level of 1.51 kJ (13.4 kip-in.). Again, any differences, although rather minor, can be attributed to variations in the wood. The average energy level for these three weak-axis tests was 1.91 kJ (16.9 kip-in.), which was actually slightly higher than the average of 1.85 kJ (16.4 kip-in.) for the strong-axis tests. This obvious error was not expected but can also be accounted for with the variations in the wood. Also, by looking at energy levels at a consistent position of 127 mm (5 in.), some error is created since energy levels depend on displacement. If more tests were conducted, the average strength, or energy levels, of the strong axis tests would probably become larger than the strength of the posts impacted on the weak axis.

Table 11a. Energy Results for MNCRT-4, MNCRT-5, and MNCRT-6 – Metric

Test No.	Impact Velocity (m/s)	Impact Angle (degrees)	Energy @ 127 mm Displacement (kJ)	Final Total Energy	
				Displacement (mm)	Energy (kJ)
MNCRT-4	7.35	90	1.93	280.2	2.48
MNCRT-5	7.05	90	2.28	314.2	2.78
MNCRT-6	6.83	90	1.51	279.9	1.88
Average	7.08	90	1.91	291.4	2.38

Table 11b. Energy Results for MNCRT-4, MNCRT-5, and MNCRT-6 – English

Test No.	Impact Velocity (mph)	Impact Angle (degrees)	Energy @ 5 in. Displacement (kip-in.)	Final Total Energy	
				Displacement (in.)	Energy (kip-in.)
MNCRT-4	16.44	90	17.1	11.03	21.94
MNCRT-5	15.77	90	20.2	12.37	24.57
MNCRT-6	15.28	90	13.4	11.02	16.64
Average	15.82	90	16.9	11.47	21.05

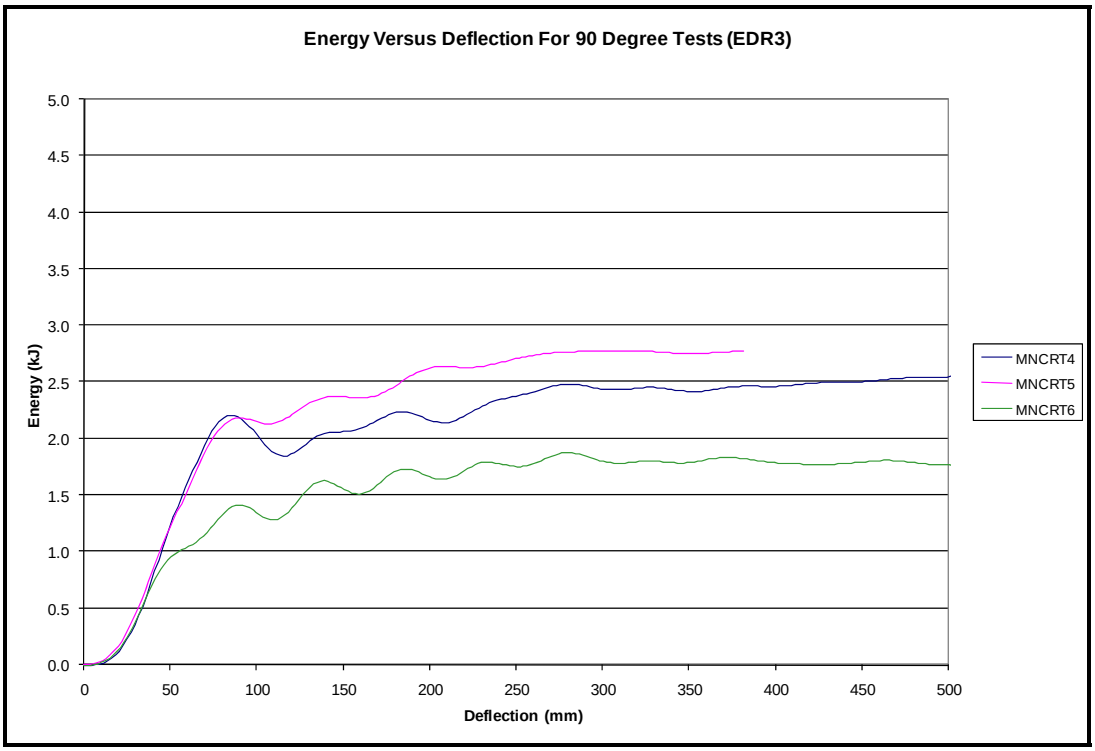

Figure 48a. Energy-Deflection Curves for MNCRT-4, 5, and 6 – Metric

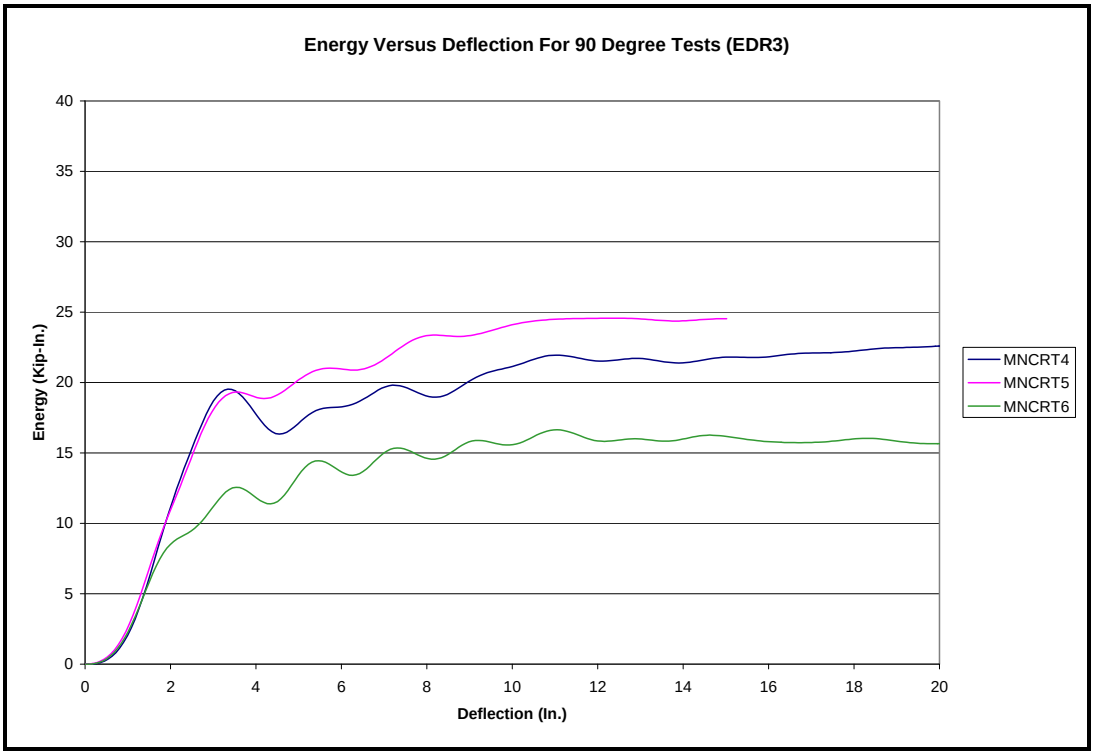

Figure 48b. Energy-Deflection Curves for MNCRT-4, 5, and 6 – English

5.4.3 Energy Results for Test Nos. MNCRT-7, MNCRT-8, and MNCRT-9

For the last three bogie tests, the CRT posts were impacted at 45 degrees, and the energy summaries are given in Table 12. The energy versus deflection curves were not as consistent as the previous impact angles, which can be seen in Figure 49. For these tests, there was a fixture issue in the rigid sleeve that had some effect on the consistency of the energy levels. The three tests averaged 2.61 kJ (23.13 kip-in.), which was higher than expected due to the fixture issue.

Table 12a. Energy Results for MNCRT-7, MNCRT-8, and MNCRT-9 – Metric

Test No.	Impact Velocity (m/s)	Impact Angle (degrees)	Energy @ 127 mm Displacement (kJ)	Final Total Energy	
				Displacement (mm)	Energy (kJ)
MNCRT-7	7.18	45	4.01	337.3	4.40
MNCRT-8	7.16	45	2.53	506.2	4.07
MNCRT-9	6.95	45	1.30	87.1	1.54
Average	7.10	45	2.61	310.2	3.34

Table 12b. Energy Results for MNCRT-7, MNCRT-8, and MNCRT-9 – English

Test No.	Impact Velocity (mph)	Impact Angle (degrees)	Energy @ 5 in. Displacement (kip-in.)	Final Total Energy	
				Displacement (in.)	Energy (kip-in.)
MNCRT-7	16.06	45	35.5	13.28	38.97
MNCRT-8	16.02	45	22.4	19.93	36.00
MNCRT-9	15.54	45	11.5	3.43	13.60
Average	15.87	45	23.13	12.21	29.52

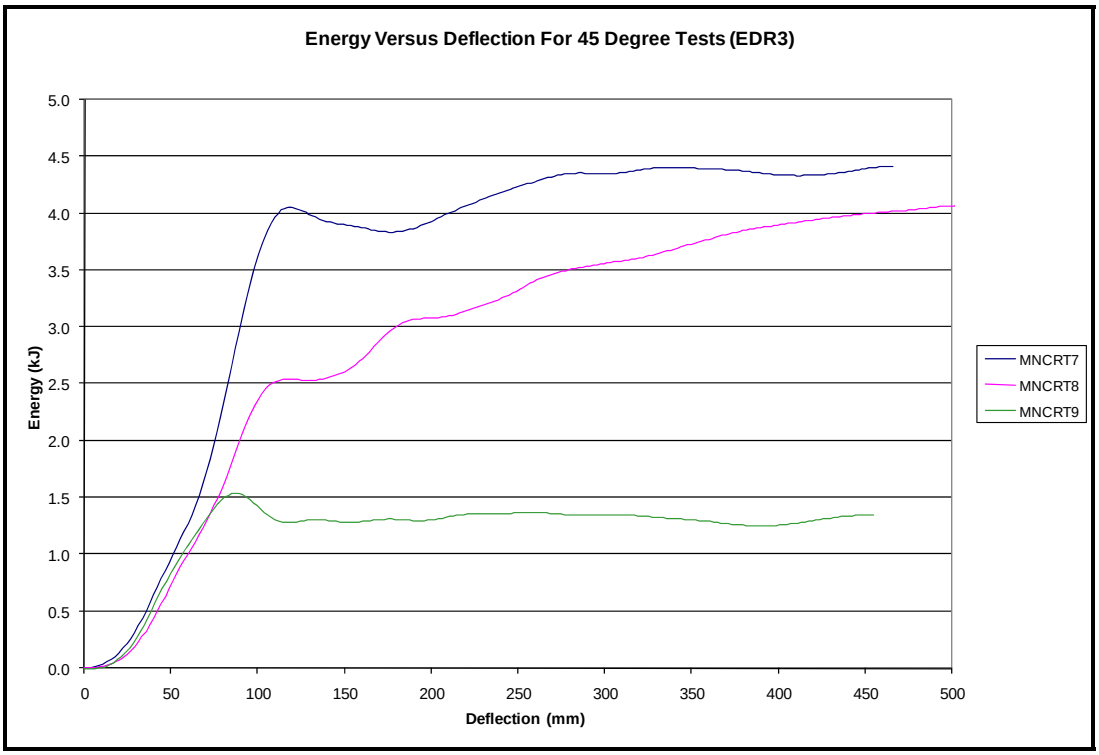

Figure 49a. Energy-Deflection Curves for MNCRT-7, 8, and 9 – Metric

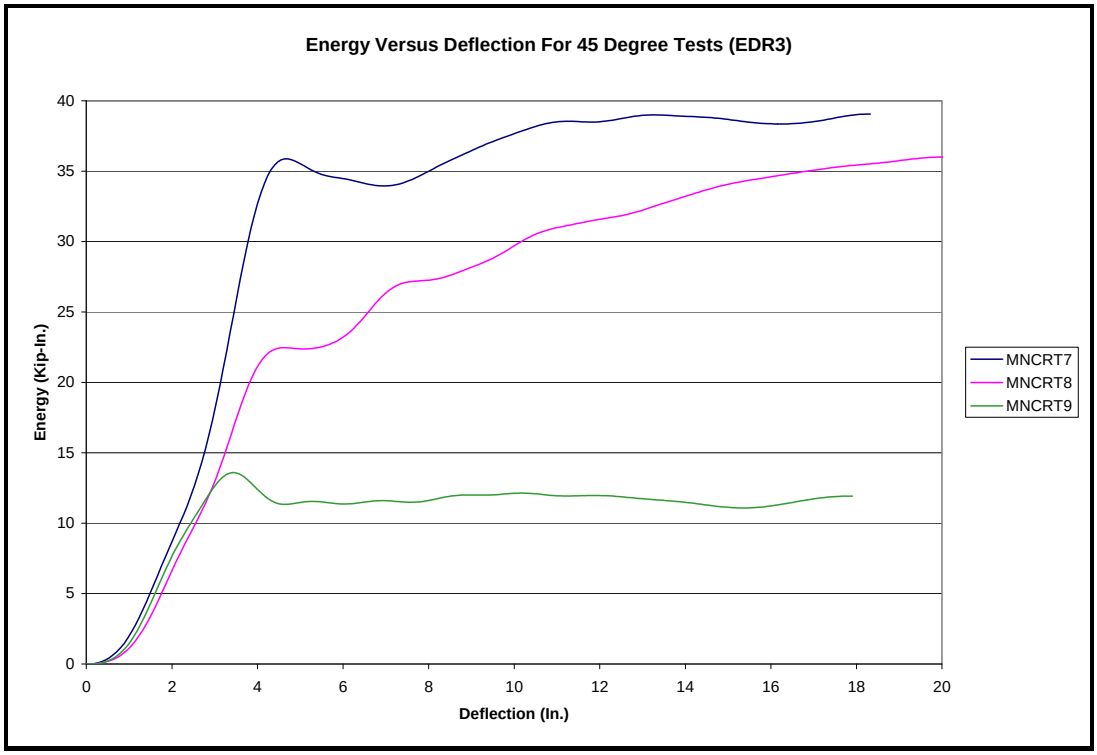

Figure 49b. Energy-Deflection Curves for MNCRT-7, 8, and 9 - English

6 CONCLUSIONS AND RECOMMENDATIONS

Dynamic impact testing of standard 152 mm x 203 mm (6 in. x 8 in.) CRT posts at different angles have been detailed and the results stated. The results from these bogie tests will aid in the future development of a Universal Breakaway Steel Post for bullnose and other non-proprietary guardrail systems.

Although only nine tests were performed with three tests at three different angles, the results of these tests provided the basic properties of the CRT post under dynamic impact testing. Based on the bogie tests and the properties of the CRT post given in Table 2, the peak forces and total energy for the strong, weak, and diagonal axis were determined and are illustrated in Figure 50. Though not clearly visible in the actual bogie tests, the strong-axis peak force of 53.4 kN (12 kips) was chosen to be exactly double the strength of the weak axis at 26.7 kN (6 kips). This decision was based on the clear wood properties of a SYP CRT wood post found in Table 2, which shows how the strong axis should have nearly double the peak force due to the different moment of inertias for the separate axes. Also, this data from the moment of inertias was independent of the differences and variation in the wood that greatly affected the nine bogie tests. For the energy levels, 51 mm (2 in.) of deflection at the peak force was chosen to be representative of the energy level. This decision stemmed from the bogie results and also from previous experience with the CRT posts knowing that the posts fracture rather quickly. From these results, there are now target force and energy values to aim for in the design of a future Universal Breakaway Steel Post.

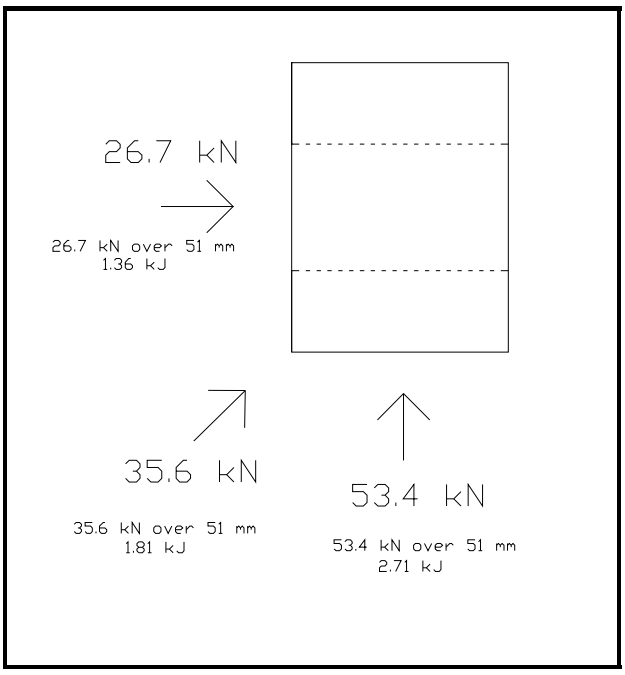

Figure 50a. Peak Forces and Energy Levels of the CRT Post - Metric

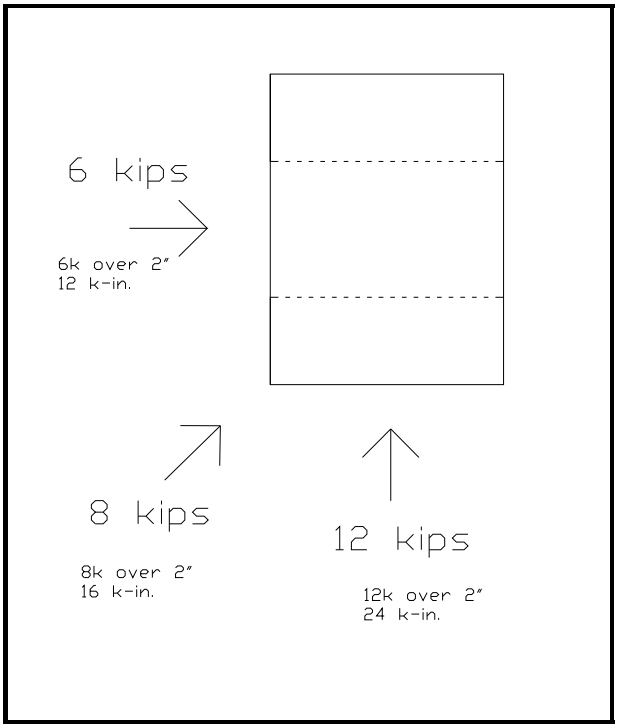

Figure 50b. Peak Forces and Energy Levels of the CRT Post - English

7 REFERENCES

1. Bielenberg, B.W., Faller, R.K., Reid, J.D., Rohde, J.R., Sicking, D.L., and Keller, E.A., *Concept Development of a Bullnose Guardrail System for Median Applications*, Final Report to the Midwest States' Regional Pooled Fund Program, MwRSF Research Report No. TRP-03-73-98, Midwest Roadside Safety Facility, University of Nebraska-Lincoln, Lincoln, Nebraska, May 1998.

2. Bielenberg, B.W., Faller, R.K., Reid, J.D., Rohde, J.R., Sicking, D.L., Keller, E.A., and Holloway, J.C., *Phase II Development of a Bullnose Guardrail System for Median Applications*, Final Report to the Midwest States' Regional Pooled Fund Program, MwRSF Research Report No. TRP-03-78-98, Midwest Roadside Safety Facility, University of Nebraska-Lincoln, Lincoln, Nebraska, December 1998.

3. Bielenberg, B.W., Faller, R.K., Reid, J.D., Rohde, J.R., Sicking, D.L., Keller, E.A., Holloway, J.C., and Supencheck, L.L., *Phase III Development of a Bullnose Guardrail System for Median Applications*, Final Report to the Midwest States' Regional Pooled Fund Program, MwRSF Research Report No. TRP-03-95-00, Midwest Roadside Safety Facility, University of Nebraska-Lincoln, Lincoln, Nebraska, June 2000.

4. Ross, H.E., Jr., Sicking D.L., and Zimmer, R.A., *National Cooperative Highway Research Report 350: Recommended Procedures for the Safety Performance Evaluation of Highway Features*. Transportation Research Board, Washington, D.C., 1993.

5. Hascall, J.A., Faller, R.K., Reid J.D., Sicking, D.L., and Kretschmann, D.E., *Investigating the Use of Small-Diameter Softwood as Guardrail Posts (Dynamic Test Results)*, Final Report to the Forest Products Laboratory – U.S. Department of Agriculture, MwRSF Research Report No. TRP-03-179-07, Midwest Roadside Safety Facility, University of Nebraska-Lincoln, Lincoln, Nebraska, March 2007.

6. Hinch, J.A., Owings R.P., and Manhard G.A., *Safety Modifications of Turned-Down Guardrail Terminals, Volumes 1, 2, and 3*, Final Report to the Federal Highway Administration, Ensco, Inc., Springfield, VA, June 1984.

7. Michie, Jarvis D., *Recommended Procedures for the Safety Performance Evaluation of Highway Appurtenances*, NCHRP Report No. 230, Transportation Research Board, Washington, D.C., March 1981.

8. Rohde, J.R., Hascall, J.A., Polivka, K.A., Faller R.K., and Sicking, D.L., *Dynamic Testing of Wooden Guardrail Posts – White and Red Pine Species Equivalency Study*, Final Report to the Midwest States' Regional Pooled Fund Program, MwRSF Research Report No. TRP-03-154-04, Midwest Roadside Safety Facility, University of Nebraska-Lincoln, Lincoln, Nebraska, September 2004.

9. Electrophysics, Moisture Meter Model MT700, Operating Instructions & Information, Ontario, Canada.

10. DynaMax User's Manual, Revision 1.75, Instrumented Sensor Technologies, Inc., Okemos, Michigan, April 1993.

11. The DADiSP Worksheet, Data Analysis and Display Software, User Reference Manuals, Version 4.0, DSP Development Corporation, Cambridge, Massachusetts, December 1991.

12. Society of Automotive Engineers (SAE), *Instrumentation for Impact Test – Part 1 – Electronic Instrumentation – SAE J211/1 MAR95*, New York City, NY, 1999.

Appendix A

A.1 Test Summary Information

A summary sheet for each test is provided in this section. Summary sheets include acceleration, velocity, and displacement versus time plots, as well as force and energy versus deflection plots.

Table A-1. Post Testing Summary

MNCRT Test Parameters
MNCRT: Control Releasing Terminal Wood Post
Test: Impact in rigid sleeve at 0, 45, and 90 degrees with respect to strong axis
Accelerometer: EDR-3 and EDR-4 Data
Bogie Weight: 728.0 kg (1,605 lbs)
Bumper Height: 632 mm (24.875 in.)
Posts: CRT Wood Post: 152 mm x 203 mm (6 in. x 8 in.)
Post Length: 1,829 mm (72 in.)

Table A-2. Post Testing Results Reference

Test No.	Impact Angle	Velocity		Embedment Depth		Embedment Type	Figure Number
		m/s	mph	mm	In.		
MNCRT-1	0	6.44	14.40	1,016	40	Rigid Sleeve	Figures A-1, A-2
MNCRT-2	0	7.11	15.9	1,016	40	Rigid Sleeve	Figures A-3, A-4
MNCRT-3	0	6.76	15.13	1,016	40	Rigid Sleeve	Figures A-5, A-6
MNCRT-4	90	7.35	16.44	1,016	40	Rigid Sleeve	Figures A-7, A-8
MNCRT-5	90	7.05	15.77	1,016	40	Rigid Sleeve	Figures A-9, A-10
MNCRT-6	90	6.83	15.28	1,016	40	Rigid Sleeve	Figures A-11, A-12
MNCRT-7	45	7.18	16.06	1,016	40	Rigid Sleeve	Figures A-13, A-14
MNCRT-8	45	7.16	16.02	1,016	40	Rigid Sleeve	Figures A-15, A-16
MNCRT-9	45	6.95	15.54	1,016	40	Rigid Sleeve	Figures A-17, A-18

Midwest Roadside Safety Facility

Bogie Test Summary

Test Information	MNDOT Wood CRT Study		
Test Number:	MNCRT-1		
Test Date:	7-Jun-2007		
Failure Type:	Post failure near breakaway hole		
Post Properties			
Post Type:	Wood CRT		
Post Size:	152 mm x 203 mm	6" x 8"	
Post Length:	182.9 cm	(72.0 in.)	
Embedment Depth:	101.6 cm	(40.0 in.)	
Category:	0		
Soil Properties			
Gradation:	0		
Moisture Content:	0.0%		
Compaction Method:	0		
Soil Density, γ_d:	0 kg/m^3	(0 pcf)	
Bogie Properties			
Impact Velocity:	6.4 m/s	(14.4 mph)	(21.1 fps)
Impact Location:	63.2 cm	(24.9 in)	above groundline
Bogie Mass:	728 kg	(1605 lbf)	
Data Acquired			
Accelerometer Data:	EDR-3		
Camera Data:	AOS1 - Perpendicular view 301"		

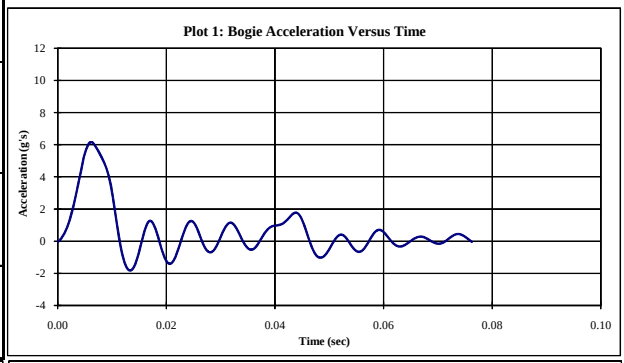

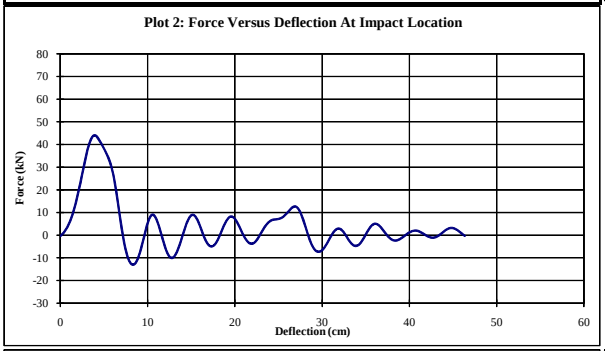

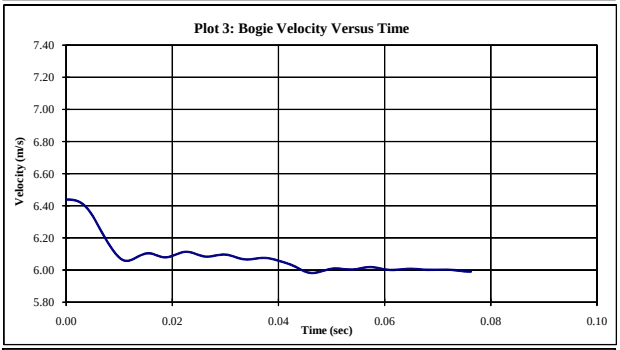

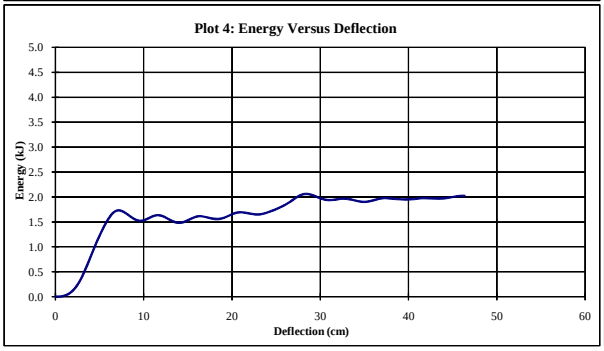

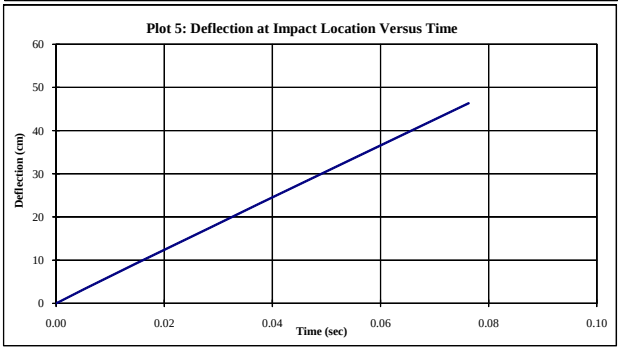

Figure A-1. Results of MNCRT-1 (EDR3)

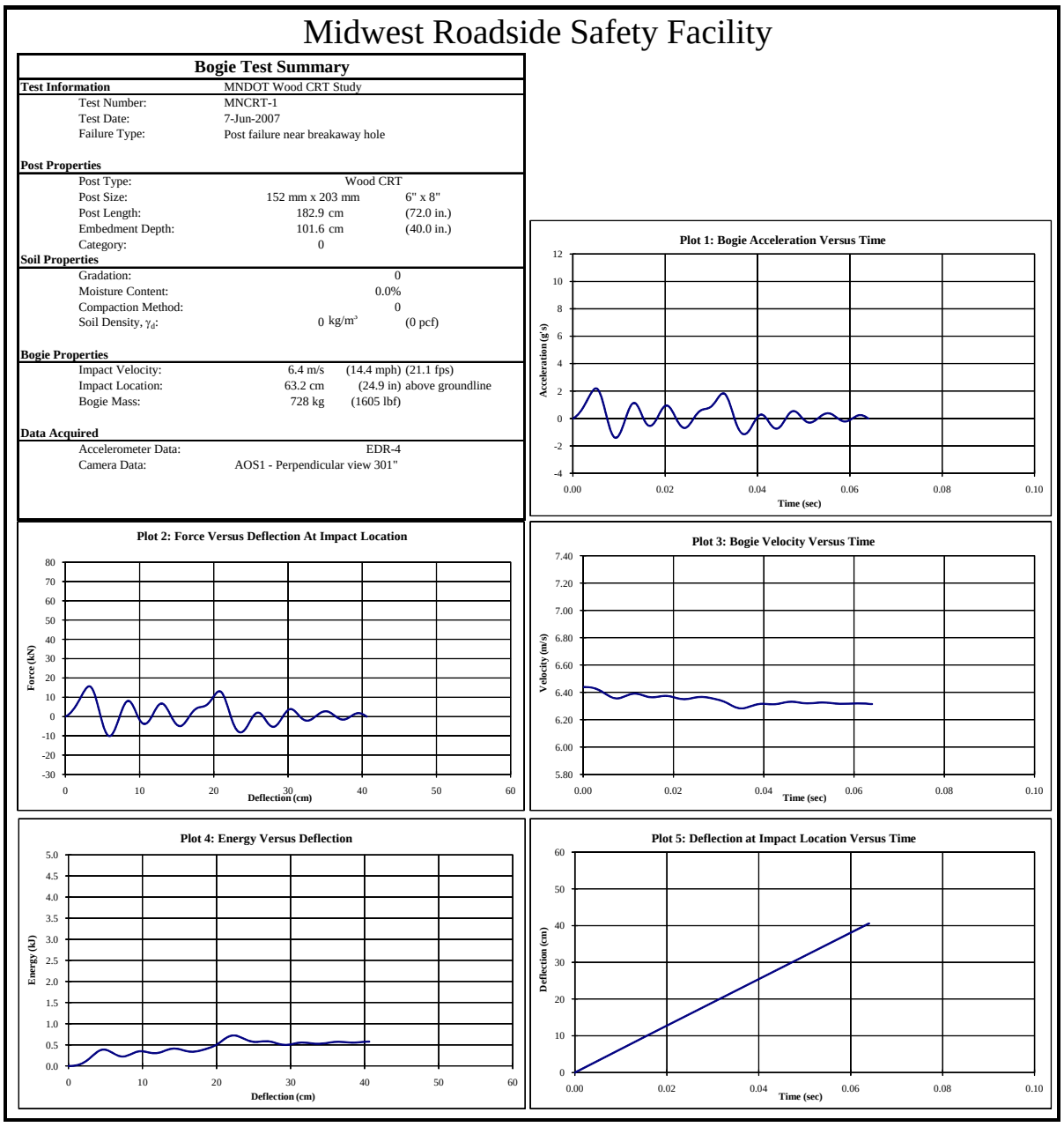

Figure A-2. Results of MNCRT-1 (EDR4)

(Invalid – Initial impact data was cutoff)

Midwest Roadside Safety Facility

Bogie Test Summary

Test Information	MNDOT Wood CRT Study		
Test Number:	MNCRT-2		
Test Date:	7-Jun-2007		
Failure Type:	Post failure near breakaway hole		
Post Properties			
Post Type:	Wood CRT		
Post Size:	152 mm x 203 mm	6" x 8"	
Post Length:	182.9 cm	(464.5 cm)	
Embedment Depth:	101.6 cm	(258.1 cm)	
Category:	0		
Soil Properties			
Gradation:	0		
Moisture Content:	0.0%		
Compaction Method:	0		
Soil Density, γ_d:	0 kg/m^3	(0 pcf)	
Bogie Properties			
Impact Velocity:	7.1 m/s	(15.9 mph)	(23.3 fps)
Impact Location:	63.2 cm	(24.9 in)	above groundline
Bogie Mass:	728 kg	(1605 lbf)	
Data Acquired			
Accelerometer Data:	EDR-3		
Camera Data:	AOS1 - Perpendicular view 301"		

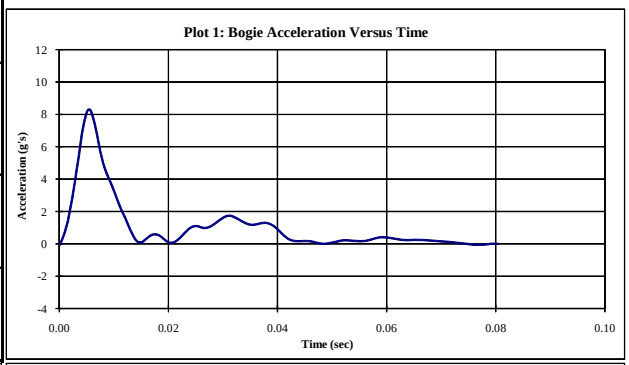

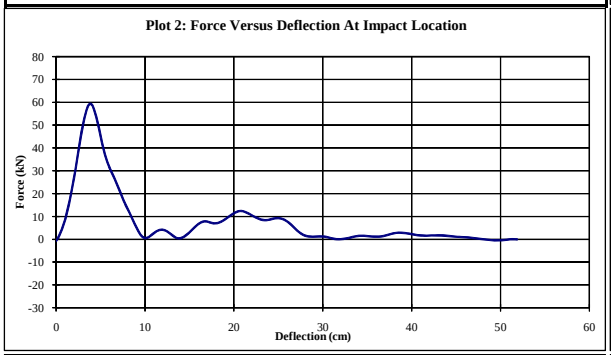

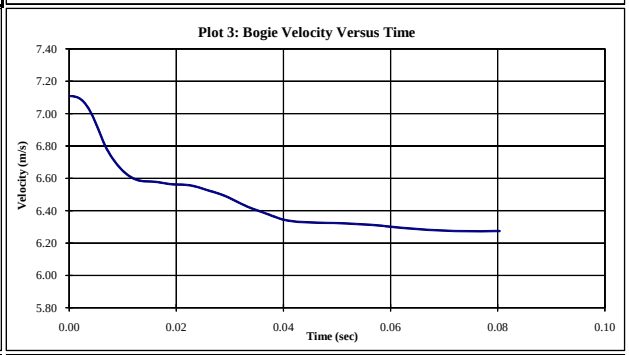

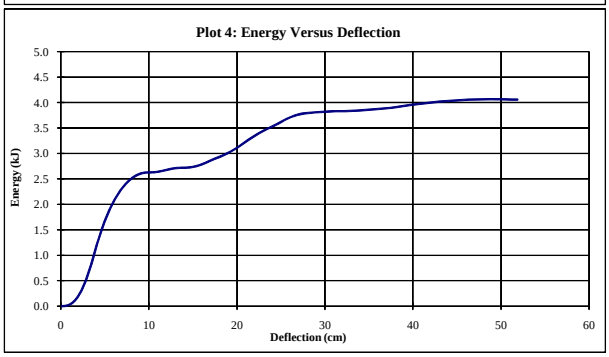

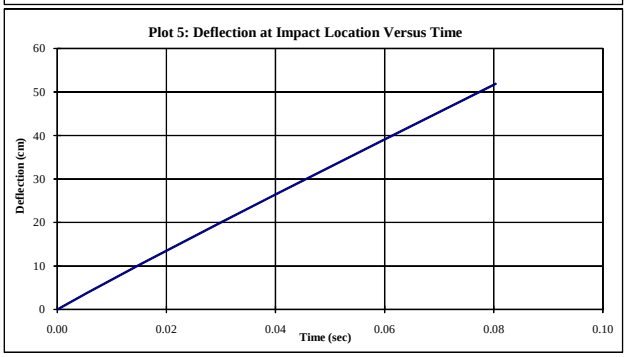

Figure A-3. Results of MNCRT-2 (EDR3)

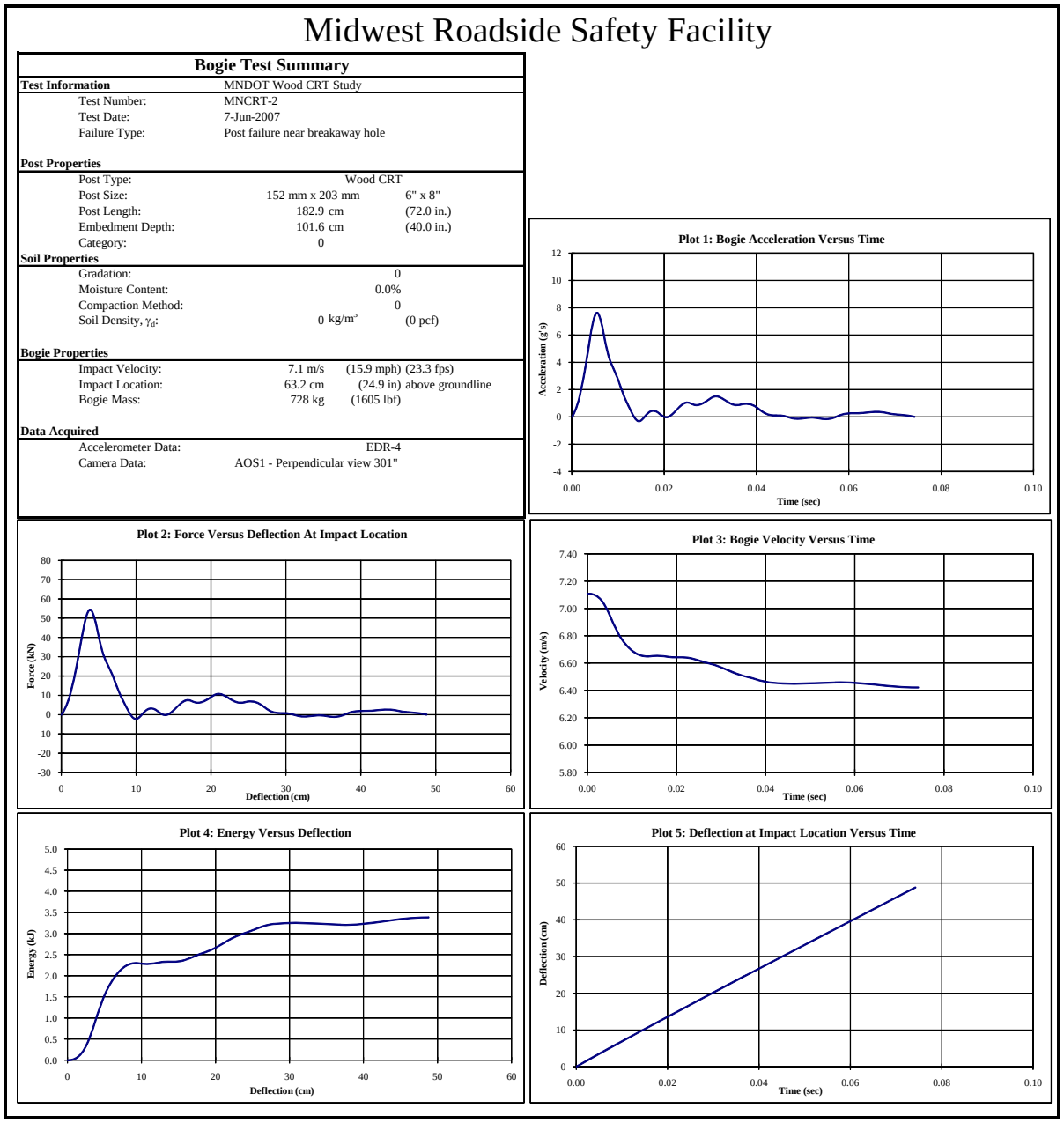

Figure A-4. Results of MNCRT-2 (EDR4)

Midwest Roadside Safety Facility

Bogie Test Summary

Test Information	MNDOT Wood CRT Study		
Test Number:	MNCRT-3		
Test Date:	7-Jun-2007		
Failure Type:	Post failure near breakaway hole		
Post Properties			
Post Type:	Wood CRT		
Post Size:	152 mm x 203 mm	6" x 8"	
Post Length:	182.9 cm	(72.0 in)	
Embedment Depth:	101.6 cm	(40.0 in)	
Category:	0		
Soil Properties			
Gradation:	0		
Moisture Content:	0.0%		
Compaction Method:	0		
Soil Density, γ_d:	0 kg/m^3	(0 pcf)	
Bogie Properties			
Impact Velocity:	6.8 m/s	(15.1 mph)	(22.2 fps)
Impact Location:	63.2 cm	(24.9 in)	above groundline
Bogie Mass:	728 kg	(1605 lbf)	
Data Acquired			
Accelerometer Data:	EDR-3		
Camera Data:	AOS1 - Perpendicular view 301"		

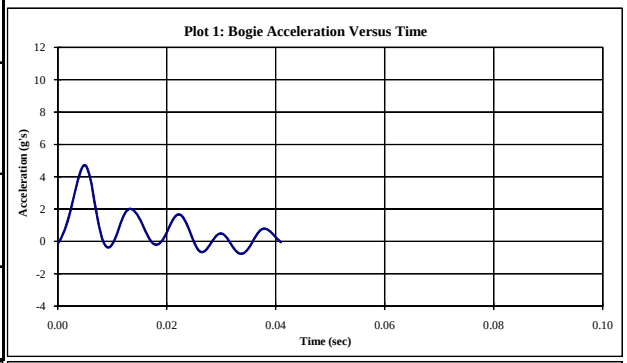

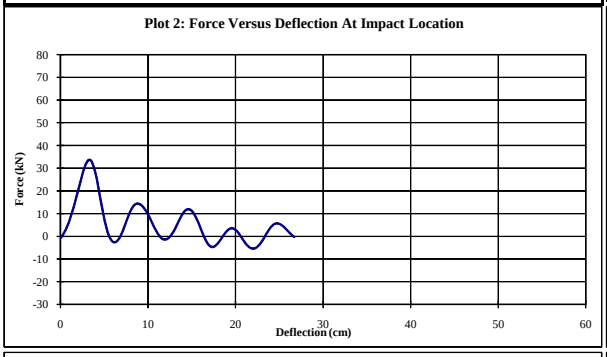

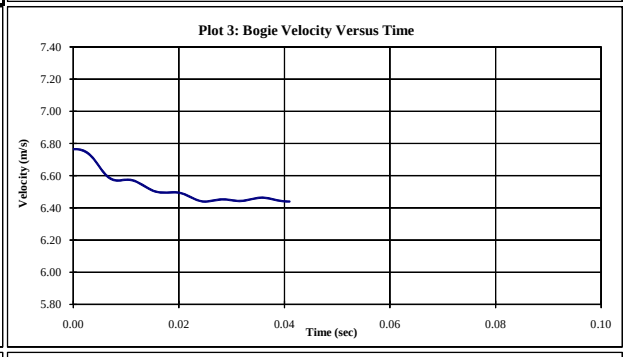

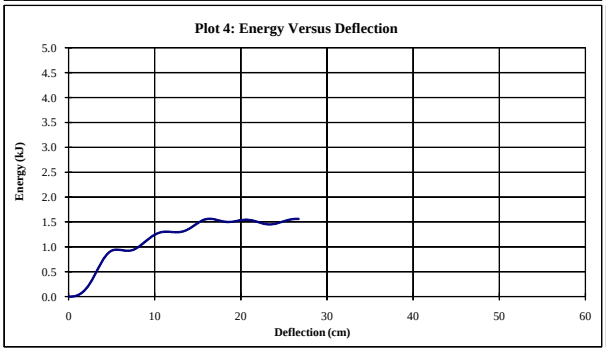

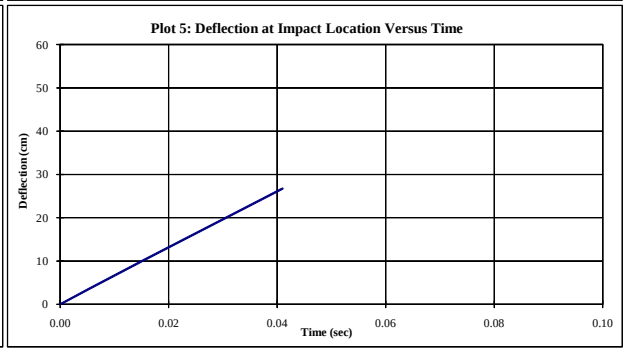

Figure A-5. Results of MNCRT-3 (EDR3)

Midwest Roadside Safety Facility

Bogie Test Summary

Test Information	MNDOT Wood CRT Study		
Test Number:	MNCRT-3		
Test Date:	7-Jun-2007		
Failure Type:	Post failure near breakaway hole		
Post Properties			
Post Type:	Wood CRT		
Post Size:	152 mm x 203 mm	6" x 8"	
Post Length:	182.9 cm	(72.0 in)	
Embedment Depth:	101.6 cm	(40.0 in)	
Category:	0		
Soil Properties			
Gradation:	0		
Moisture Content:	0.0%		
Compaction Method:	0		
Soil Density, γ_d:	0 kg/m^3	(0 pcf)	
Bogie Properties			
Impact Velocity:	6.8 m/s	(15.1 mph)	(22.2 fps)
Impact Location:	63.2 cm	(24.9 in)	above groundline
Bogie Mass:	728 kg	(1605 lbf)	
Data Acquired			
Accelerometer Data:	EDR-4		
Camera Data:	AOS1 - Perpendicular view 301"		

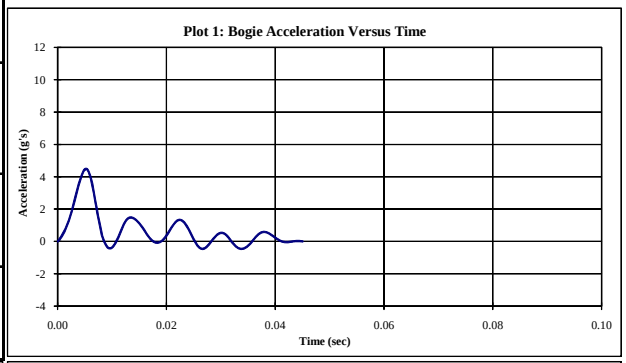

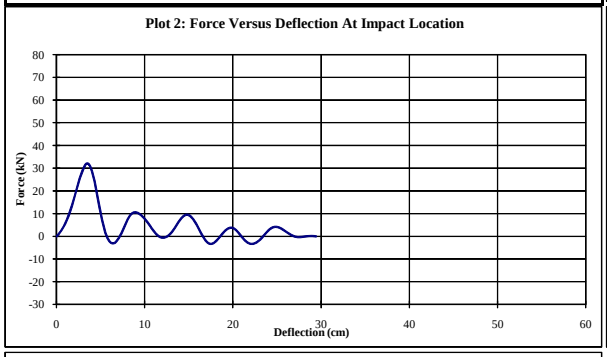

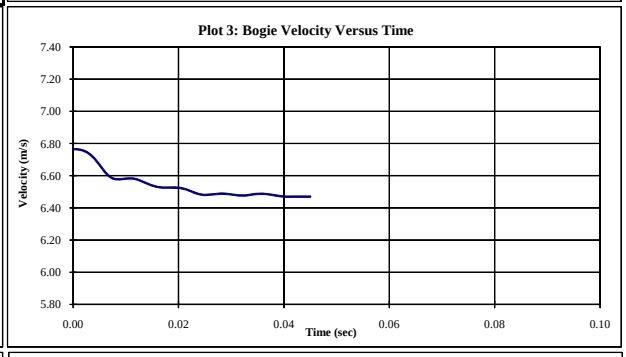

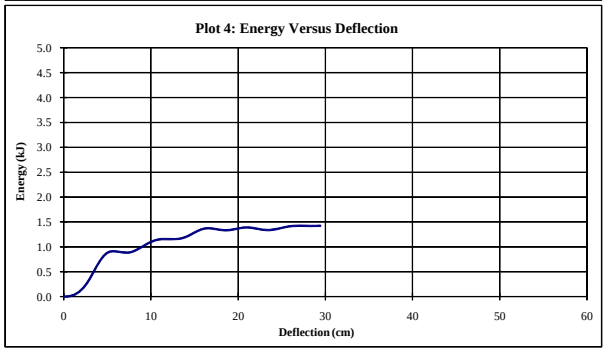

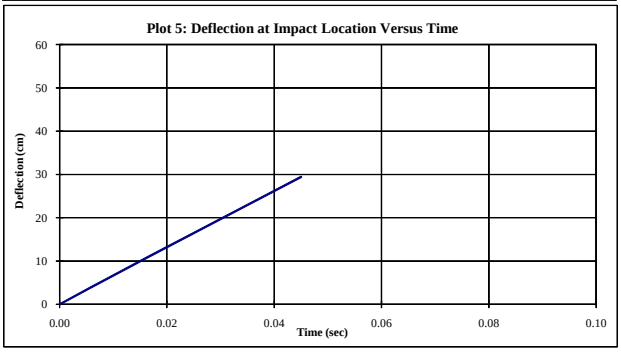

Figure A-6. Results of MNCRT-3 (EDR4)

Midwest Roadside Safety Facility

Bogie Test Summary

Test Information	MNDOT Wood CRT Study		
Test Number:	MNCRT-4		
Test Date:	7-Jun-2007		
Failure Type:	Post failure near breakaway hole		
Post Properties			
Post Type:	Wood CRT		
Post Size:	152 mm x 203 mm	6" x 8"	
Post Length:	182.9 cm	(72.0 in.)	
Embedment Depth:	101.6 cm	(40.0 in.)	
Category:	0		
Soil Properties			
Gradation:	0		
Moisture Content:	0.0%		
Compaction Method:	0		
Soil Density, γ_d:	0 kg/m³	(0 pcf)	
Bogie Properties			
Impact Velocity:	7.3 m/s	(16.4 mph)	(24.1 fps)
Impact Location:	63.2 cm	(24.9 in)	above groundline
Bogie Mass:	728 kg	(1605 lbf)	
Data Acquired			
Accelerometer Data:	EDR-3		
Camera Data:	AOS1 - Perpendicular view 301"		

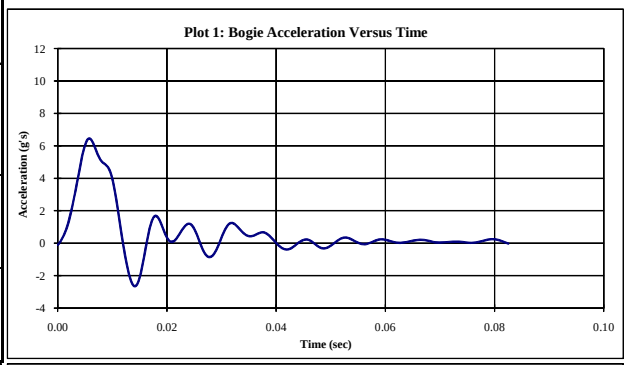

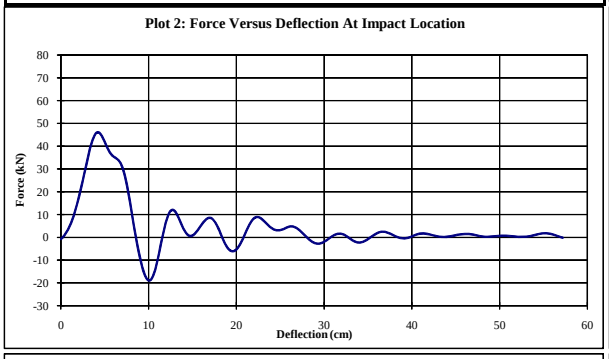

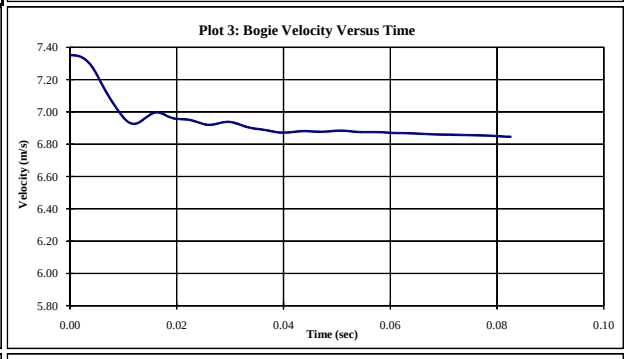

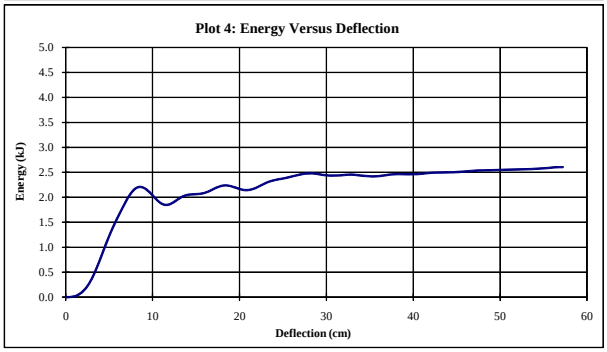

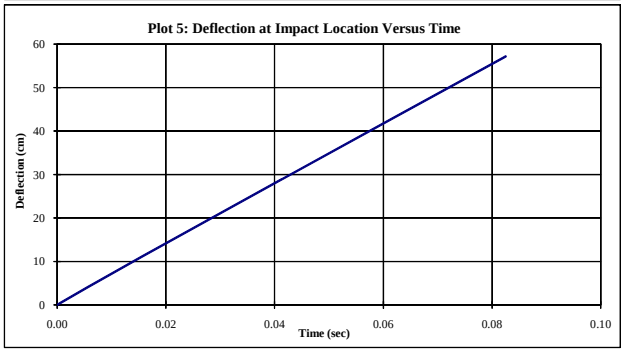

Figure A-7. Results of MNCRT-4 (EDR3)

Midwest Roadside Safety Facility

Bogie Test Summary

Test Information	MNDOT Wood CRT Study		
Test Number:	MNCRT-4		
Test Date:	7-Jun-2007		
Failure Type:	Post failure near breakaway hole		
Post Properties			
Post Type:	Wood CRT		
Post Size:	152 mm x 203 mm	6" x 8"	
Post Length:	182.9 cm	(72.0 in.)	
Embedment Depth:	101.6 cm	(40.0 in.)	
Category:	0		
Soil Properties			
Gradation:	0		
Moisture Content:	0.0%		
Compaction Method:	0		
Soil Density, γ_d:	0 kg/m³	(0 pcf)	
Bogie Properties			
Impact Velocity:	7.3 m/s	(16.4 mph)	(24.1 fps)
Impact Location:	63.2 cm	(24.9 in)	above groundline
Bogie Mass:	728 kg	(1605 lbf)	
Data Acquired			
Accelerometer Data:	EDR-4		
Camera Data:	AOS1 - Perpendicular view 301"		

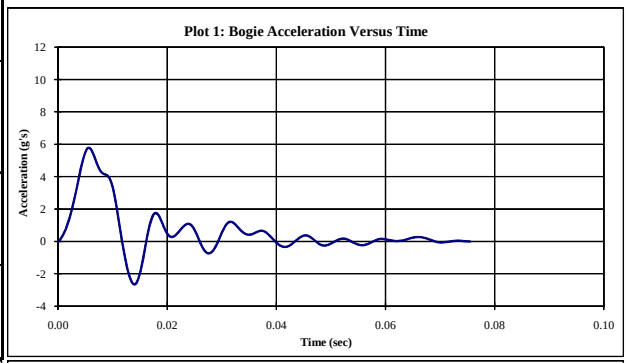

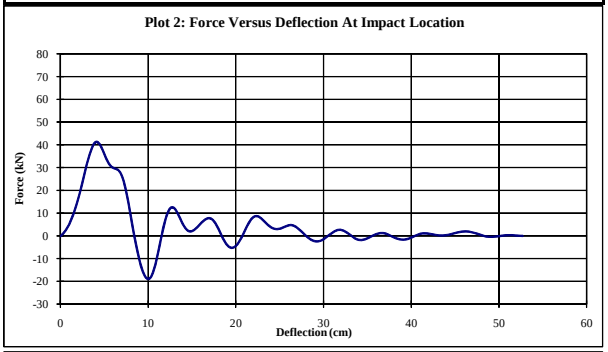

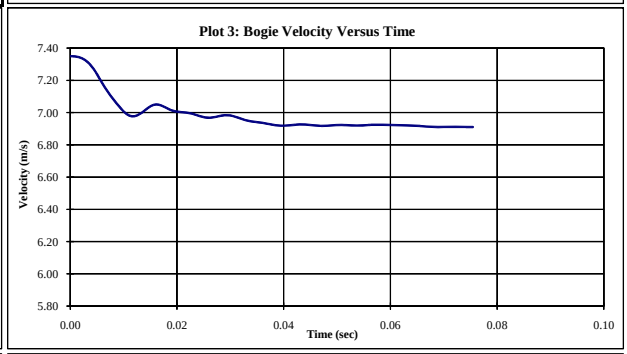

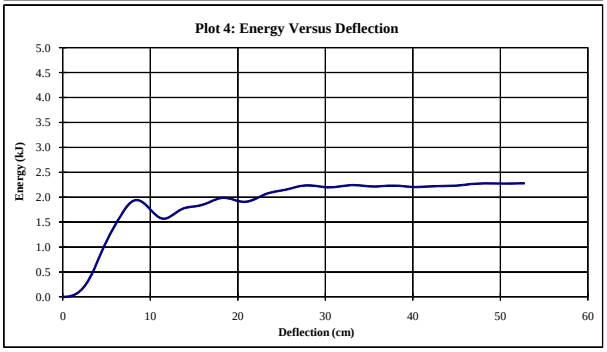

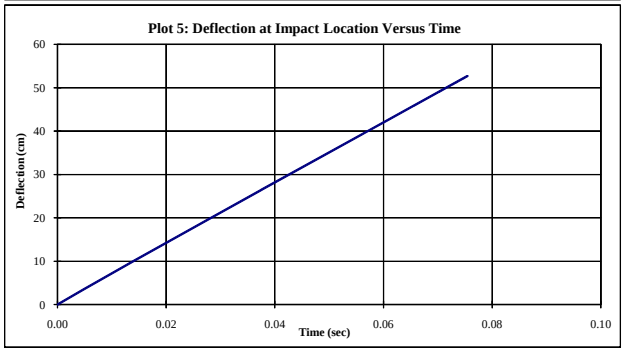

Figure A-8. Results of MNCRT-4 (EDR4)

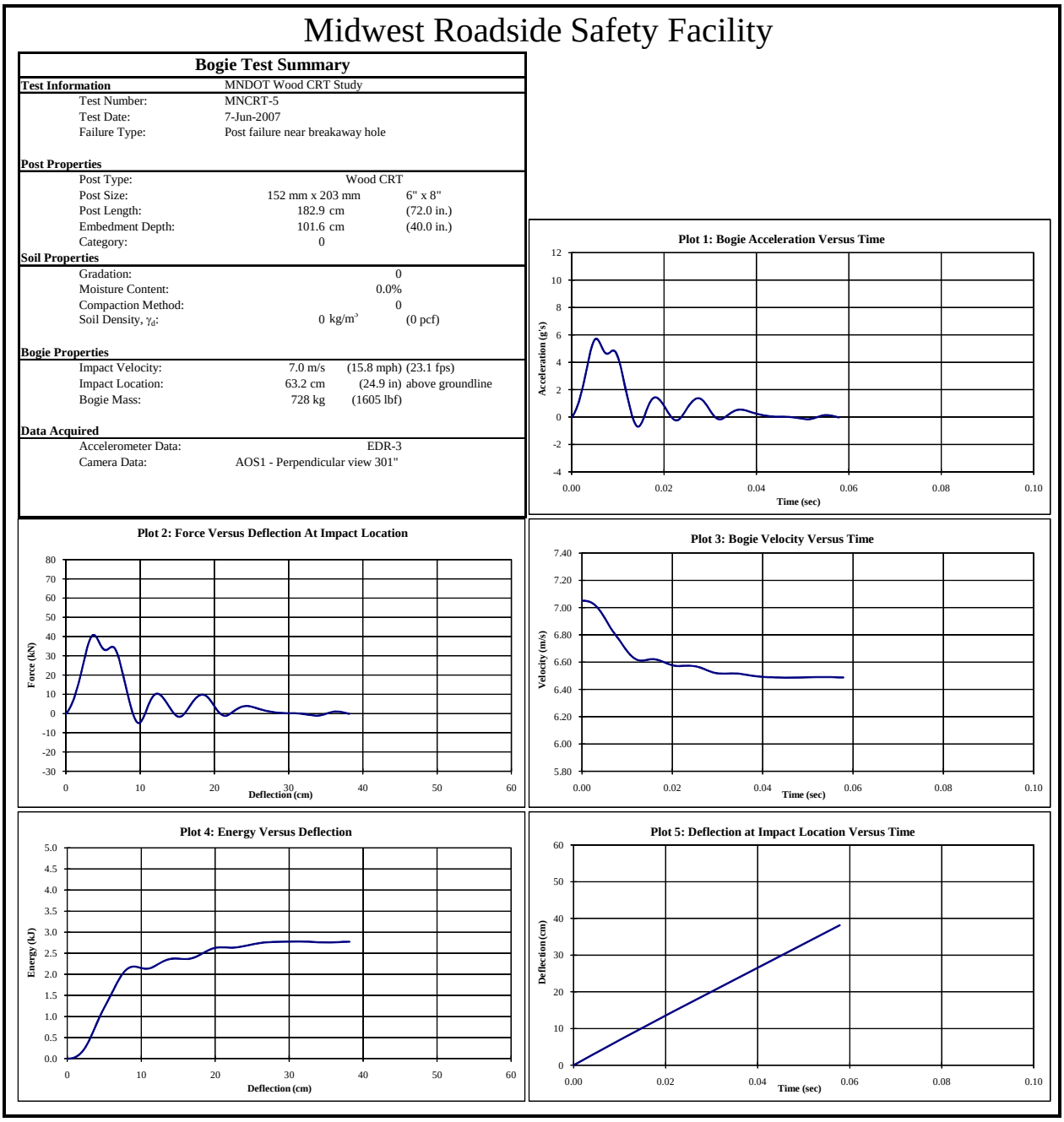

Figure A-9. Results of MNCRT-5 (EDR3)

Midwest Roadside Safety Facility

Bogie Test Summary

Test Information	MNDOT Wood CRT Study		
Test Number:	MNCRT-5		
Test Date:	7-Jun-2007		
Failure Type:	Post failure near breakaway hole		
Post Properties			
Post Type:	Wood CRT		
Post Size:	152 mm x 203 mm	6" x 8"	
Post Length:	182.9 cm	(72.0 in.)	
Embedment Depth:	101.6 cm	(40.0 in.)	
Category:	0		
Soil Properties			
Gradation:	0		
Moisture Content:	0.0%		
Compaction Method:	0		
Soil Density, γ_d:	0 kg/m^3	(0 pcf)	
Bogie Properties			
Impact Velocity:	7.0 m/s	(15.8 mph)	(23.1 fps)
Impact Location:	63.2 cm	(24.9 in)	above groundline
Bogie Mass:	728 kg	(1605 lbf)	
Data Acquired			
Accelerometer Data:	EDR-4		
Camera Data:	AOS1 - Perpendicular view 301"		

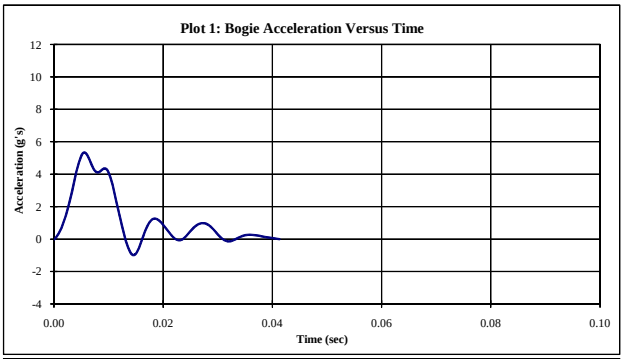

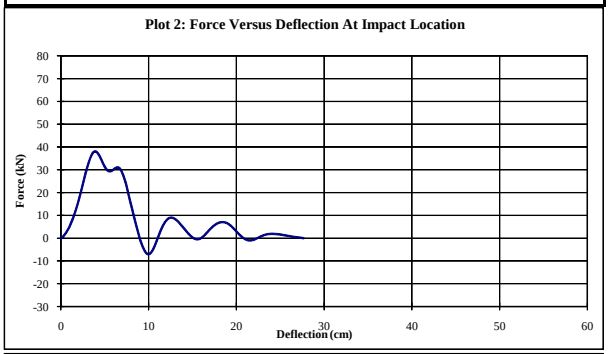

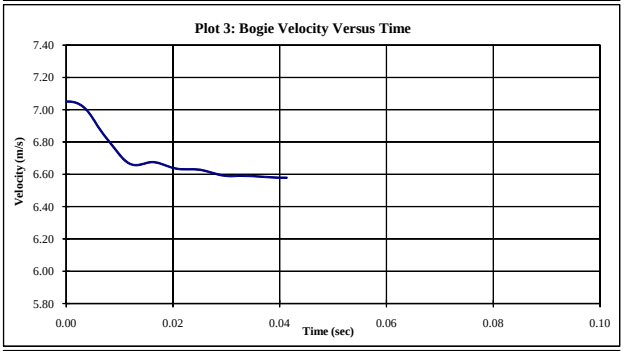

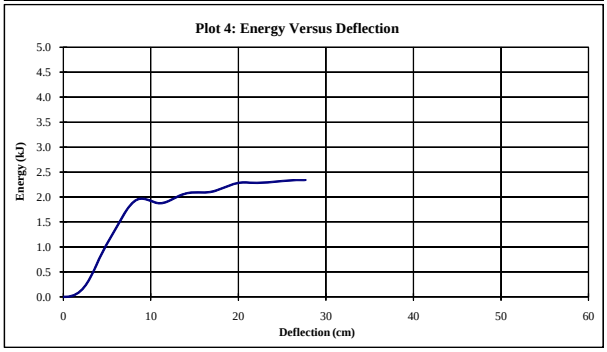

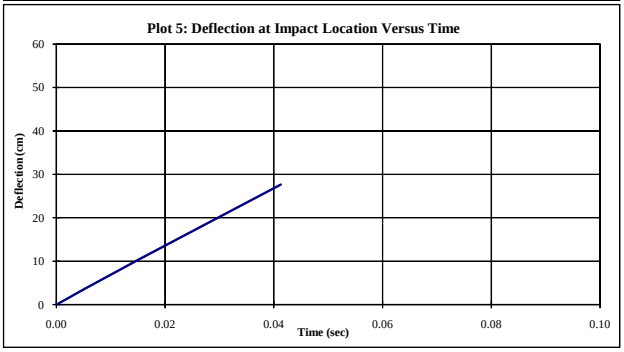

Figure A-10. Results of MNCRT-5 (EDR4)

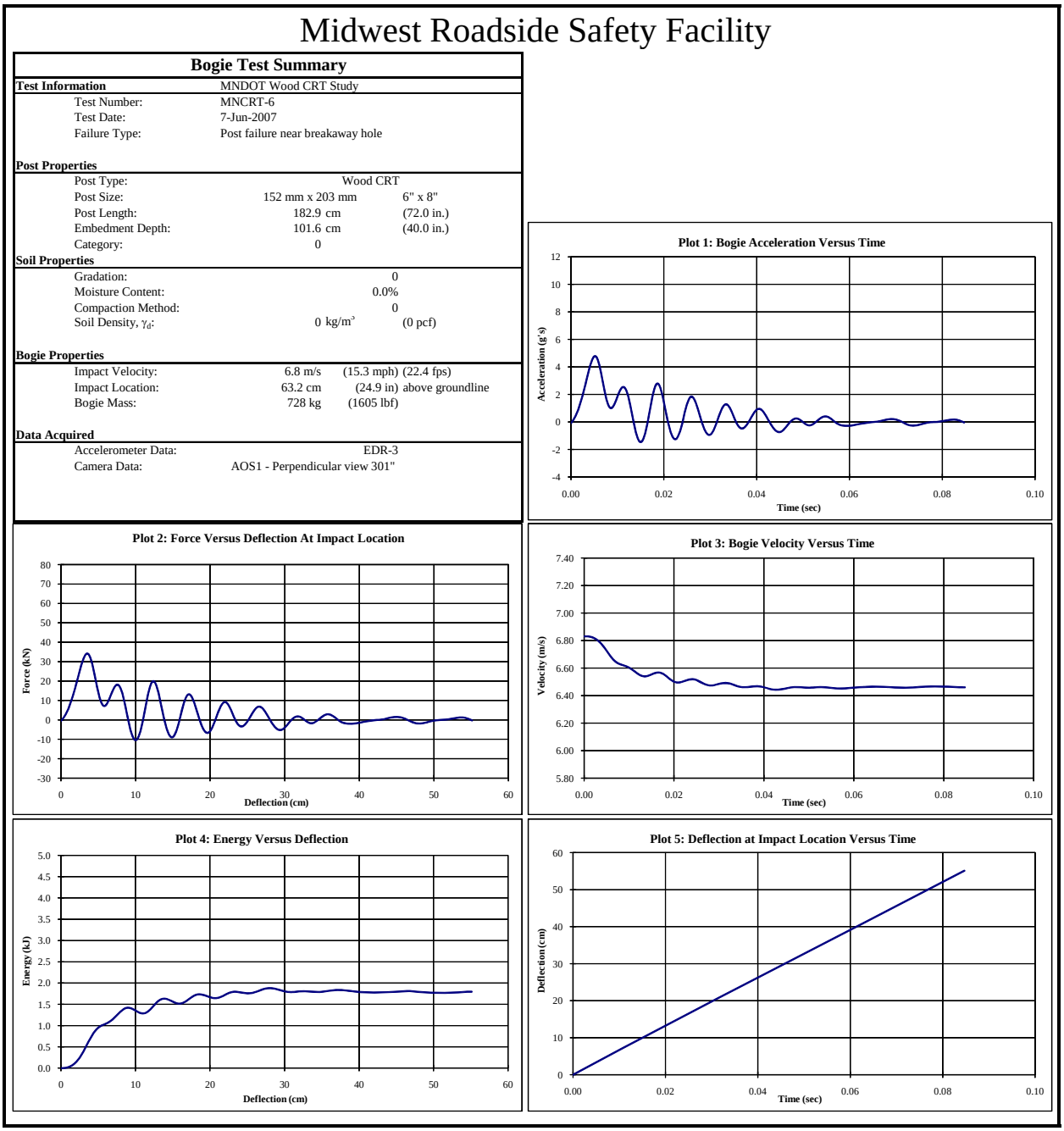

Figure A-11. Results of MNCRT-6 (EDR3)

Midwest Roadside Safety Facility

Bogie Test Summary

Test Information	MNDOT Wood CRT Study		
Test Number:	MNCRT-6		
Test Date:	7-Jun-2007		
Failure Type:	Post failure near breakaway hole		
Post Properties			
Post Type:	Wood CRT		
Post Size:	152 mm x 203 mm	6" x 8"	
Post Length:	182.9 cm	(72.0 in.)	
Embedment Depth:	101.6 cm	(40.0 in.)	
Category:	0		
Soil Properties			
Gradation:	0		
Moisture Content:	0.0%		
Compaction Method:	0		
Soil Density, γ_d:	0 kg/m^3	(0 pcf)	
Bogie Properties			
Impact Velocity:	6.8 m/s	(15.3 mph)	(22.4 fps)
Impact Location:	63.2 cm	(24.9 in)	above groundline
Bogie Mass:	728 kg	(1605 lbf)	
Data Acquired			
Accelerometer Data:	EDR-4		
Camera Data:	AOS1 - Perpendicular view 301"		

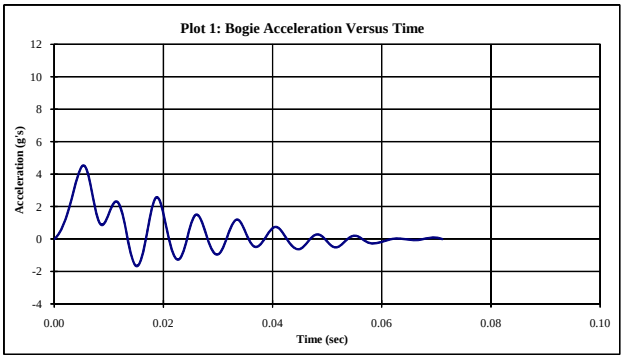

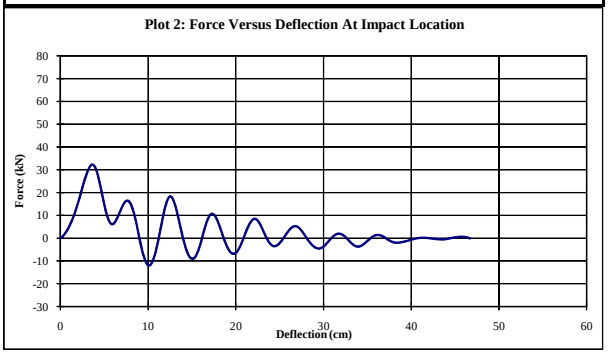

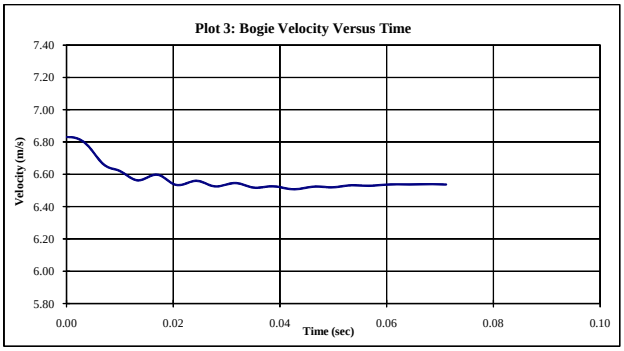

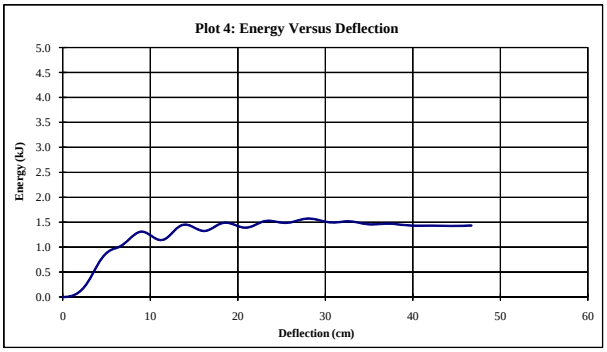

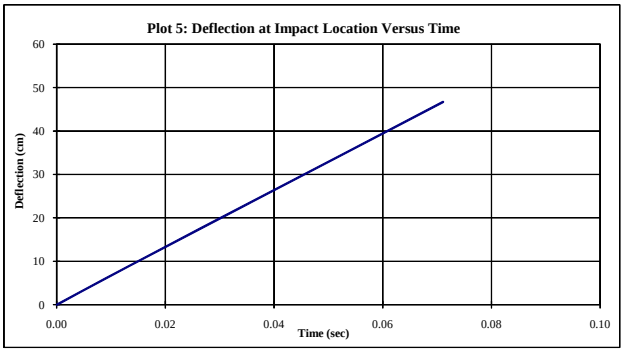

Figure A-12. Results of MNCRT-6 (EDR4)

Midwest Roadside Safety Facility

Bogie Test Summary

Test Information	MNDOT Wood CRT Study		
Test Number:	MNCRT-7		
Test Date:	7-Jun-2007		
Failure Type:	Post failure near breakaway hole		
Post Properties			
Post Type:	Wood CRT		
Post Size:	152 mm x 203 mm	6" x 8"	
Post Length:	182.9 cm	(72.0 in.)	
Embedment Depth:	101.6 cm	(40.0 in.)	
Category:	0		
Soil Properties			
Gradation:	0		
Moisture Content:	0.0%		
Compaction Method:	0		
Soil Density, γ_d:	0 kg/m^3	(0 pcf)	
Bogie Properties			
Impact Velocity:	7.2 m/s	(16.1 mph)	(23.6 fps)
Impact Location:	63.2 cm	(24.9 in)	above groundline
Bogie Mass:	728 kg	(1605 lbf)	
Data Acquired			
Accelerometer Data:	EDR-3		
Camera Data:	AOS1 - Perpendicular view 301"		

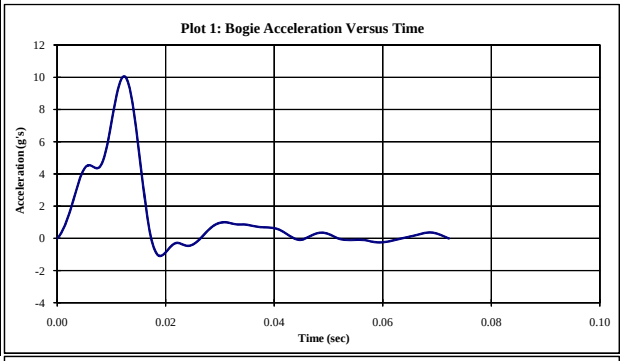

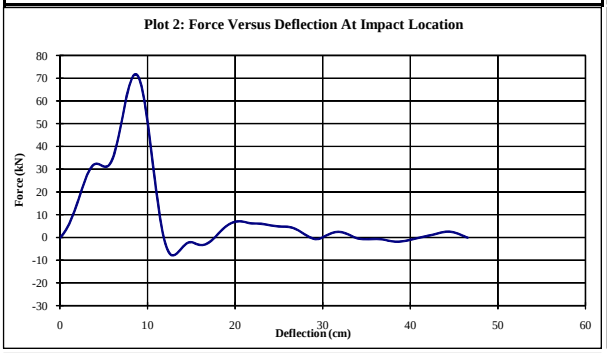

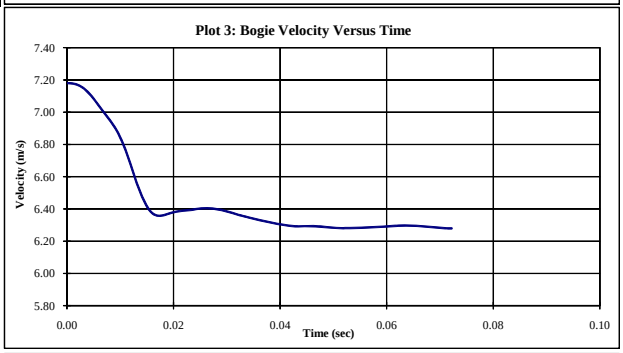

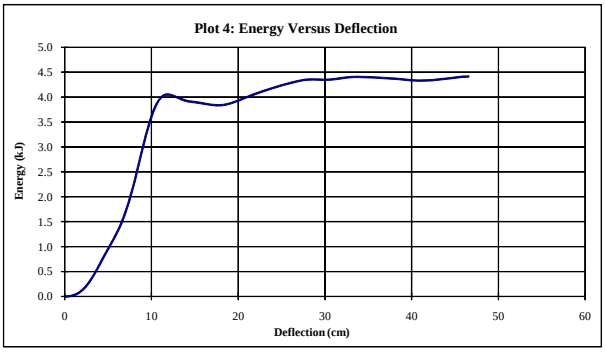

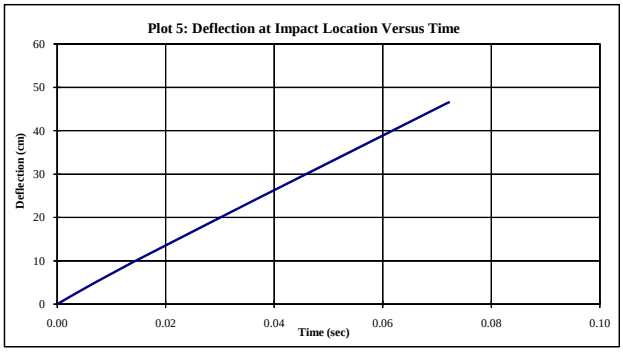

Figure A-13. Results of MNCRT-7 (EDR3)

Midwest Roadside Safety Facility

Bogie Test Summary

Test Information	MNDOT Wood CRT Study		
Test Number:	MNCRT-7		
Test Date:	7-Jun-2007		
Failure Type:	Post failure near breakaway hole		
Post Properties			
Post Type:	Wood CRT		
Post Size:	152 mm x 203 mm	6" x 8"	
Post Length:	182.9 cm	(72.0 in.)	
Embedment Depth:	101.6 cm	(40.0 in.)	
Category:	0		
Soil Properties			
Gradation:	0		
Moisture Content:	0.0%		
Compaction Method:	0		
Soil Density, γ_d:	0 kg/m^3	(0 pcf)	
Bogie Properties			
Impact Velocity:	7.2 m/s	(16.1 mph)	(23.6 fps)
Impact Location:	63.2 cm	(24.9 in)	above groundline
Bogie Mass:	728 kg	(1605 lbf)	
Data Acquired			
Accelerometer Data:	EDR-4		
Camera Data:	AOS1 - Perpendicular view 301"		

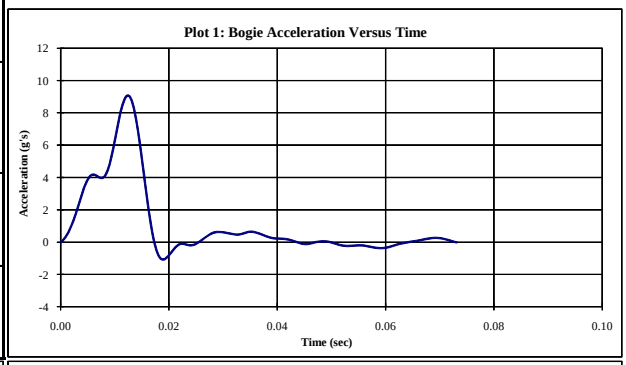

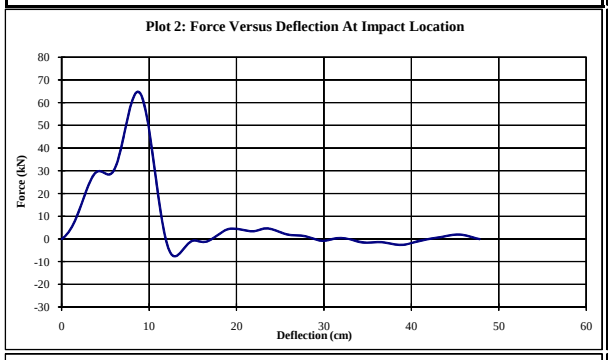

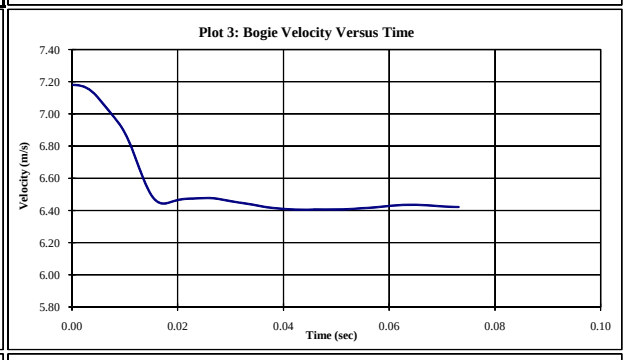

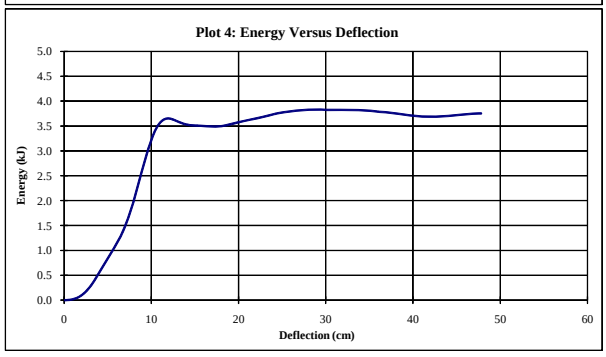

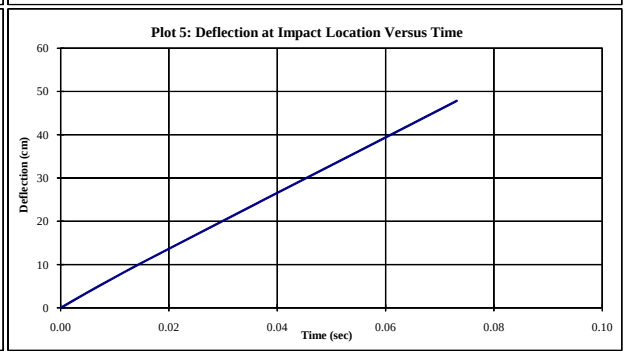

Figure A-14. Results of MNCRT-7 (EDR4)

Midwest Roadside Safety Facility

Bogie Test Summary

Test Information	MNDOT Wood CRT Study		
Test Number:	MNCRT-8		
Test Date:	8-Jun-2007		
Failure Type:	Post failure near breakaway hole		
Post Properties			
Post Type:	Wood CRT		
Post Size:	152 mm x 203 mm	6" x 8"	
Post Length:	182.9 cm	(72.0 in.)	
Embedment Depth:	101.6 cm	(40.0 in.)	
Category:	0		
Soil Properties			
Gradation:	0		
Moisture Content:	0.0%		
Compaction Method:	0		
Soil Density, γ_d:	0 kg/m^3	(0 pcf)	
Bogie Properties			
Impact Velocity:	7.2 m/s	(16.0 mph)	(23.5 fps)
Impact Location:	63.2 cm	(24.9 in)	above groundline
Bogie Mass:	728 kg	(1605 lbf)	
Data Acquired			
Accelerometer Data:	EDR-3		
Camera Data:	AOS1 - Perpendicular view 301"		

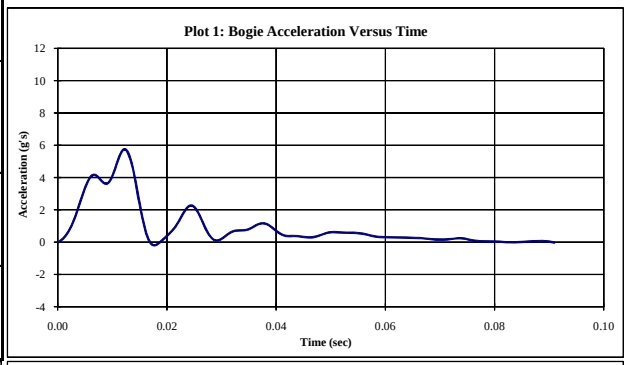

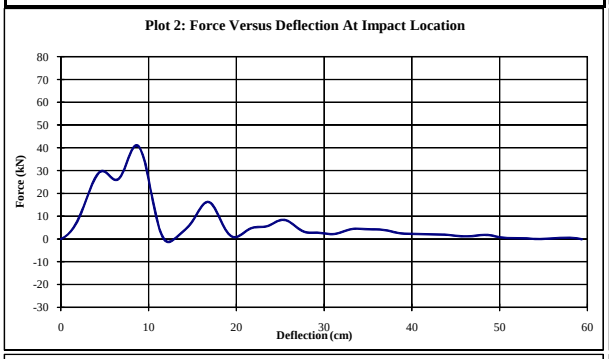

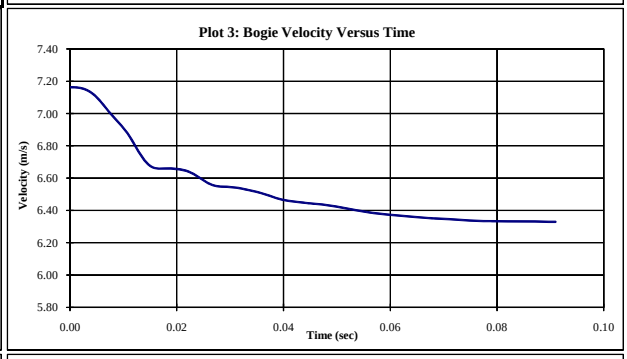

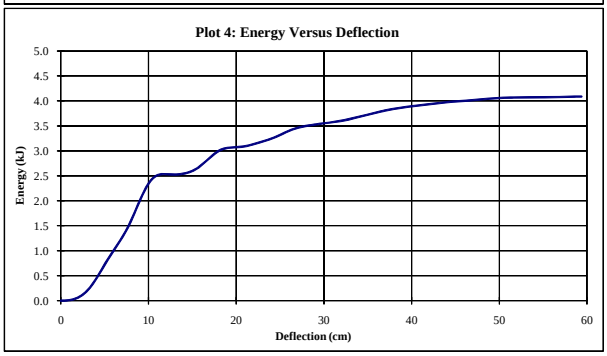

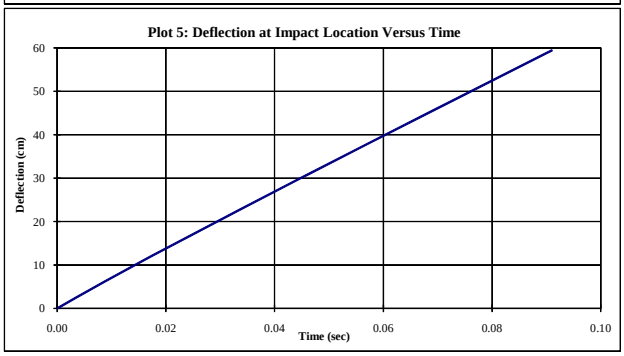

Figure A-15. Results of MNCRT-8 (EDR3)

Midwest Roadside Safety Facility

Bogie Test Summary

Test Information	MNDOT Wood CRT Study		
Test Number:	MNCRT-8		
Test Date:	8-Jun-2007		
Failure Type:	Post failure near breakaway hole		
Post Properties			
Post Type:	Wood CRT		
Post Size:	152 mm x 203 mm	6" x 8"	
Post Length:	182.9 cm	(72.0 in.)	
Embedment Depth:	101.6 cm	(40.0 in.)	
Category:	0		
Soil Properties			
Gradation:	0		
Moisture Content:	0.0%		
Compaction Method:	0		
Soil Density, γ_d:	0 kg/m^3	(0 pcf)	
Bogie Properties			
Impact Velocity:	7.2 m/s	(16.0 mph)	(23.5 fps)
Impact Location:	63.2 cm	(24.9 in)	above groundline
Bogie Mass:	728 kg	(1605 lbf)	
Data Acquired			
Accelerometer Data:	EDR-4		
Camera Data:	AOS1 - Perpendicular view 301"		

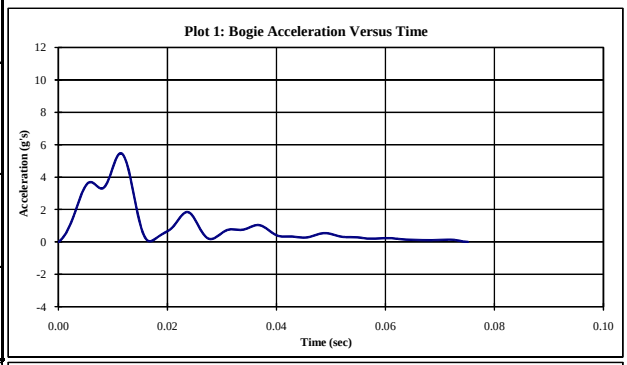

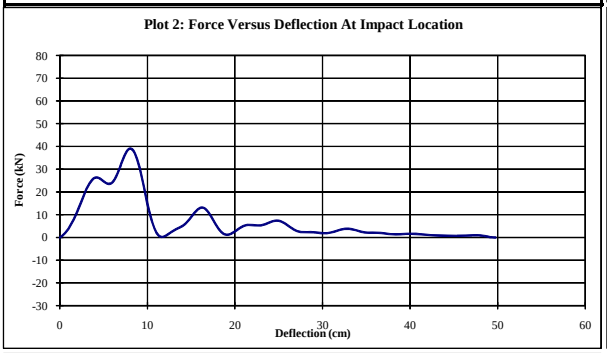

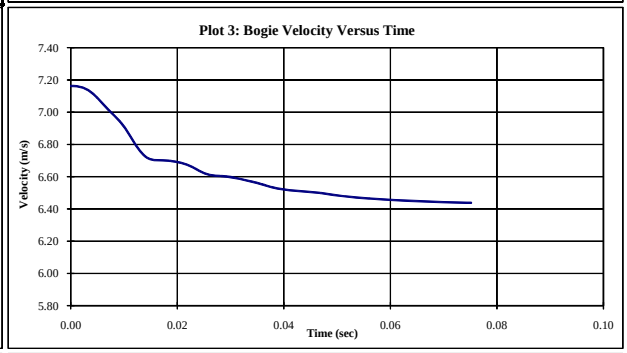

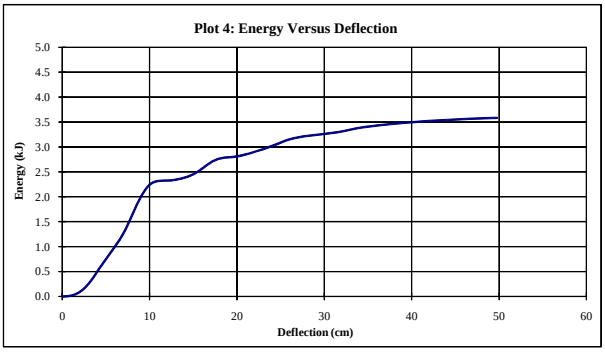

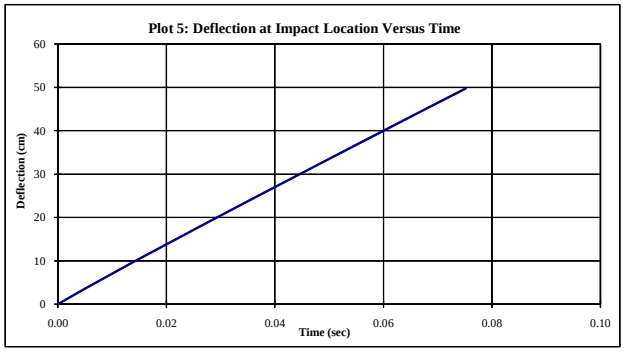

Figure A-16. Results of MNCRT-8 (EDR4)

Midwest Roadside Safety Facility

Bogie Test Summary

Test Information	MNDOT Wood CRT Study		
Test Number:	MNCRT-9		
Test Date:	8-Jun-2007		
Failure Type:	Post failure near breakaway hole		
Post Properties			
Post Type:	Wood CRT		
Post Size:	152 mm x 203 mm	6" x 8"	
Post Length:	182.9 cm	(72.0 in.)	
Embedment Depth:	101.6 cm	(40.0 in.)	
Category:	0		
Soil Properties			
Gradation:	0		
Moisture Content:	0.0%		
Compaction Method:	0		
Soil Density, γ_d:	0 kg/m³	(0 pcf)	
Bogie Properties			
Impact Velocity:	6.9 m/s	(15.5 mph)	(22.8 fps)
Impact Location:	63.2 cm	(24.9 in)	above groundline
Bogie Mass:	728 kg	(1605 lbf)	
Data Acquired			
Accelerometer Data:	EDR-3		
Camera Data:	AOS1 - Perpendicular view 301"		

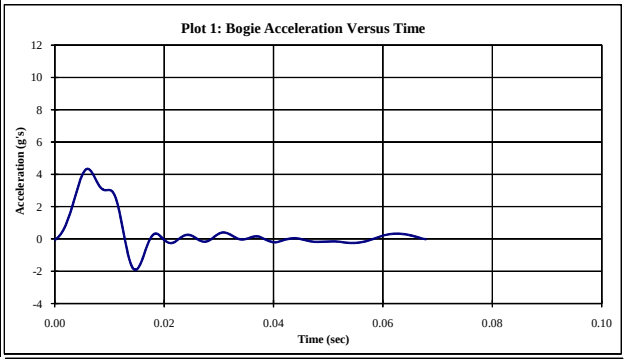

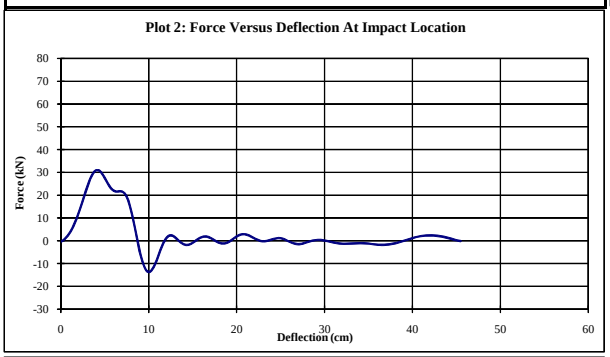

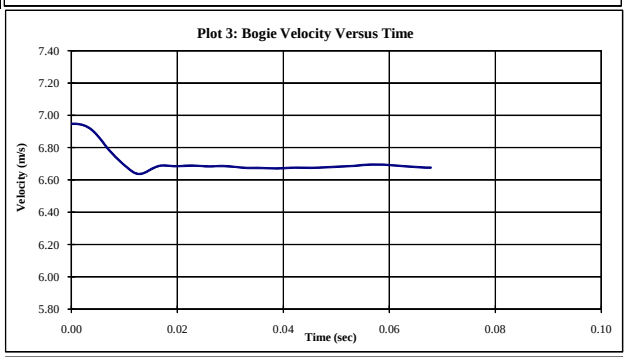

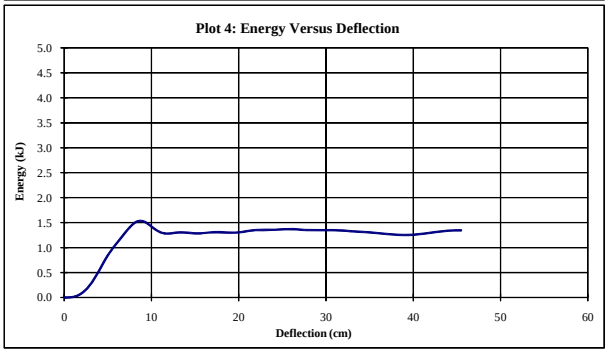

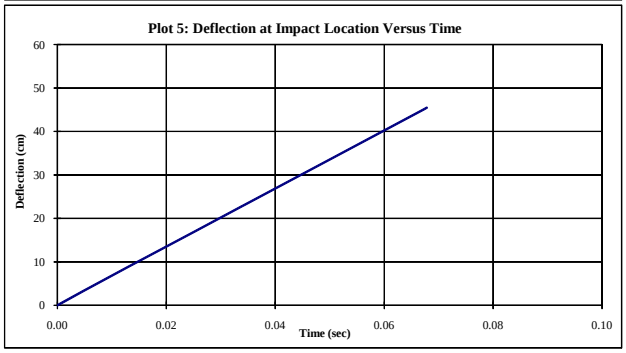

Figure A-17. Results of MNCRT-9 (EDR3)

Midwest Roadside Safety Facility

Bogie Test Summary

Test Information	MNDOT Wood CRT Study		
Test Number:	MNCRT-9		
Test Date:	8-Jun-2007		
Failure Type:	Post failure near breakaway hole		
Post Properties			
Post Type:	Wood CRT		
Post Size:	152 mm x 203 mm	6" x 8"	
Post Length:	182.9 cm	(72.0 in.)	
Embedment Depth:	101.6 cm	(40.0 in.)	
Category:	0		
Soil Properties			
Gradation:	0		
Moisture Content:	0.0%		
Compaction Method:	0		
Soil Density, γ_d:	0 kg/m^3	(0 pcf)	
Bogie Properties			
Impact Velocity:	6.9 m/s	(15.5 mph)	(22.8 fps)
Impact Location:	63.2 cm	(24.9 in)	above groundline
Bogie Mass:	728 kg	(1605 lbf)	
Data Acquired			
Accelerometer Data:	EDR-4		
Camera Data:	AOS1 - Perpendicular view 301"		

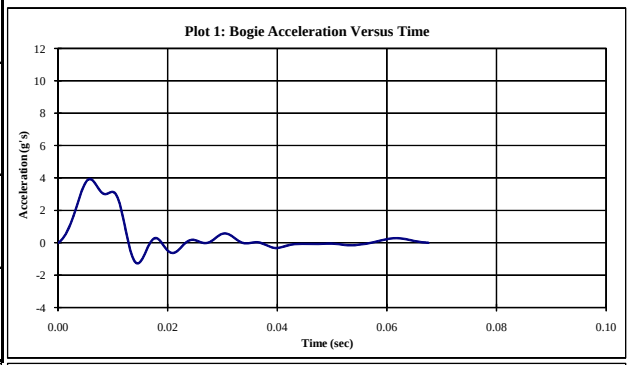

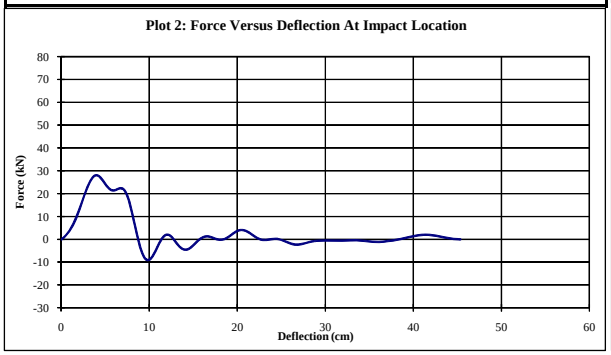

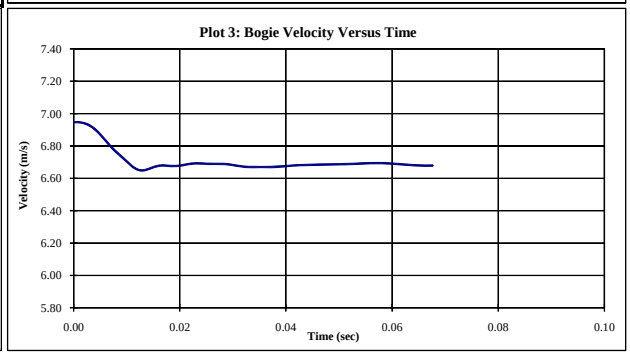

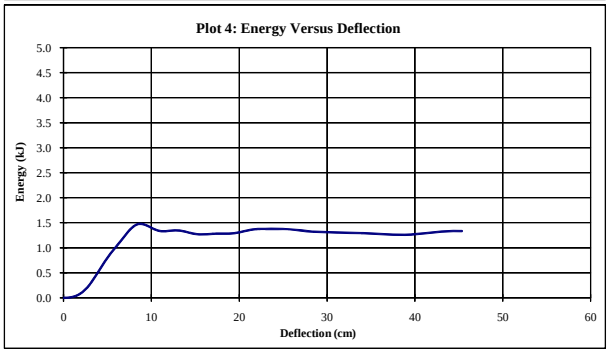

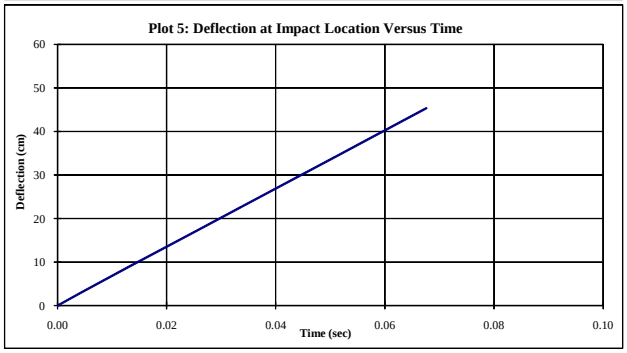

Figure A-18. Results of MNCRT-9 (EDR4)